FIELD TRIP GUIDE

GSA PENROSE MEETING

SUBDUCTION TO STRIKE-SLIP TRANSITIONS ON PLATE BOUNDARIES

JANUARY 21-22, 1999

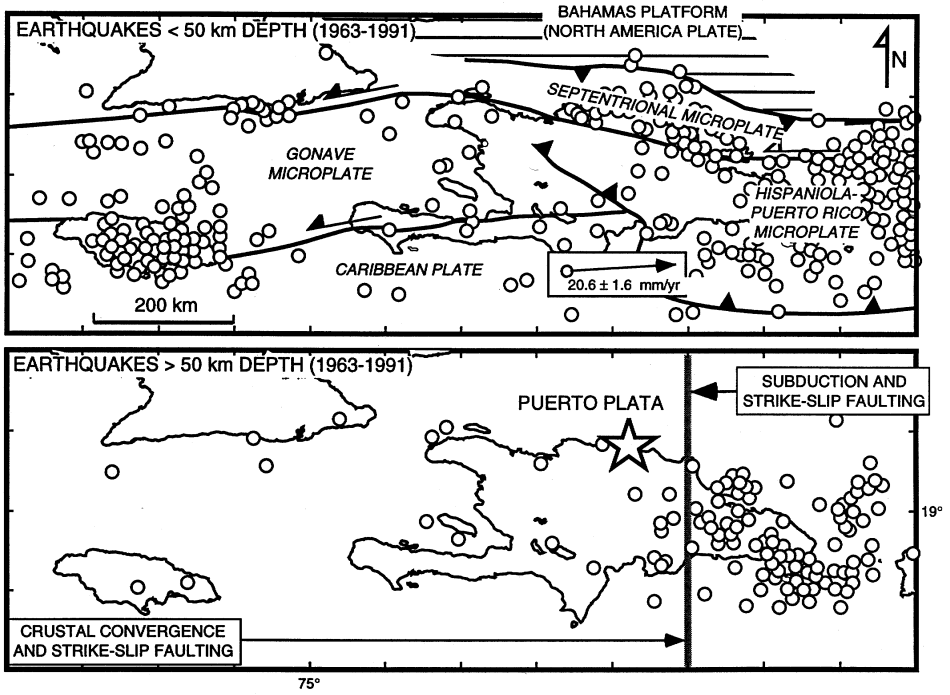

PUERTO PLATA VILLAGE CARIBBEAN RESORT

PUERTO PLATA

DOMINICAN REPUBLIC

TABLE OF CONTENTS

OVERVIEW OF THE FIELD TRIP AND ORGANIZATIONAL INFORMATION

PAUL MANN

Welcome to the Dominican Republic and the North America-Caribbean plate boundary zone!

ROUTE AND SCOPE OF THE FIELD TRIP

This two day field trip will provide you with an overview of some of the more accessible localities related to different aspects of the subduction to strike-slip transition on this plate boundary (Figs. 1, 2). Stops A and B of Day One will show you the subduction-related geology of the North Coast. Stop C on Day One focusses on rocks at the subduction-strike-slip transition interval in the Cordillera Septentrional. Stops D and E on Day One will examine young deformation associated with recent strike-slip faulting in the Cibao Valley.

On Day Two, we will resume our look at the recent strike-slip faulting in the Cibao Valley at Stops F and G and then drive to coastal Stop H, the site of a deadly tsunami runup related to the 1946 magnitude 8 earthquake. Stops H and Ia will attempt to integrate recent advances in marine geophysical mapping of the offshore areas of the Dominican Republic and Puerto Rico with what we have shown you onland. Stop Ib will attempt to integrate recent advances in GPS-based geodesy in our understanding of the plate boundary zone. Stop J will conclude the trip with a visit to ancient blueschist rocks that do not occur in the area of Stops A and B on Day One.

You will see a great variety of landscapes, microclimates and geology that are all controlled by the recent tectonic activity of the area. It is our hope that this trip will stimulate some of you to return to this and other parts of Hispaniola either for vacationing or to carry out research of your own on the many active and paleotectonic problems that remain to be solved.

ORGANIZATIONAL INFORMATION

- **Loading up in the morning.** We have timed the route and all the stops are feasible if we depart on time in the morning and leave at the recommended times from the various stops. The first hurtle will be to leave on time in the morning from the hotel. **We will leave promptly at 7:30 am on Day One and 8:00 am on Day Two.** The busses will be available for boarding at 7:15 am on Day One and 7:45 am on Day Two. Please be on time with all of your field gear.
- **Lunches and drinks.** The hotel will be providing us with box lunches and drinks. You will also have the opportunity to buy cold drinks at the lunch stops. You might want to bring some extra water in a bottle or canteen.
- **Places on busses and head counts.** We would suggest that you sit on the same bus for both days. This would help the leaders on each bus to make a head count at the end of each stop to make sure we don't leave anyone behind. Each bus will have one or more of the field trip leaders on it. If you notice someone missing after a stop, please tell the leader.
- **Toilets and emergency stops.** There will be no restrooms on the busses. However, we have arranged for restroom stops about every 2 hours. If you need to stop more frequently than that, let the leader know.
- **Procedure at each stop.** Stops will be led by the various people indicated. After unloading at each stop, please congregate in a tight group so the leader can give you an overview of stop and suggest features for you to observe. Please take note of the leader's personal safety suggestions in the stop descriptions.
- **Problems?** For problems of any type, see one of the leaders, Lois Elms, or Christine Herridge-Guerrero.

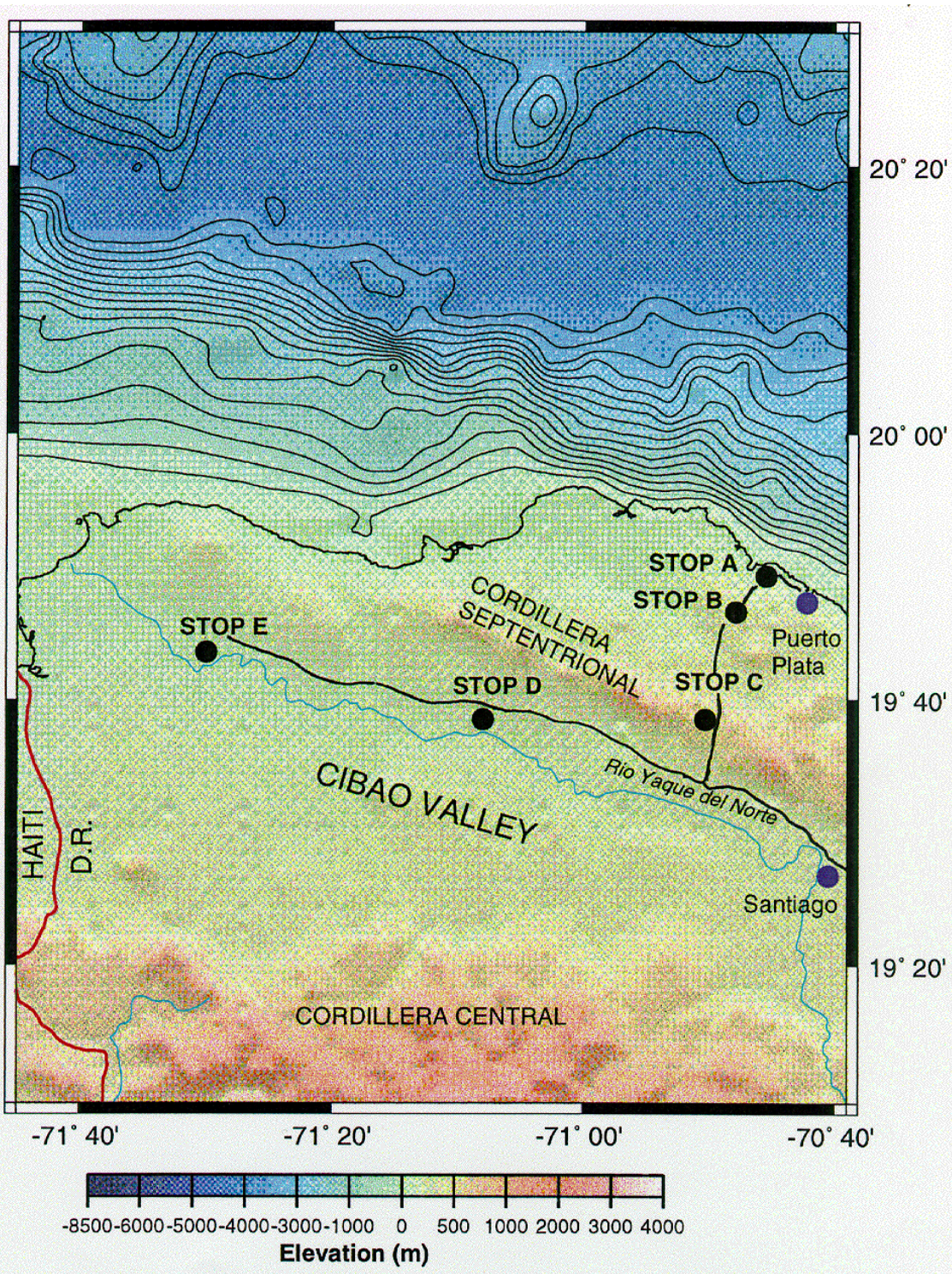

Figure 1. DAY 1 FIELD TRIP STOPS. Onshore and offshore digital elevation map of northern Hispaniola. Onshore topography is based on the GTOPO3 database compiled by USGS, offshore bathymetry is predicted seafloor topography from satellite altimetry with ship soundings (Smith and Sandwell, 1997.)

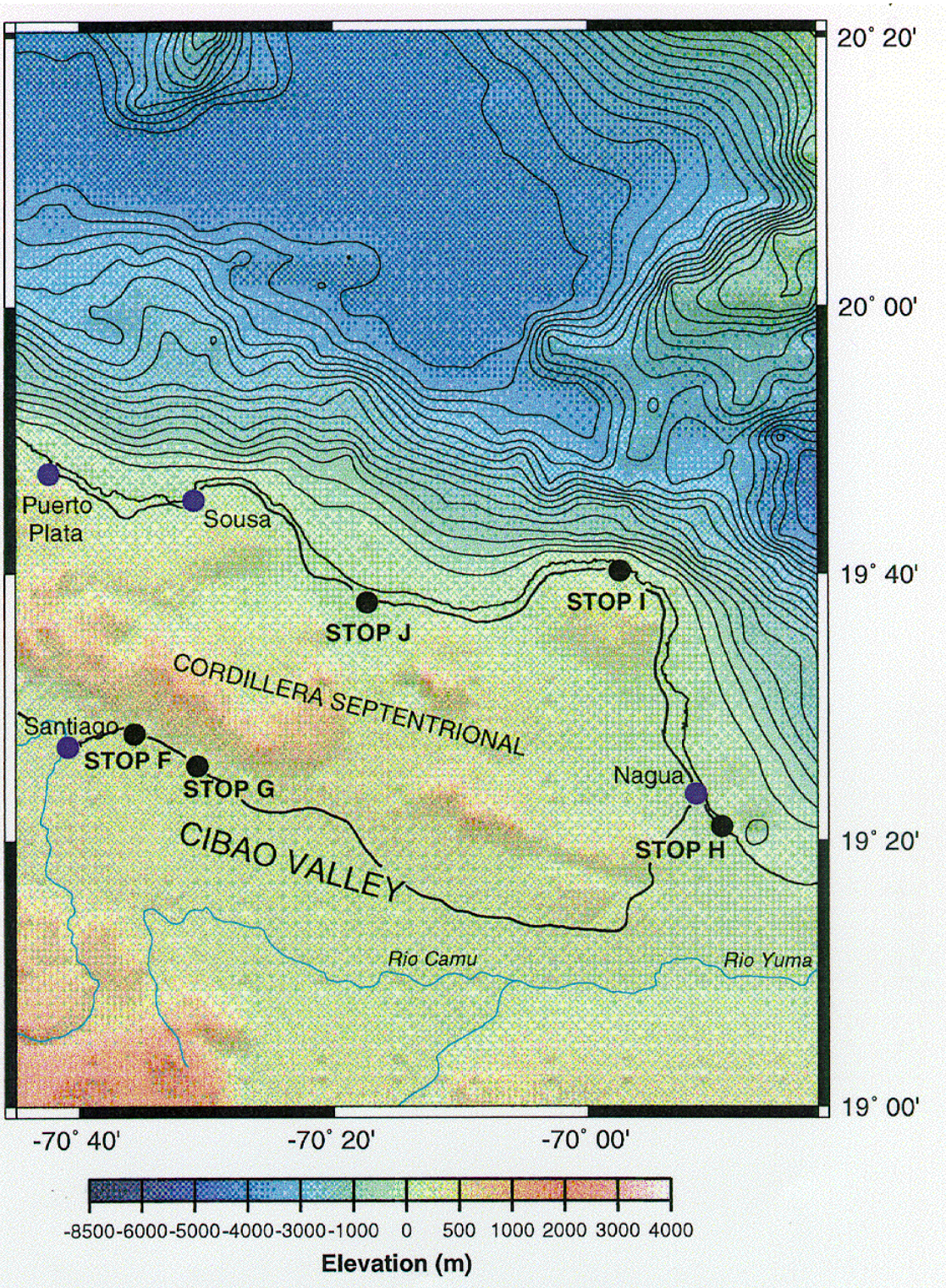

Figure 2. DAY 2 FIELD TRIP STOPS. Onshore and offshore digital elevation map of northern Hispaniola. Onshore topography is based on the GTOPO3 database compiled by USGS, offshore bathymetry is predicted seafloor topography from satellite altimetry with ship soundings (Smith and Sandwell, 1997.)

OVERVIEW OF THE FIELD TRIP ON THE NORTH COAST OF THE DOMINICAN REPUBLIC

JAMES DOLAN

MAIN OBJECTIVES

Our objectives on the North Coast will include a wide range of topics related to both the active and ancient tectonics of subduction to strike-slip transition areas. To facilitate discussion during these stops and on the busses between stops, I have appended six illustrations with long captions. These maps and interpretations are derived from our paper in the recent Geological Society of America Special Publication 326 (published December, 1998). We will have display copies of GSA SP 326 available at the conference and will bring one copy in each of the four busses.

North Coast field trip objectives and topics will include:

• discussion of the tectonic origin of historical earthquakes and tsunamis and their relation to the submarine thrust front of the North Hispaniola deformed belt mapped north of Hispaniola (Fig. 1). This topic is most relevant to Stops H, Ia, and Ib on Day Two.

• discussion of the origin, geometry, and exhumation of subducted slabs in the mantle that have been mapped using the hypocenters of deep and intermediate depth earthquakes beneath Hispaniola and Puerto Rico (Fig. 2). This topic is most relevant to Stops A and B on Day One and Ia, Ib and J on Day Two.

• examination of outcrops of older rocks formed during the Eocene and older subduction phase of the North America-Caribbean plate boundary and their relation to active structures of the North Hispaniola deformed belt (Fig. 3). This topic is most relevant Stops A and B on Day One and Stop J on Day Two.

• discussion of strain partitioning relations between onland strike-slip faults - including the Septentrional and Camu - and offshore thrust faults and folds - including the ones in the North Hispaniola deformed belt (Fig. 4A, 4B). This topic is most relevant to Stops H, Ia, and Ib on Day Two.

• discussion of North America-Caribbean slab intersection in the mantle beneath the Dominican Republic and Puerto Rico and its implications for surface tectonics and earthquake potential (Fig. 5). This topic is most relevant to Stops H, Ia, and Ib on Day Two.

All of these discussion topics will be discussed in relation to other transition areas during the meeting at the conference center and will be addressed during our final discussion on the last day of the meeting.

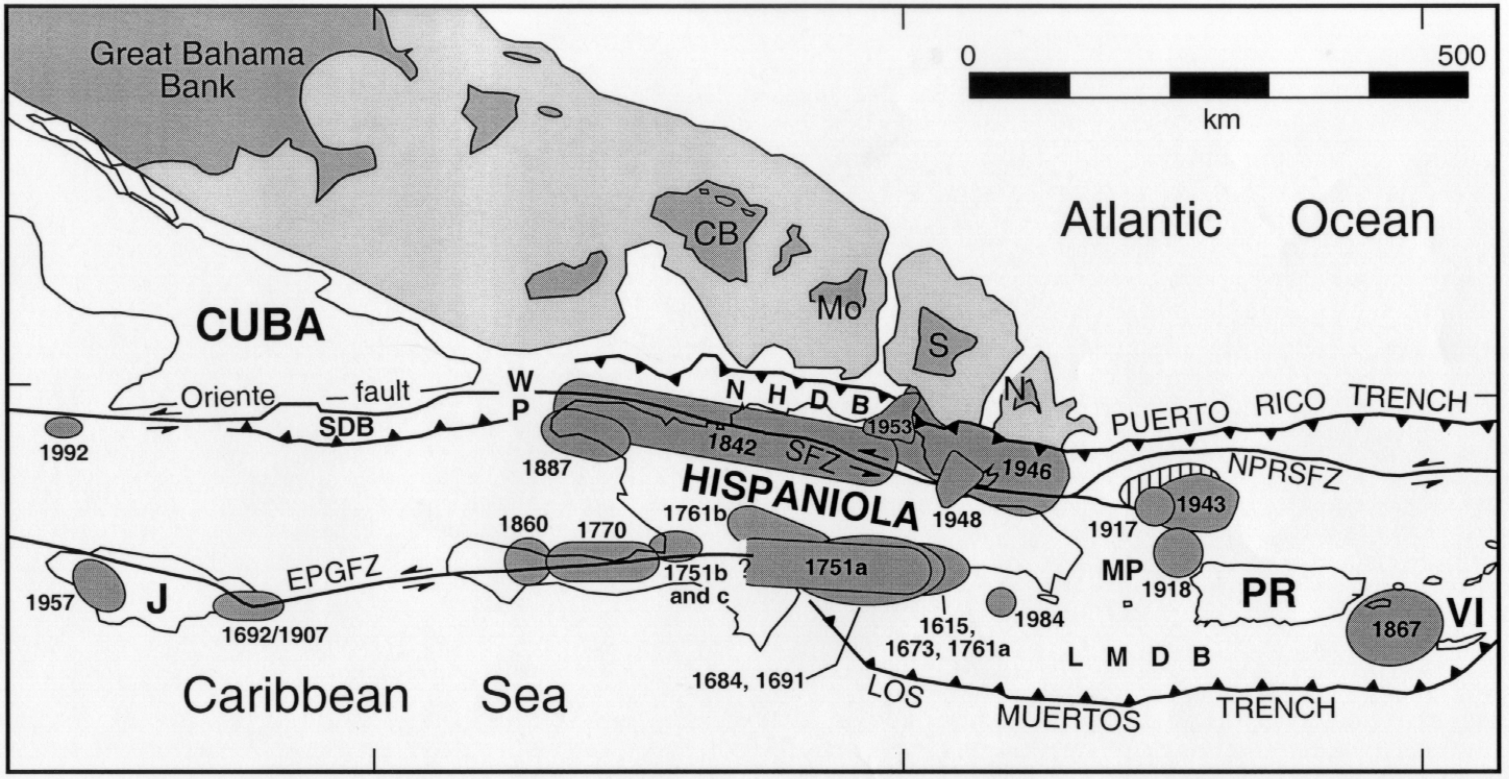

FROM DOLAN AND WALD (1998)

Figure 1. Neotetctonic map of north-central Caribbean region showing great width (250 km) and complexity of northern Caribbean plate boundary zone (NCPBZ) as well as location of major historical earthquakes (year of occurrence shown for each event; 1751a event occurred in October and 1751b event occurred in November). Geologic data compiled from Dolan and et al. (1998), Mann et al. (1984; 1998), Masson and Scanlon (1991), Edgar (1991), Dillon et al. (1992), and Case and Holcombe (1980). Earthquake data compiled from Kelleher et al. (1973), Chalas-Jimenez (1989), McCann and Pennington (1990), and Mann et al. (1998). CB is Caicos bank; EPGFZ is Enriquillon-Plantain Garden fault zone; J is Jamaica; LMDB is Los Muertos deformed belt; Mo is Mouchoir bank; MP is Mona Passage; N is navidad bank; NHDB is northern Hispaniola deformed belt; NPRSFZ is northern Puerto Rico slope fault zone; PR is Puerto Rico; S is Silver bank; SDB is Santiago deformed belt; SFZ is Septentrional fault zone; VI is Virgin Islands; WP is Windward passage.

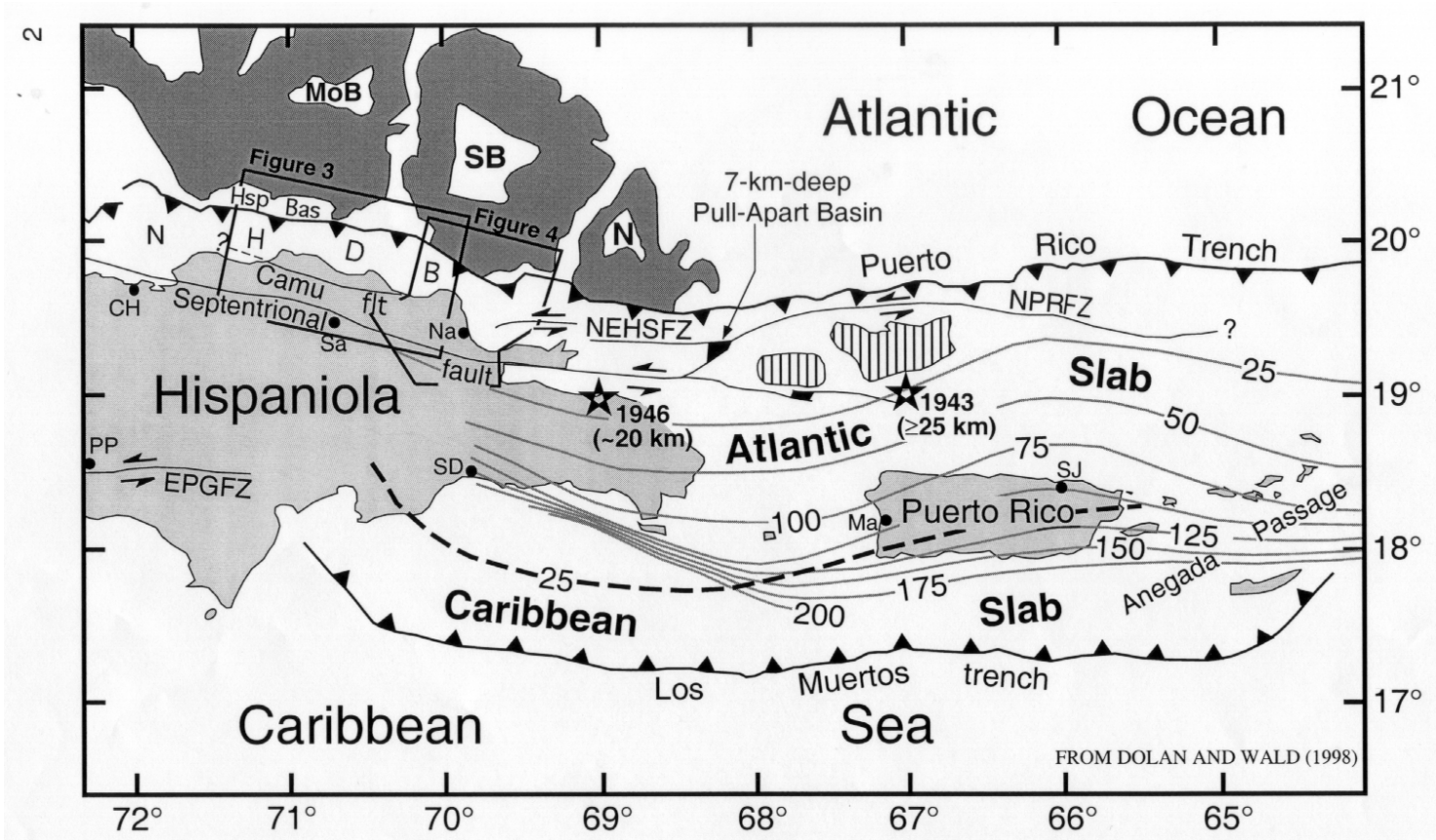

Figure 2. Structure contour map of underthrust Atlantic and Caribbean slabs in north-central Caribbean region. Depth contour interval is 25 km. Contours are from Dolan et al. (1998), and are based on cross sections of recent seismicity from ISC catalog. Slab contours shown as solid gray lines are constructed along the top of a south-dipping zone of seismicity interpreted to represent the top of the underthrust slab of Atlantic oceanic lithosphere of the North America Plate. Slab contours shown by black dashed line are constructed along top of north-dipping upper limit of a north-dipping zone of seismicity thought to represent the top of underthrust Caribbean lithosphere. Note the epicenters and approximate focal depths of the 1943 Northern Mona Passage and 1946 Northeastern Hispaniola earthquakes, which are discussed in this paper. The minimum focal depth shown for the 1943 event was determined in this study. The approximate focal depth for the 1946 event is from Russo and Villasenor (1995). Dark shading denotes limits of Bahamas carbonate province (from Dolan et al., 1998). Black circles show locations of major cities. CH is Cap Haitien, Haiti; E-PGF is Enriquillo fault zone from Mann et al. (1984); Ma is Mayaguez, Puerto Rico; MoB is Mouchoir bank; Na is Nagua, Dom. Rep.; N is Navidad bank; NHDB is northern Hispaniola deformed belt, which includes the northern Hispaniola accretionary prism; NPRSFZ is northern Puerto Rico fault zone compiled from Masson and Scanlon (1991) and Dolan et al. (1998); PP is Port-au-Prince, Haiti; Sa is Santiago, Dom. Rep.; SB is Silver bank; SD is Santo Domingo, Dom. Rep.. Hsp Bas is Hispaniola Basin. Irregular black areas northeast of Hispaniola denote pull-apart basins at left steps along the Septentrional fault system.

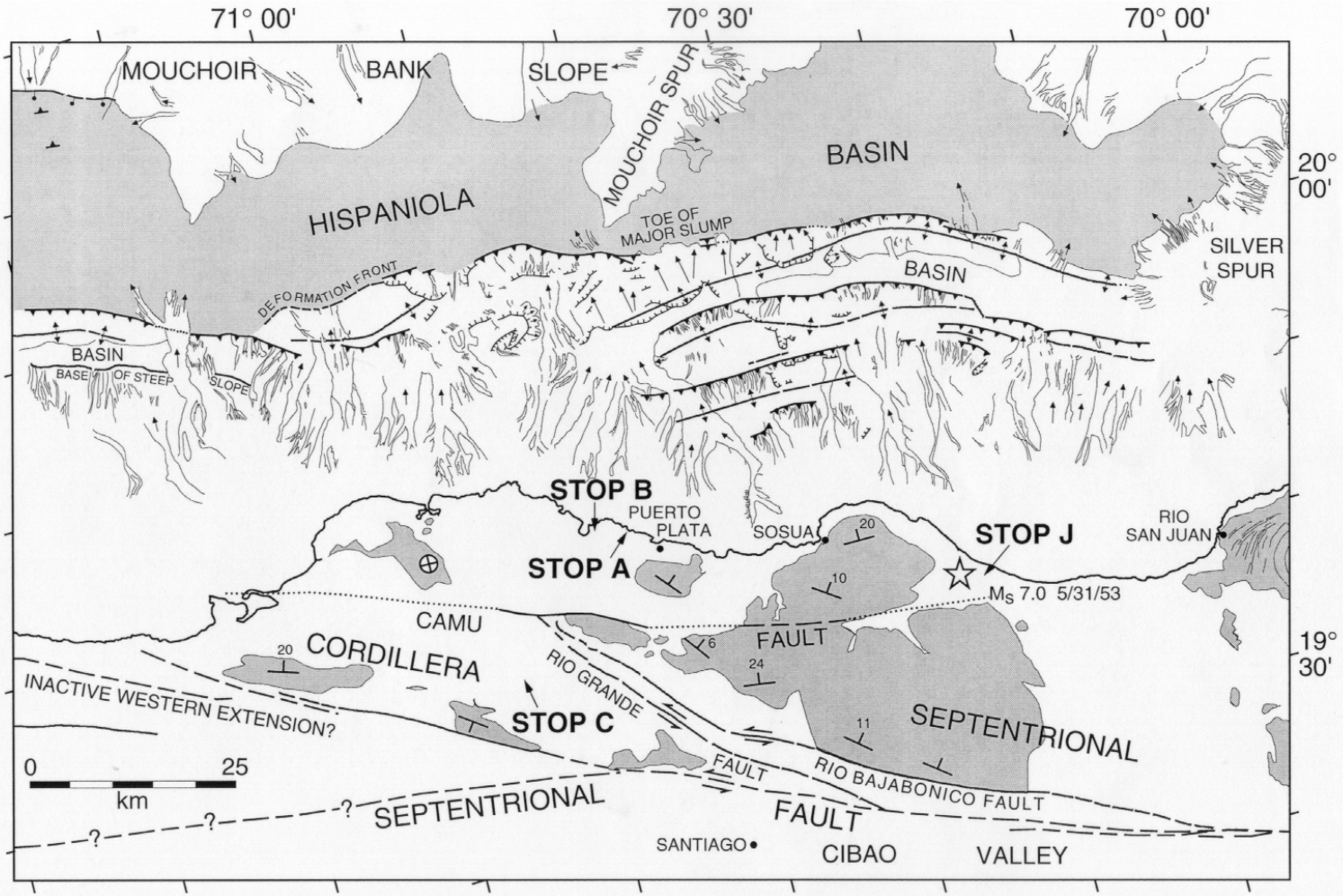

Figure 3. Major structures onshore and offshore northern Dominican Republic. Gray shading onshore denotes outcrop of Miocene-Pliocene Villa Trina Formation limestones. Offshore shading denotes flat-floored, turbidite-filled basins. Onshore data from de Zoeten and Mann (1991) and de Zoeten et al. (1991). Epicenter (star) of 1953 Sosua earthquake from International Seismological Summary of 1953 (1961).

Figure 4A. SeaMARC II side-scan sonar image of central part of the survey area showing the well-developed Silver Spur collision. Onshore data are an SAR image processed by Tim Dixon (used with kind permission).

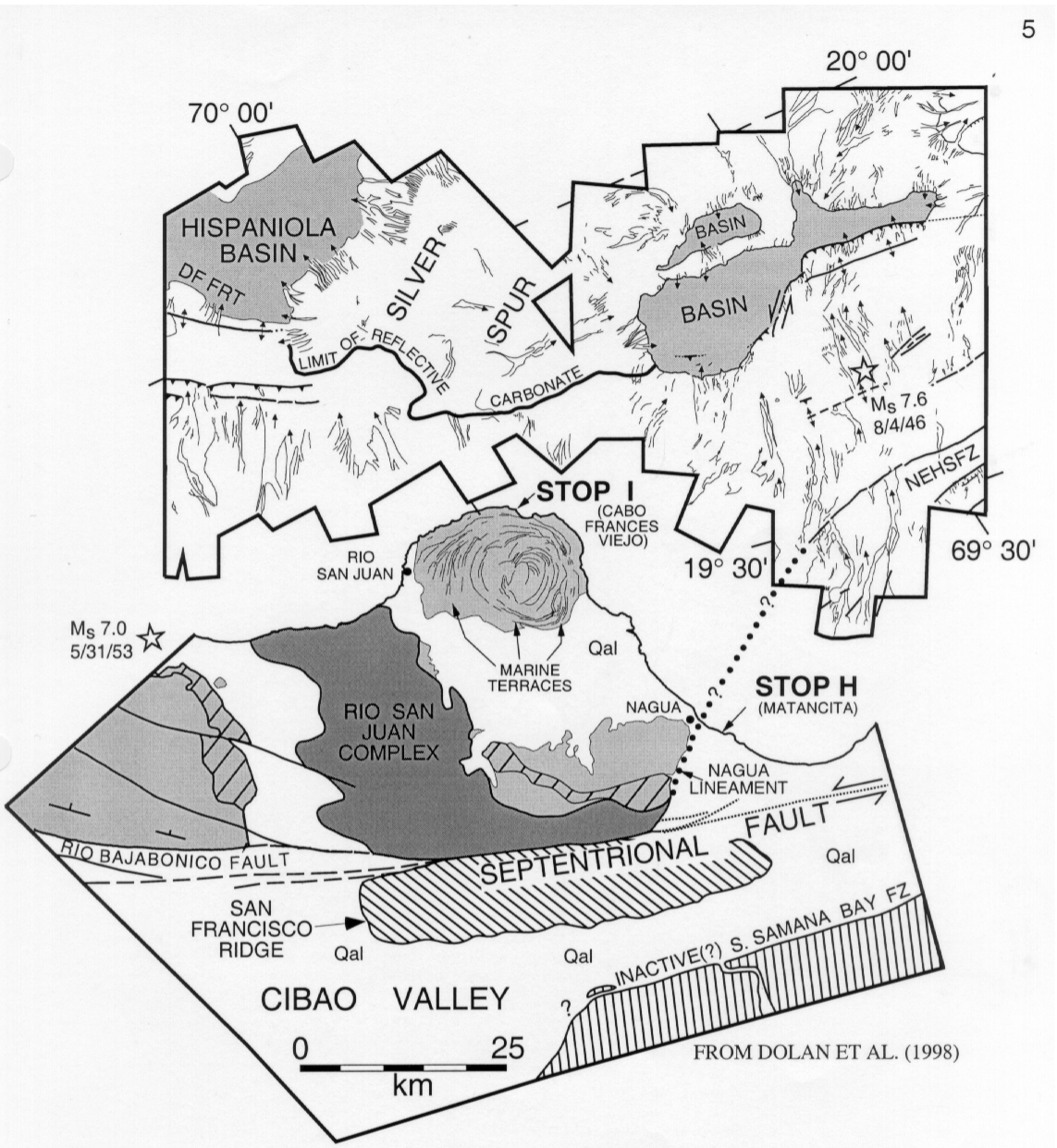

Figure 4B. Line drawing of major structural and sedimentary features observed on SeaMARC II side-scan sonar data offshore and SAR image onshore northern Hispaniola. DF FRT is deformation front of eastern-most part of northern Hispaniola accretionary prism, where no frontal thrust fault is present. Deformation front within Silver Spur collision zone is poorly defined due to poor penetration of seismic reflection data, but is taken to be at southern limit of reflective carbonate outcrop. Note curvature of western part of Northeastern Hispaniola Slope fault zone (NHSFZ) into alignment with the north-northeast-trending Nagua topographic lineament. We postulate an oblique, left-lateral-normal fault connecting these two features (dotted line). We speculate that this fault transfers slip from the Septentrional fault to the NHSFZ. Pale shading is outcrop of upper Miocene-lower Pliocene Villa Trina Formation (from De Zoeten and Mann, 1991; De Zoeten and others, 1991). Diagonal hatching denotes outcrop of resistant, reefal La Piedra member of Villa Trina Formation (modified from De Zoeten and others, 1991). Deposition of the Villa Trina Formation limestones on Rio San Juan Peninsula probably continued into the Pleistocene. Vertical hatching denotes outcrop of Miocene-lower Pliocene Cevicos Formation limestone.

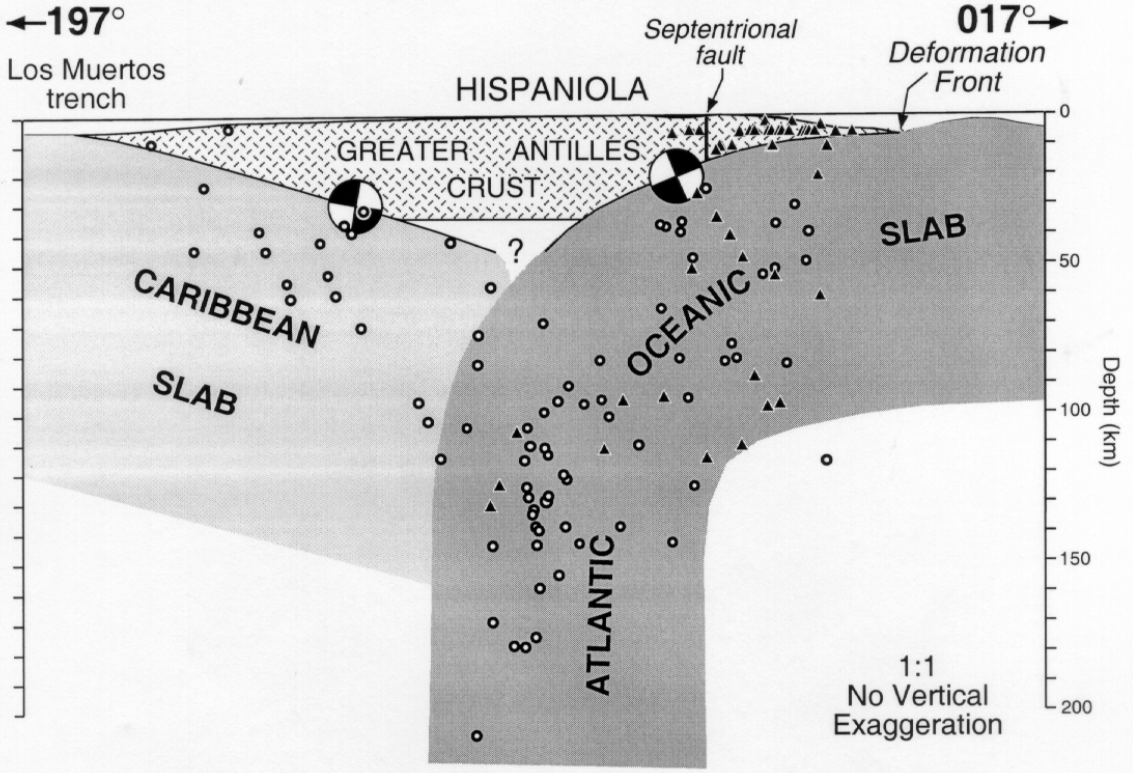

Figure 5. Cross section oriented 017° through eastern part of Hispaniola-Bahamas collision zone showing recent seismicity in the region of the 1946 Northeastern Hispaniola earthquake (modified from Dolan et al. 1998). Heavy line at top of figure represents bathymetry-topography along center line of cross section. No vertical exaggeration. Note that although the profile is oriented approximately perpendicular to regional strike, the profile is oblique to some tectonic and topographic features. Shading denotes approximate thickness of different lithospheric plates, based on assumptions that Atlantic plate consists of normal oceanic lithosphere ~90-100 km thick, and that the thicker crust of the Caribbean plate (Edgar et al., 1971; Case et al., 1990) results in a thicker lithosphere. All seismicity data from NEIC catalog 1962-1992 except as noted. Only earthquakes with well-defined depths have been used; earthquakes assigned default depths of 10 km and 33 km were not used in constructing these sections. Triangles denote 1946 aftershocks relocated by Russo and Villasenor (1995). Note the very well-defined, shallowly southwest-dipping zone of 1946 aftershocks. Also note the diffuse, southward dipping zone of seismicity associated with underthrusting of Atlantic oceanic crust and Bahamas platform carbonates. These shallow aftershocks extend almost to the deformation front defined by SeaMARC II side-scan sonar data (Dolan et al., 1998), suggesting that the 1946 mainshock may have locally ruptured all the way to the sea floor in this collisional region of enhanced mechanical coupling. Note the near-total absence in the recent ISC data of well-located earthquakes associated with the south-dipping plate interface between underthrust Atlantic oceanic crust and Hispaniola that ruptured during the 1946 Northeastern Hispaniola earthquake. In contrast, the relocated 1946 aftershocks define a shallowly southwest-dipping plane approximately along our proposed 1946 mainshock rupture surface. Note that the deeper relocated 1946 aftershocks occur within a long-lived zone of deep background seismicity defined by the past 30 years of ISC catalog data. The gentle southwestward dip of the shallow 1946 aftershock zone, coupled with its location north of the Septentrional fault, confirms that the 1946 mainshock occurred along the shallowly southwest-dipping plate interface, rather than along a strand of the Septentrional fault system, as has been suggested by Russo and Villasenor (1995). Focal mechanisms are shown for the 1946 Northeast Hispaniola mainshock (Dolan and Wald, 1998) and for the Ms 6.7 earthquake of 6-24-84, which occurred along the north-dipping Los Muertos Trench zone of underthrusting (from Byrne et al., 1985).

OVERVIEW OF THE FIELD TRIP IN THE CIBAO VALLEY

PAUL MANN

MAIN OBJECTIVES

Our objective in the Cibao Valley will be to visit exposures of the Septentrional fault zone which accommodates part of the active left-lateral strike-slip motion between the North America and Caribbean plates in northern Hispaniola (Fig. 1). We will also visit a sediment liquefaction site formed during multiple large earthquake shocks that have affected fluvial sediments deposited within the valley.

The Cibao Valley and the Motagua Valley of Guatemala in Central America are the only two subaerial exposures of this interplate strike-slip fault system along its 3,200 km length (Fig. 1). The Motagua fault in Guatemala is a better studied segment of the plate boundary than the segment we will visit here because a 230-km-long segment of the Motagua fault ruptured in 1976 with about 1 m of left-lateral slip. This catastrophic M 7.1 earthquake took the lives of 22,780 Guatemalans and left more than one million homeless in a country with a total 1976 population of about 5.5 million people. Despite recent advances seafloor mapping of the fault zone, landbased studies of the plate boundary in the Cibao and Motagua Valleys will remain critical for fully understanding the tectonics and earthquake potential of the North America-Caribbean plate boundary.

LANDSAT IMAGES SHOWING THE TRIP ROUTE IN THE CIBAO VALLEY

Figures 2-6 are Landsat images kindly processed by Michael Rymer of the U. S. Geological Survey. Carol Prentice and Luis Peña originally interpreted these images as part of their 1998 GSA poster session and later made these digital images available to me for use in this guide. I have expanded their original annotations of the images to show:

- our trip route in the Cibao Valley for both days.
- major cities and towns along the trip route.
- major fault scarps and lineaments (blue arrows) including some shown to me by Luis Peña based on his recent work in 1998 (see meeting abstracts).
- the late Neogene carbonate margin along the southern edge of the Cibao Valley.
- the liquefaction sites (red X's) studied by Tish Tuttle, Carol Prentice, and Luis Peña including the one we will visit at Stop E.
- lineaments that to our knowledge have not been studied in the field.

For those of you who would like to closely follow our position on the images as we drive along, I would suggest that you buy a tourist road map at the hotel gift shop before the field trip. These maps would name more towns and rivers that would help in establishing your location. If you have any questions about our location or the position of scarps and other tectonic features as we are driving through the Cibao Valley, please ask one of the leaders in your bus.

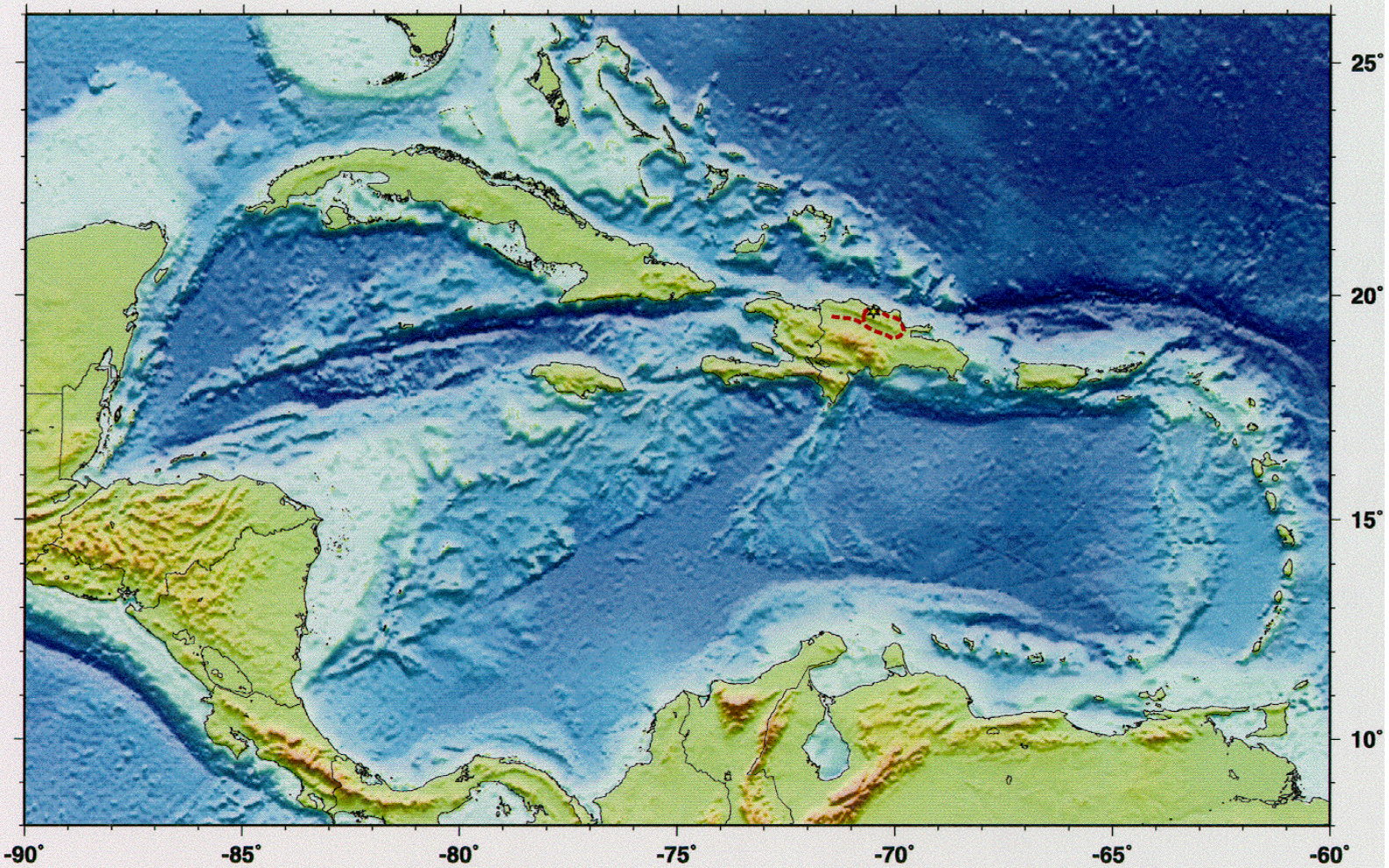

Figure 1. Predicted bathymetry of the Caribbean region based on GEOSAT gravity data from Smith and Sandwell, 1997, *Science*, 277:1956-1962. The star shows the location of Puerto Plata and the red line in the northern Dominican Republic shows route of Penrose field trip.

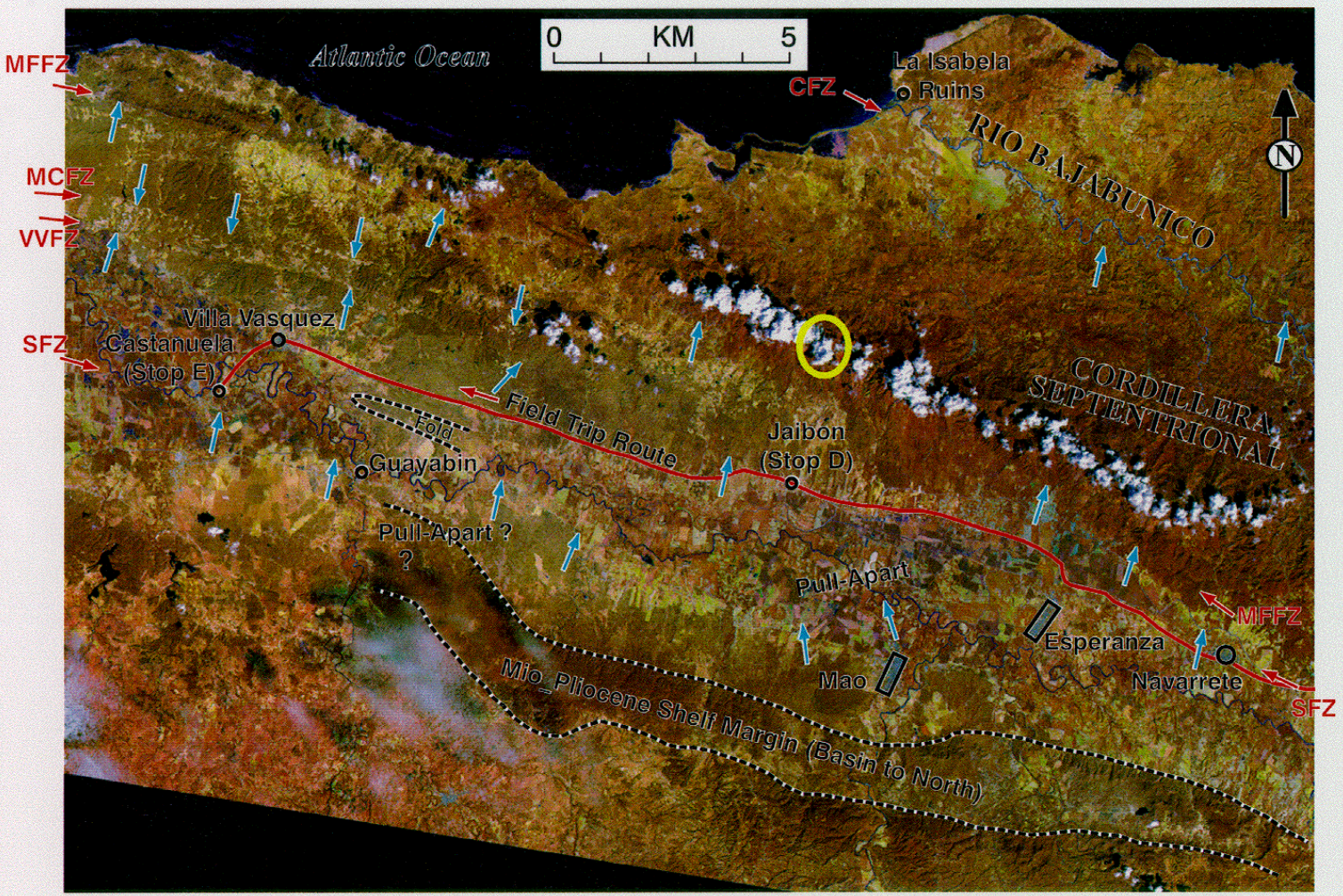

Figure 2. Landsat image showing main tectonic features and the route (red line) of the field trip for Day One in the west-central Cibao Valley. Blue arrows highlight major fault scarps. Yellow circle surrounds same clouds that appear on Figure 3 to determine overlap. Images in Figures 2-6 kindly produced by M. Rymer, USGS. Key to abbreviations: MFFZ = Mountain Front FZ; MCFZ = Monte Criste FZ; VVFZ = Villa Vasquez FZ; SFZ = Septentrional FZ; CFZ = Camu FZ

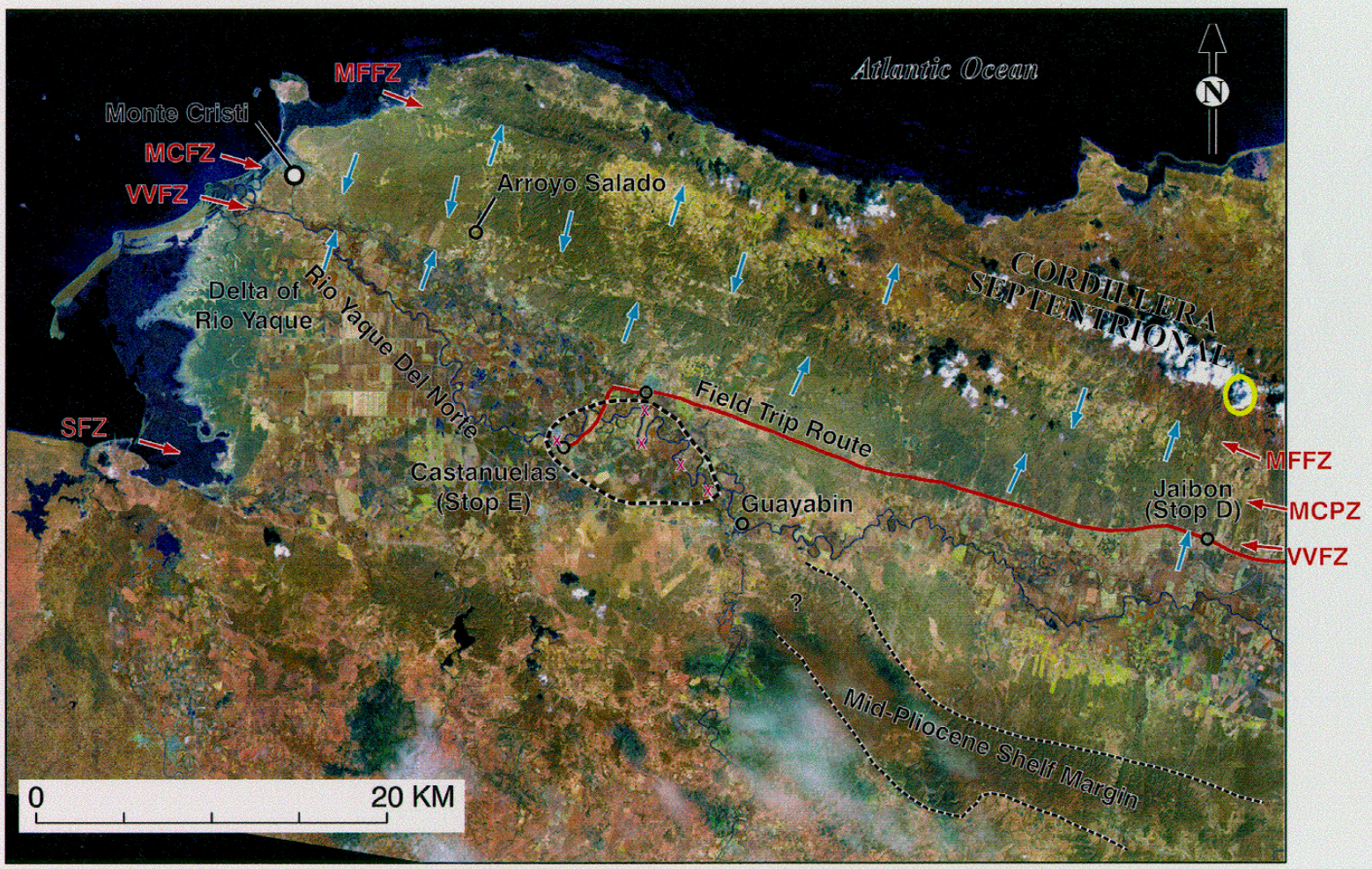

Figure 3. Landsat image showing main tectonic features and the route of the field trip for Day One in the western Cibao Valley. Yellow circle surrounds same clouds that appear on Figure 2 to determine overlap. Blue arrows highlight major fault scarps. Red X's in dashed, circled area are liquefaction sites of Tuttle et al. (this meeting). Key to abbreviations: MFFZ = M ntain Front FZ; MCFZ = Monte Criste FZ; VVFZ = Villa quez FZ; SFZ = Septentrional FZ; CFZ = Camu FZ

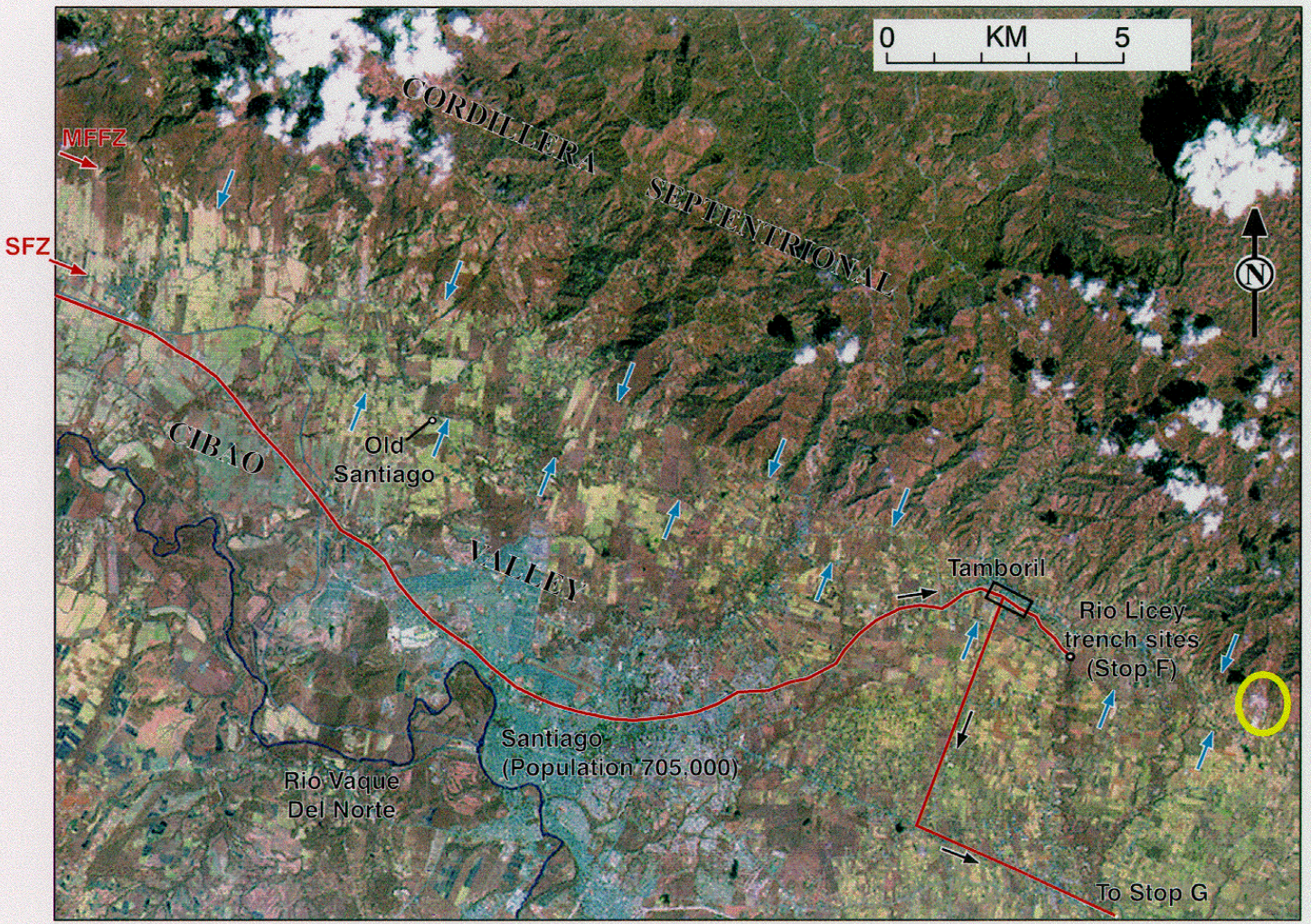

Figure 4. Landsat image showing main tectonic features and the route of the field trip in the Santiago area of the central Cibao Valley on day two. Yellow circle surrounds same clouds that appear on Figure 5 to determine overlap. Blue arrows highlight major fault scarps. Key to abbreviations: MFFZ = Mountain nt FZ; SFZ = Septentrional FZ.

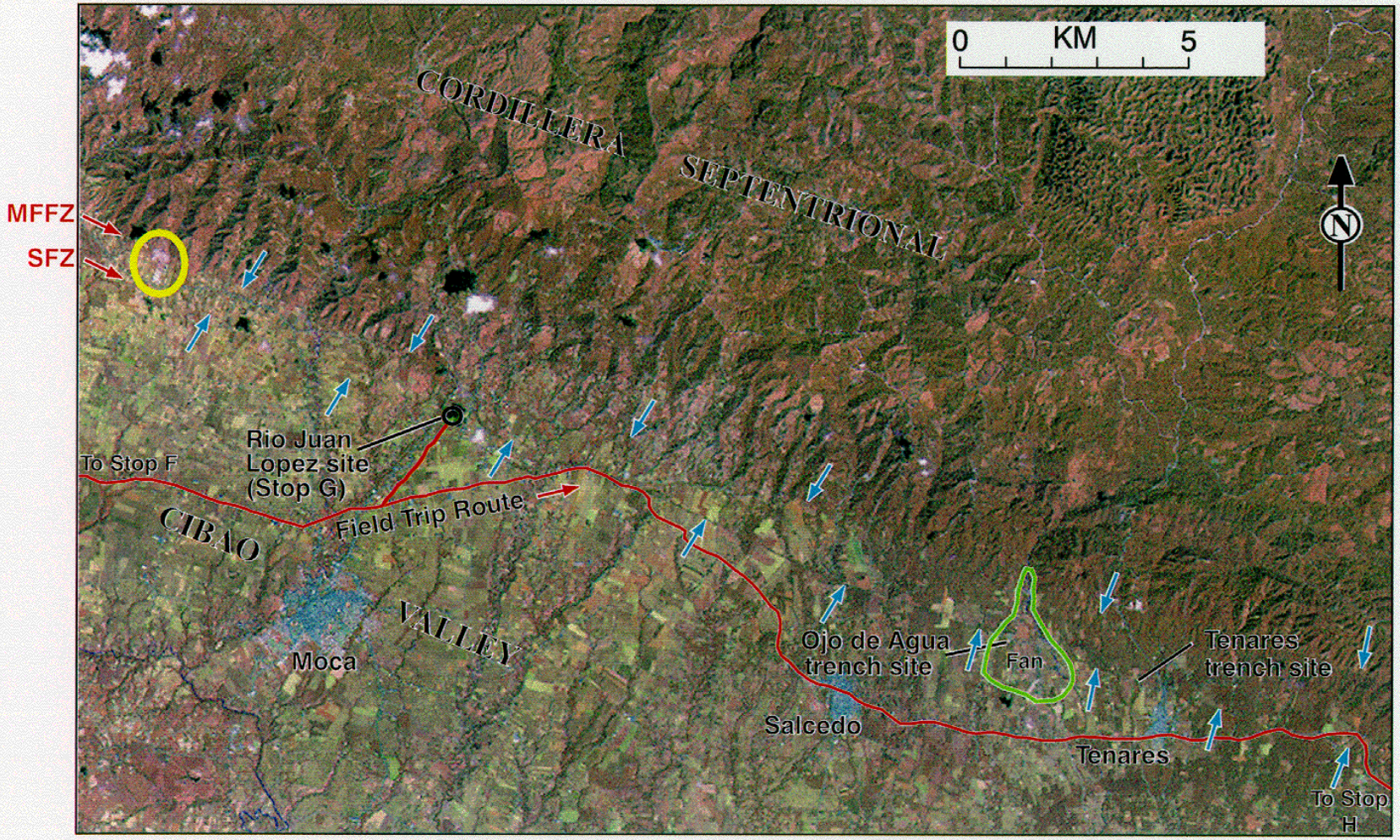

Figure 5. Landsat image showing main tectonic features and the route of the field trip in the Moca-Salcedo area of the east-central Cibao Valley on day two. Yellow circle surrounds same clouds that appear on Figure 4 to determine overlap. Blue arrows highlight main fault scarps. Key to abbreviations: MFFZ = Mountain Front FZ; SFZ = Septentrional FZ.

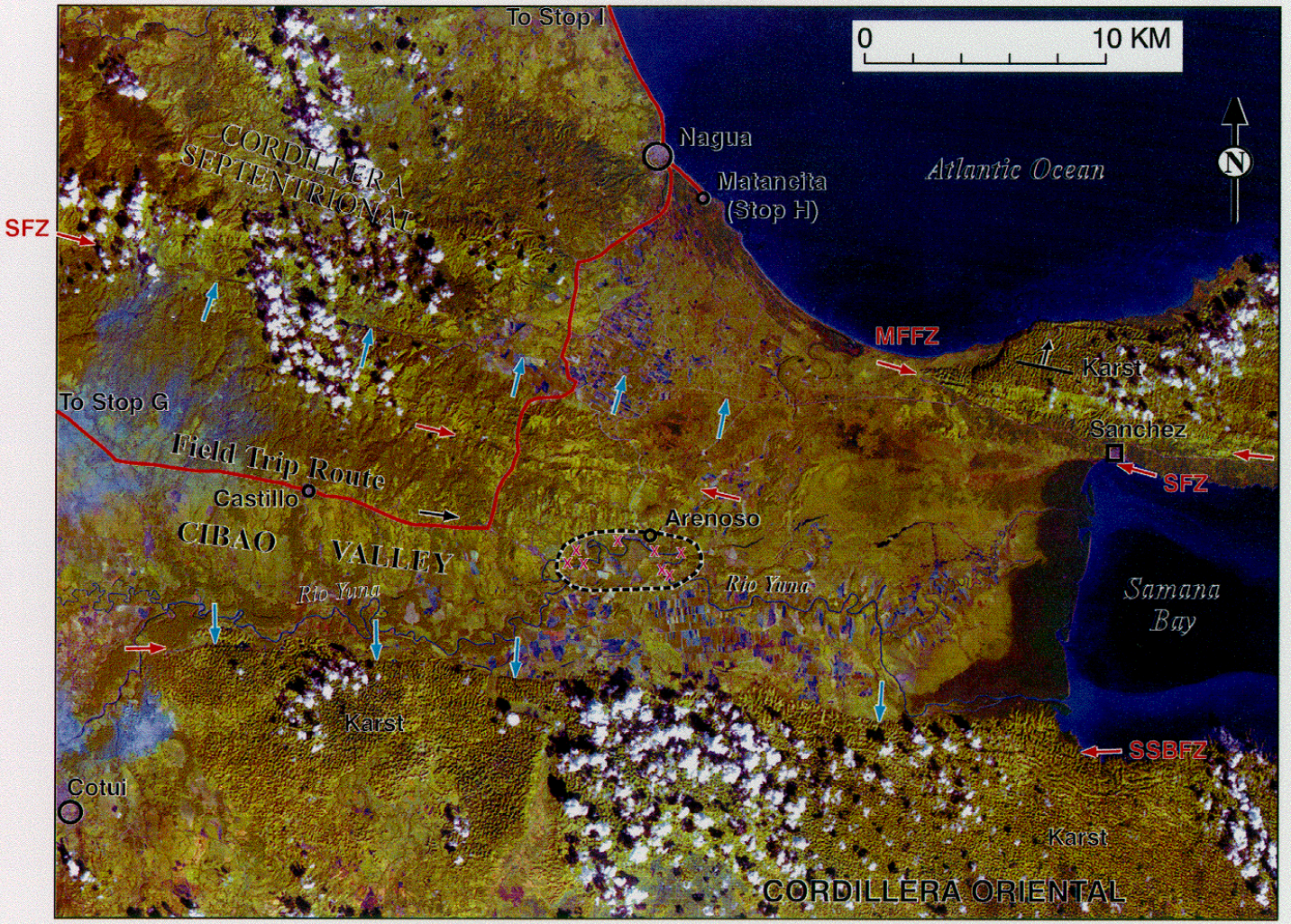

Figure 6. Landsat image showing main tectonic features and the route of the field trip in the eastern Cibao Valley. Blue arrows highlight major fault scarps. Red X's in dashed, circled area indicate liquefaction sites of Tuttle et al. (this meeting). Key to abbreviations: MFFZ = Mountain Front FZ; SSBFZ = Sou amana Bay FZ; SFZ = Septentrional FZ.

DAY ONE, STOP A: SERPENTINITES, NORTH COAST OF DOMINICAN REPUBLIC

LEADERS: JAMES PINDELL AND GRENVILLE DRAPER

LOCATION AND REGIONAL SETTING FOR STOPS A AND B

Stops A and B are located close together in the fault-bounded (10-30 km) "Puerto Plata Inlier" (PPI) that is flanked by the coastline to the north, the Camu Fault and Neogene carbonate rocks to the south, and Neogene carbonate rocks to the east and west (Fig. 1A). The PPI exposes rocks belonging to a Cretaceous-Eocene fore-arc or subduction complex (serpentinite-bearing Puerto Plata Basement Complex and the Imbert Formation) from beneath a Neogene carbonate cover (Villa Trina Formation; Fig. 1C). The linear, east-west striking Camu Fault bounding the PPI's south side is sinistral and stratigraphically north-side up at the PPI contact, which is confirmed by structures along the fault, but the Neogene carbonate rocks on the south flank of the fault sit morphologically higher (Cordillera Septentrional), suggesting relatively faster erosion rates within the PPI. Projecting northeastward from the Camu Fault and occurring within in PPI itself, the alluvial Maimon Valley separates two structurally distinct parts of the PPI (Fig. 1A). To the west of the Valley, the Basement Complex rocks form a morphologically mature landscape, whilst equivalent and other rocks to the east of the Valley comprise a relatively high relief, immature morphology (Fig. 1B).

We interpret this morphological difference to indicate recent/active diapirism of relatively buoyant/mobile lithologies/mélanges of the Puerto Plata Basement Complex east of the Maimon Valley (Fig. 1B). This is further suggested by the occurrence of the Franciscan-like San Marcos mud-diapir/flow unit which clearly extrudes and "flows" northward across all strata in the PPI from a portion of the trace of Camu fault which we believe was/is a conduit for mud diapirs (Pindell, 1985; Pindell and Draper, 1991). This diapirism, or faulting associated with it, has also disrupted the formerly continuous Neogene carbonate cover (Fig. 1C).

The isolated occurrence of Neogene carbonates of Pico Isabel, which rests on the Basement Complex, appears to have been tectonically dislocated from the Neogene carbonate section outside the PPI. The buoyant and highly mobile San Marcos unit (and several serpentinite bodies) fills the void created by this dislocation (Fig. 1B, C). Field relations prevent a clear understanding of the nature of that dislocation, **but we consider that a half graben (master E-dipping fault surfacing at Maimon Bay "graben"?) has formed along the north side of the sinistral Camu Fault (Fig. 1A, B).**

Although the San Marcos unit probably derives from the Cretaceous to Eocene subduction complex below (e.g., Nagle, 1974), it has also picked up knockers as young as Middle Miocene during diapirism and subsequent sub-horizontal gravitational flow (Pindell, 1985; Pindell and Draper, 1991) (Fig. 1C). The unit today maps as a Late Miocene-Pleistocene lobate, wedge-shaped deposit. This two-part history has caused confusion, namely that the San Marcos might represent a Miocene subduction mélange (e.g., Bourgois et al., 1982). Such an interpretation throws considerable discrepancy into regional models of Caribbean evolution.

GEOLOGIC HISTORY OF THE PUERTO PLATA INLIER

Lower Cretaceous-Eocene rocks comprise the Puerto Plata Basement Complex (PPBC) of the PPI (Pindell and Draper, 1991). The PPBC consists of dismembered, variably sheared masses of serpentinite, tectonized harzburgite, cumulate gabbroic rock, and mafic/intermediate volcanic rock which in at least one area is pillowed with red interpillow cherts (Fig. 1C). The PPBC is interpreted as remnants of an ophiolite. Montgomery et al. (1994a, b) claim that the inter-pillow cherts are non-Tethyan (Boreal). They propose that the ophiolite represents pieces of Caribbean forearc basement rather than obducted portions of [Tethyan] Proto-Caribbean Seaway subducted beneath the Greater Antilles arc.

The PPBC is overlain by two units of similar faunal age. One is the Paleocene-Early Eocene Imbert Formation consisting of off-white crystal tuffs, vari-colored cherts, and sandy

to pebbly turbiditic rocks (Fig. 1C). Coarse clastic beds are more common low in this formation, and contain sand and pebbles of serpentinite, volcanic and metamorphic rock, and limestone. The second unit overlying the PPBC consists of sedimentary serpentinite conglomerates and algal-limestone buildups or patch reefs of the ?early Paleogene shallow-water La Isla Formation (Fig. 1C). La Isla limestone buildups and serpentinite conglomerates contain fragments of one another, and corals were observed in growth attachment to serpentinite cobbles, indicating coeval, shallow-water deposition of the conglomerate and limestone. Imbert Formation is believed to be older than La Isla because it is more deformed and because Imbert deposition occurred in deeper water than La Isla deposition, possibly prior to or during uplift from forearc platform to photic water depths. The period of La Isla deposition and probably longer thereafter was a time of erosion across much of the PPI, leading to an angular unconformity between Imbert and younger units. The Eocene uplift and erosional hiatus is interpreted as recording convergence and collision between the Greater Antilles island arc and the Bahamas Bank.

In Late Eocene-Oligocene, shelf deposition is indicated by basal conglomerates and terrigenous, mica-bearing sands and marine shales of the Luperon Formation. Tectonism during this period was apparently minor, but a few conglomerates occur locally. Deformation and erosion (emergence?) occurred again in the Early Miocene, but deposition was renewed in the Middle to Late Miocene with the carbonate rocks (terrigenous input greatly reduced) of Villa Trina Formation. The Early Miocene uplift, deformation, and change in sedimentation may pertain to strike-slip separation of northern Hispaniola from southeastern Cuba along the Oriente Transform Fault (Pindell and Barrett, 1990).

Major regional uplift has occurred again since Pliocene, elevating Villa Trina Formation and its Pliocene reefal cap to several hundred meters throughout northern Hispaniola, and exposing ?Pleistocene reefal limestones/beachrock along coastal areas. This uplift is due to highly oblique convergence of Hispaniola with the easternmost Bahamas Bank by motion along the Oriente transform. Finally, since ?Pliocene and probably associated with the Pliocene-Recent uplift, the San Marcos mud unit carrying mm to 100 m sized blocks of all the above mentioned lithologies (and others) diapirically rose to the surface and flowed horizontally across areas of the Imbert, Luperon and Villa Trina Formations.

THE CAMU FAULT AND MAIMON VALLEY

The Camu Fault defines the PPI's southern limit. Fault gouge, breccias and steep dips are common in the fault zone, involving Neogene Villa Trina carbonates. Kinematic indicators show dominantly sinistral, strike-slip motion on the fault zone. No definitive strike-slip offset markers are known, but the PPBC can be correlated with similar rocks across the Camu to the east in Río San Juan Complex (see Stop I), possibly suggesting a 50-60 km displacement of late Neogene-Recent age. The Villa Trina Formation of the Septentrional is topographically higher than the PPI north of the Camu, but along the PPI's length the Camu juxtaposes older rocks to the north with younger rocks to the south. Thus, the Camu has a post-Miocene north side up component as well. The north side's relative uplift is in addition to the regional uplift of the Cordillera Septentrional. The fault's linearity for nearly 100 km suggests a steep dip near the surface. Thus, at the PPI the Camu Fault is likely a high angle, sinistral, up to the north fault of uncertain lateral displacement (but probably tens of kilometers), with post-Miocene (and possibly earlier) motion. Vertical displacement may be on the order of 300 m (thickness of Villa Trina flanking the PPI).

The Maimon Valley is also fault controlled, and has been interpreted as a graben in an E-W trending sinistral shear model (Mann et al., 1984). Vertical structural offset may be on the order of 200 m as indicated by present elevation differences of La Isla Limestone outcrops within vs to the west of Maimon Valley. Fault breccias occur along the valley's west flank and on the southward extension of the east flank. The east flank quite distinctly separates immature topography to the east, which we believe is diapirically generated, from more mature

morphological areas to the west. The Maimon Valley fault zone clearly defines the western limit of the most active tectonism in the PPI.

We suggest that the east flank of the valley is the hanging wall of a NE-trending half graben whose master fault dips E from the trace of Maimon Valley. Further, the diapirically-generated topography within this hanging wall may extrude along collapse faults within the hanging wall, thereby creating locally high, immature reliefs. We note that north of Imbert, and east of the west boundary fault of Maimon Valley, the Luperon and Imbert formations dip homoclinally west, possibly indicating rotation of the hanging wall of the half-graben.

DESCRIPTION

Stop A is a roadcut on the main highway at Cofresi west of Puerto Plata. The outcrop provides one of the best exposures of serpentinite within the PPI.

WORDS OF CAUTION! High speed truck and car traffic is present on this highway. Please do not attempt to cross to the outcrop on the opposite side of the highway and stay as far off the road as possible. If you are using a geologic hammer, please use protective eyewear.

Interpretation of the many serpentinite bodies in the Puerto Plata region is difficult because serpentinites occur in four different associations:
1) as coherent, fault bounded slices ("massive serpentinite" of Nagle, 1966) associated with pillow basalts in the Puerto Plata basement complex (PPBC),
2) as a brecciated serpentinite that outcrops in the area west of Maimon Bay,
3) as serpentinite debris flows in the Paleocene age Imbert Formation,
4) as blocks ("knockers") in the San Marcos unit.

It is possible that association 2) and 3) are the same.

We interpret the Cofresi body at this stop as being a massive serpentized peridotite that is part of the PPBC.

This outcrop of the PPBC serpentinite is massive and serpentization is 95-100%. Nagle (1966) considered that it was derived from harzburgites and dunites. Occasional inclusions of microdiorite and diabase can be found (one is exposed on the south side of the road about 0.5 km west of the Cofresi outcrop). Also present at this outcrop are dikes of white to green inclusions (possibly disrupted dikes) of rodingite (metasomatic rock of grossular garnet + calcic pyroxene ? epidote ? vesuvianite + other calcic minerals). If you have a rock hammer and geologic hammer, please share with a neighbor.

The association with pillow basalts suggests to us that the serpentinites represent a hydrated slice of sub-oceanic mantle peridotite, either incorporated into the accretionary complex of a Late Cretaceous, south dipping subduction zone, or representing the arc forearc basement. Non-Tethyan fauna from between the pillows suggests an origin related to the far-travelled arc basement.

REFERENCES

Bourgois, J., Vila, J-M., Llinas, R., and Tavares, I., 1982, Datos geologicos nuevos acerca de la region de Puerto Plata, (Republica Dominicana): in Transactions, Caribbean Geological Conference, 9th, Santo Domingo, Dominican Republic, p. 35-38.

Bowin, C., and Nagle, F., 1982, Igneous and metamorphic rocks of northern Dominican Republic: an uplifted subduction zone complex: in Transactions, Caribbean Geological Conference, 9th, Santo Domingo, Dominican Republic,, p. 39-50.

Mann, P., Burke, K., and Matumoto, T., 1984, Neotectonics of Hispaniola: plate motion, sedimentation, and seismicity at a restraining bend: Earth and Planetary Science Letters, v. 70, p. 311-324.

Montgomery, H. Pessagno, E. A., Jr., Lewis, J. A., and Schellekens, J. H., 1994a, Paleogeography of the Jurassic fragments in the Caribbean: Tectonics, v. 13, p. 725-732.

Montgomery, H., Pessagno, E. A., Jr., and Pindell, J. L., 1994b, A 195 Ma terrane in a 165 Ma ocean: Pacific origin of the Caribbean plate: GSA Today, v. 4, p. 1-6.
Nagle, F., 1966, Geology of the Puerto Plata area, Dominican Republic [Ph.D. thesis]: Princeton University, 171 p.
Nagle, F., 1974, Blueschist, eclogite, paired metamorphic belts, and the early tectonic history of Hispaniola: Geological Society of America Bulletin, v. 85, p. 1461-1466.
Nagle, F., 1979, Geology of the Puerto Plata area, Dominican Republic, in Hispaniola, tectonic focal point of the Caribbean; three tectonic studies in the Dominican Republic, Miami Geological Society, Miami, p. 1-28.
Pindell, J. L., 1985, Plate tectonic evolution of the Gulf of Mexico and Caribbean region [Ph.D Thesis]: Durham University, England, 287 p.
Pindell, J. L., and Barrett, S. F., 1990, Geologic evolution of the Caribbean region: A plate-tectonic perspective, in Dengo, G., and Case, J. E., eds., The Caribbean Region: Boulder, Colorado, Geological Society of America, The Geology of North America, v. H., p. 405-432.
Pindell, J., and Draper, G., 1991, Stratigraphy and geological history of the Puerto Plata area, northern Dominican Republic. in: Mann, P., Draper, G., and Lewis, J.F., eds., Geologic and tectonic development of the North America-Caribbean plate boundary in Hispaniola: Boulder, Co., GSA Special Paper 262, 97-114.

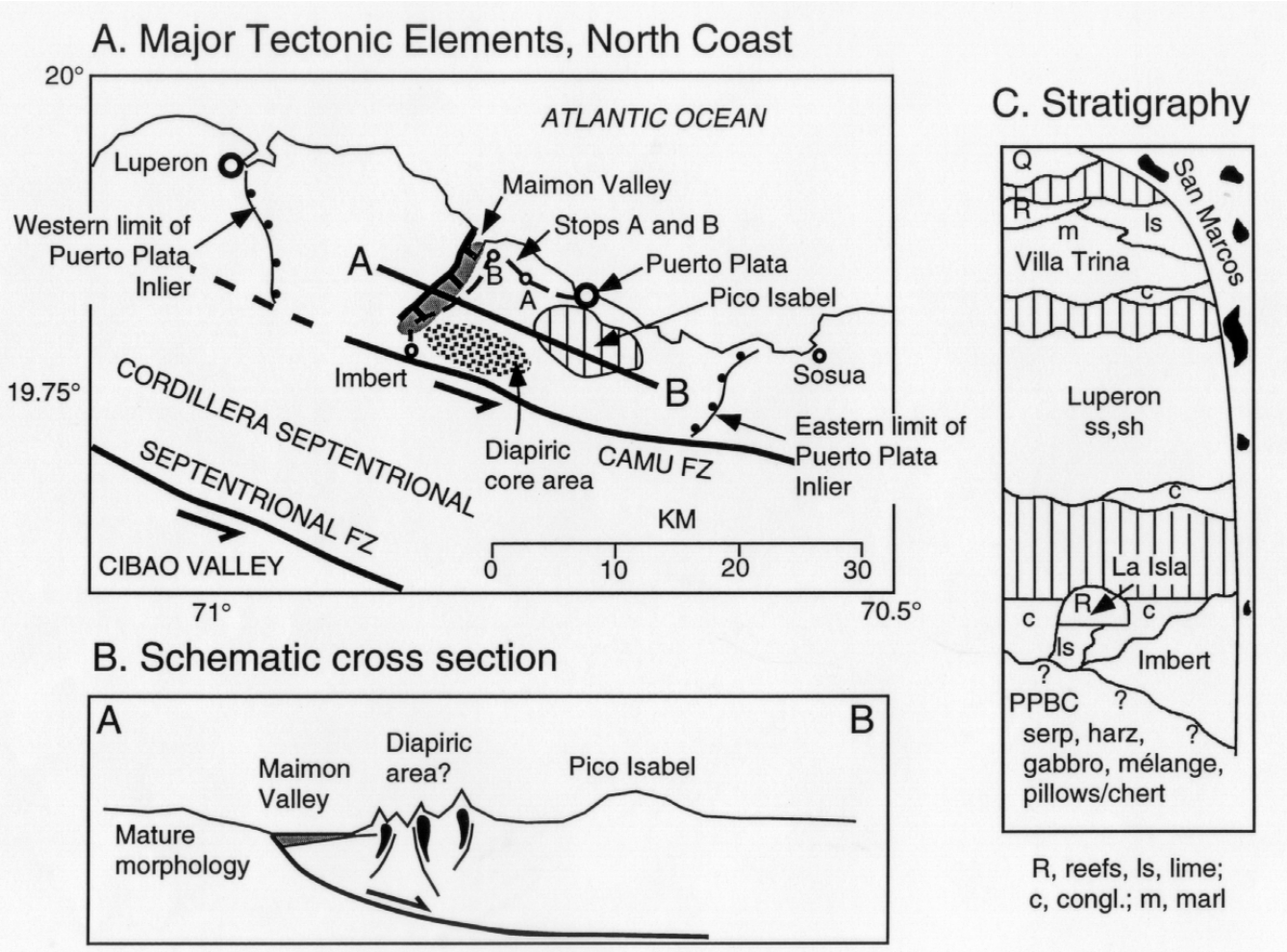

Figure 1. A. Major tectonic elements of the Puerto Plata area based on Pindell and Draper (1991) and location of Stops A and B on Day One. B. Schematic cross section. C. Stratigraphy of the Puerto Plata area based on Pindell and Draper (1991).

DAY ONE, STOP B: MIOCENE TO RECENT DIAPIR-FED MUDFLOWS, NORTH COAST OF DOMINICAN REPUBLIC

LEADERS: JAMES PINDELL AND GRENVILLE DRAPER

LOCATION AND REGIONAL SETTING

Stop B is within the San Marcos unit that is comprised blocks of various well-lithified rock-types chaotically contained within a non-lithified mud matrix with Eocene fauna (Nagle, 1979) (Fig. 1C of Stop A). The matrix is gray to brown, soft, non-lithified mud or argillite, with shear striations on freshly broken surfaces of any orientation. The blocks include all components of PPBC plus metamorphic rocks (marbles, greenschists, blueschists, amphibolites). Slabs of blueschist occur east and north of Imbert. Also, cream colored Villa Trina marls/limes are common in the San Marcos matrix, for which a Middle Miocene age was determined SW of Pico Isabela and elsewhere.

San Marcos unit occurs in two primary lobes projecting north from Camu Fault, one flanking Pico Isabela, the other northeast of Imbert (Fig. 1A of Stop A). A third area occurs 4 km north-northwest of Imbert. It is commonly associated with fractured, mobilized serpentinite. South of Pico Isabel around El Cupey, the unit is more than 300 m thick, but thins east, west, and north. South of El Cupey, the Camu River has eroded much San Marcos material, leaving an abrupt "wall" of exposed Villa Trina carbonate bounding the south side of the PPI.

The San Marcos unit is nowhere observed to lie between Imbert and Luperon Formations, as Nagle (1966; 1974) had suggested, nor beneath the Villa Trina Formation. In contrast, it overlies Luperon with angular unconformity, and appears in one area to overlie Villa Trina. At Pico Isabela, San Marcos surrounds, rather than underlies, the carbonate section. As defined by field relations, San Marcos unit is the youngest unit of the PPI except for Quaternary coastal and fluvial deposits (Fig. 1C of Stop A). The occurrence of Miocene carbonate in San Marcos indicates a post-Middle Miocene age for its emplacement or deposition, even though the matrix is dominantly composed of Eocene material (Nagle, 1966).

Production of San Marcos unit involved mixing of diverse types of lithified blocks in a pervasively sheared clay mud matrix. As possible modes of production, we consider (1) tectonic mélange formation during (a) the close of subduction in the Eocene (Bowin and Nagle, 1982) or (b) Miocene "tangential tectonics" (Bourgois et al., 1982); (2) sedimentary olistostromal deposition (Nagle, 1966); and (3) mud and serpentinite diapirism and extrusion with subsequent lateral flow. We disfavor a tectonically produced mélange of (1) Eocene age because San Marcos is younger than Eocene, and (2) Miocene age because Luperon Formation, which underlies the San Marcos unit, is very little deformed except near Neogene or active strike-slip faults. We disfavor Neogene olistostromal deposition for lack of a reasonable source area and of a sufficiently deep depocenter (judged from Villa Trina facies).

We conclude that mud diapirism and subsequent lateral flow (post-Miocene) is responsible for San Marcos unit as it maps out today. First, San Marcos muds are commonly associated with brecciated serpentinites, locally intruding as well as resting upon the serpentinites and other PPBC constituents. Second, diapirism provides a mechanism for emplacing San Marcos in shallow water and/or subaereal conditions. Third, diapirism and lateral flow explains the outwardly thinning lobate shapes of mapped occurrences of the San Marcos unit. Fourth, diapirism explains the pervasive shear stria, or slickensides, of the matrix. As for timing of diapirism, the Villa Trina shows no interstratification with or contamination by San Marcos, suggesting post-Villa Trina diapirism. We associate the diapirism with post-Miocene tectonism on Camu and Maimon fault systems, and regional uplift of the Cordillera Septentrional. We agree with Nagle (1966) based on his X-ray clay composition work that the source of the matrix is likely the tuffs of the Imbert Formation

plus the serpentinites of the PPBC; large volumes of these units may have been tectonically mixed during Eocene subduction and uplift. Thus, the Eocene San Marcos fauna (Nagle, 1966) are Imbert equivalent, but do not date the final emplacement of the unit. Components of the PPI's mappable stratigraphy and other minor lithologies (marble, greenschist, amphibolite, and blueschist) may have been incorporated into the mobile matrix either during subduction or during diapirism and lateral flow.

WORDS OF CAUTION AT STOP B! High speed truck and car traffic is present on this highway. Please do not attempt to cross to the outcrop on the opposite side of the highway and stay as far off the road as possible.

SIGNIFICANCE FOR FOREARC GEOLOGY

The ability of buoyant lithologies and mélanges to mobilize diapirically to the surface and, in so doing, to incorporate cover rocks that are far younger than the true age of subduction, is a process which must be considered when interpreting the period of subduction from the rock assemblages of subduction mélanges. Further, we should expect to see such reworking of buoyant materials especially in zones of highly oblique convergence, where the strike-slip component of motion often occurs at trench-parallel faults (such as Camu Fault) which can easily serve as migration conduits for buoyant materials from depth to the surface.

REFERENCES

Bourgois, J., Vila, J-M., Llinas, R., and Tavares, I., 1982, Datos geologicos nuevos acerca de la region de Puerto Plata, (Republica Dominicana): in Transactions, Caribbean Geological Conference, 9th, Santo Domingo, Dominican Republic, p. 35-38.

Bowin, C., and Nagle, F., 1982, Igneous and metamorphic rocks of northern Dominican Republic: an uplifted subduction zone complex: in Transactions, Caribbean Geological Conference, 9th, Santo Domingo, Dominican Republic,, p. 39-50.

Nagle, F., 1966, Geology of the Puerto Plata area, Dominican Republic [Ph.D. thesis]: Princeton University, 171 p.

Nagle, F., 1974, Blueschist, eclogite, paired metamorphic belts, and the early tectonic history of Hispaniola: Geological Society of America Bulletin, v. 85, p. 1461-1466.

Nagle, F., 1979, Geology of the Puerto Plata area, Dominican Republic, in Hispaniola, tectonic focal point of the Caribbean; three tectonic studies in the Dominican Republic, Miami Geological Society, Miami, p. 1-28.

Pindell, J. L., 1985, Plate tectonic evolution of the Gulf of Mexico and Caribbean region [Ph.D Thesis]: Durham University, England, 287 p.

Pindell, J., and Draper, G., 1991, Stratigraphy and geological history of the Puerto Plata area, northern Dominican Republic. in: Mann, P., Draper, G., and Lewis, J.F., eds., Geologic and tectonic development of the North America-Caribbean plate boundary in Hispaniola: Boulder, Co., GSA Special Paper 262, 97-114.

DAY ONE, STOP C: UPLIFTED TERTIARY SEDIMENTARY BASINS OF THE CORDILLERA SEPTENTRIONAL
LEADER: PAUL MANN

LOCATION

Stop C is located at the south end of a tunnel on the Puerto Plata-Santiago highway that passes under the 1000 m high topographic divide of the Cordillera Septentrional. We will park the busses on the shoulder after passing through the tunnel. Please spread out along the outcrop to examine marine sedimentary rocks rocks of the Eocene-Oligocene Altamira Formation.

WORDS OF CAUTION! High speed truck and car traffic is present on this highway. Please do not attempt to cross to the outcrop on the opposite side of the highway and stay as far off the road as possible. Please be careful of falling rocks and use protective eyewear while hammering.

SETTING

Regional tectonics. The Cordillera Septentrional ("Northern Range") forms an elongate, east-northeast-trending mountain range that rises to a maximum elevation of 1249 m (Fig. 1A, B). The range is partially bounded by seismically-active, strike-slip and reverse faults related to left-lateral displacement between the North America and Caribbean plates across Hispaniola (de Zoeten and Mann, 1991). Transpression across northern Hispaniola is probably a response to highly oblique subduction of the Bahama carbonate platform (Dolan et al., in press, STOP I).

The basement of the area can be divided into the Altamira block to the west and the La Toca block to the east separated by the left-lateral Rio Grande fault zone (Fig. 1B). Basement of the La Toca block in the eastern part of the study area consists of Upper Cretaceous to Eocene andesitic tuffs and tonalites of the Pedro García Formation (Fig. 1B). Basement of the Altamira block in the western part of study area consists of Upper Paleocene to Lower Eocene pelagic carbonate rocks of the Los Hidalgos Formation that are crosscut by dikes and sills of the Palma Picada intrusives (Fig. 1B).

Sedimentary cover. Well-dated, Upper Eocene to Lower Miocene deep-marine siliciclastic sedimentary rocks of the Altamira and Las Lavas Formations unconformably overlie arc-related basement of the Altamira block (Fig. 1B). These two formations together consist of about 4000 m of thin- to medium-bedded sandstone interbedded with conglomerate. About 1200 m of Oligocene to Lower Miocene siliciclastic sedimentary rocks of the La Toca Formation unconformably overlie, or are locally faulted against, igneous rocks of the Pedro García Formation.

Middle Miocene to Lower Pliocene shallow-marine limestone of the Villa Trina Formation forms the youngest sedimentary unit in the Cordillera Septentrional and is at least 250 m thick. The limestone exhibits both conformable and unconformable contacts with the underlying siliciclastic rocks of the La Toca and Altamira Formations, respectively. Dips in the Villa Trina Formation define a large, post-Early Pliocene anticline that coincides with the topographically highest part of the Cordillera Septentrional. The angular contact between the Villa Trina Formation and the underlying siliciclastic formations is generally found in the western and central Cordillera Septentrional whereas conformable or disconformable contacts are found in the eastern part of the range.

Regional structure. In our study area, ages of rock units indicate two large half-dome or anticlinal structures adjacent to the Septentrional and Rio Bajabonico fault zones (Fig. 2A, B) (de Zoeten and Mann, 1991). Tilting related to the Paradero half-dome along the Septentrional fault zone accounts for the northeast dips observed over much of the Altamira block. Folding related to the Pedro Garcia anticline accounts for the northeast

dips observed over much of the La Toca block. The Altamira fault zone abruptly truncates fold axes developed in the central part of the study area near Stop C.

Main tectonic phases affecting the Cordillera Septentrional. The main phases are summarized on the block diagrams and captions of Figure 3:

- Paleocene to middle Eocene phase records the termination of arc activity and uplift of arc basement rocks probably as the result of early interaction between the Hispaniola arc and the Bahama carbonate platform
- late Eocene to early Miocene phase marks the first major deposition of deep marine siliciclastics; and
- late Miocene to early Pliocene phase records simultaneous tectonic uplift of northern Hispaniola to near sea level and subsequent deposition of shallow marine limestones of the Villa Trina Formation.

DESCRIPTION OF THE CANADA BONITA MEMBER (ALTAMIRA FORMATION)

Terminology. In our stratigraphic and sedimentologic study of the Altamira, Las Lavas and La Toca Formations, we used the facies classification for deep-marine siliciclastic rocks that was developed by Pickering and others (1986). This classification, a modification of Mutti and Ricci Lucchi's (1978) lithofacies classification, facilitates facies descriptions and interpretations in the field. The Pickering and others (1986) classification is a comprehensive and purely descriptive scheme used to subdivide lithologies into mappable facies. Four of the seven facies classes proposed by Pickering and others (1986) were recognized in the central Cordillera Septentrional. The letter-number code shown in on the sections in Figure 4 is modified from Pickering and others (1986) was used for all measured sections done in the study.

Biostratigraphy. Ages of stratigraphic units are based on their fossil content (Fig. 1A). Reworked older fauna, however, are an inherent problem associated with resedimented turbidite deposits in the area and so the youngest ages were picked to represent the time of deposition.

Outcrop distribution and general stratigraphy. The Altamira Formation extends over a 200 km^2 area from the Rio Grande fault zone to a poorly defined western limit near El Mamey (Fig. 1A, B). The Altamira Formation consists of thin- to medium-bedded sandstone and siltstone couplets, with minor interbedded conglomerates and thick bedded sandstones. The Altamira Formation is divided into two members: 1) a 50-m-thick basal conglomerate, the Ranchete Member, which makes up a minor part of the total thickness of the Altamira Formation, and lies unconformably above rocks of the Los Hidalgos Formation, and the Palma Picada intrusions; and 2) the Canada Bonita Member, an approximately 2500-m-thick section of alternating sandstone and siltstone with interbedded conglomerate; this member composes most of the thickness of the Altamira Formation (Fig. 2B).

Sedimentary rocks of the Altamira Formation overlie the basal conglomerate of the Ranchete Member in an arcuate belt stretching 40 km across the center of the study area (Fig. 1A). This unit is here named the Canada Bonita Member of the Altamira Formation, after the village of Canada Bonita, 7 km north of Navarette. The Canada Bonita Member is composed of 80% very thin- to medium-bedded, sandstone and siltstone couplets (facies types: C2.2, C2.3, D2.2); 15% conglomerates (A1.1, A2.1), and 5% thick-bedded sandstones (B2.1, C2.1).

Sandstone and siltstone of the Canada Bonita Member are blue-gray, calcite-cemented, feldspathic litharenite, which weathers to an orange-tan color. The Bouma facies T_{de} of the sandstone and siltstone couplet of the Altamira Formation typically lack mud-sized particles. These upper divisions consist predominantly of coarse- to fine-grained silt with only minor clay.

Clasts in conglomerates of the Canada Bonita Member range in size from granules to boulders, but most commonly range in size from pebbles to cobbles. The clasts are equidimensional or oblate in shape, and subrounded to well rounded. In general, clasts are composed of: 1) recrystallized limestones (~60%), including biomicrites, dark-gray, green, and banded argillites, and carbonaceous silts derived from the underlying Los Hidalgos Formation; 2) plutonic porphyries (~20%); 3) bioclastic limestones (~10%); and 4) sandstones and volcanic fragments (~10%). The conglomerate matrix is a gray to light brown, fossiliferous volcaniclastic sand.

Age and paleobathymetry. Biostratigraphic analysis on 37 samples indicates that the Altamira Formation ranges in age from middle or upper Eocene to upper Oligocene (Fig. 1A). Ten samples from the lower part of the Altamira Formation exposed near El Mamey have been well dated as middle to upper Eocene using calcareous nannofossils and foraminifera. These dates constrain the upper age limit of the underlying Ranchete Member as upper Eocene. The lower age limit of the Ranchete Member is constrained by the lower Eocene age of the underlying Los Hidalgos Formation.

Several samples from the Canada Bonita Member collected along the Santiago-Puerto Plata highway suggest upper Eocene ages (Fig. 1A). However, Bourgois et al. (1982, 1983) and S. Monechi (pers. comm.) determined that three samples from beds stratigraphically below the upper Eocene sample localities contain distinct Oligocene faunas. No northwest-striking faults separating the sample localities along the Santiago-Puerto Plata highway were recognized. This suggests that upper Eocene calcareous nannofossils are reworked and that deposition of the Altamira Formation continued into late Oligocene time. Paleoenvironmental studies on the benthonic foraminiferal assemblage indicate upper bathyal water depths (150-500 m).

Measured sections. Five sections of the Altamira Formation were measured along or adjacent to the Santiago-Puerto Plata highway (Fig. 4A). The rocks are gently folded into an anticline-syncline pair. These measured sections all describe variations within a 1000-1500 m thick section of lateral equivalent rocks of the upper Canada Bonita Member of the Altamira Formation. The Calabaza measured section is separated from the Northern Canada Bonita and Southern Canada Bonita sections by the north-south striking Altamira fault zone (Fig. 4A).

Despite the structural complexity related to folding and the presence of the Altamira fault zone, there are many similarities between all five sections near the Santiago-Puerto Plata highway that allow the various sections to be correlated. For example, all three section are overlain by the basal conglomerate of the Las Lavas Formation and all three sections consist predominantly of thin- to medium-bedded sandstones and siltstones (C2.2, C2.3, D2.2) and associated conglomerates (A1.1, A2.1).

Thin-bedded sandstone and siltstone couplets of the Canada Bonita Member have a sand/silt ratio greater than 1:1, are tabular, laterally continuous for at least 10 m; exhibit sharp basal contacts, and are overlain by medium- to coarse-grained, structureless or poorly graded sand (T_{bd}, T_{abd}). Thin parallel laminae are very common throughout the lower division of beds. These laminae are defined by 0.5-4 mm biogenic carbonate grains composed mostly of red algae and benthonic foraminifera. The silty upper division of C2.2 and C2.3 sandstone and siltstone couplets contain isolated stringers of medium to coarse sand, are locally parallel laminated, and are commonly bioturbated by Skolithos, Planolites, and Glockeria.

The thick-bedded sandstones of the Canada Bonita Member have sand/silt ratios greater than 1:1 and exhibit erosional basal contacts with local load and groove casts. The lower division of beds are massive or coarse-tail graded and capped by parallel laminae which are defined by concentrations of coarser grained carbonate material (T_{bd},T_{abd}). Siltstones are commonly thin (3-10 cm), mud-poor, parallel-laminated, and occasionally show bioturbation by Skolithos and Glokeria. Beds are tabular and exhibit good lateral continuity at the outcrop scale.

No vertical cycles were recognized in the Canada Bonita Member, except for rare, thin (1-3 m) thickening-up cycles within rhythmically bedded, thin, sand/silt couplets. Two 2-7 m thick, thinning-upward intervals of C2.1-C2.3 facies are found 450 and 470 m above the base of the Guananico section. Both intervals are composed of lithic-rich calcarenites (T_{abd}). These are the only calciturbidites found in the Altamira Formation. Their lateral extent or geometry could not be determined.

Paleocurrents. Twenty-eight groove casts measured from the bottom of medium- to thick-bedded sandstones indicate a northwest to southeast (110°) mean paleocurrent trend. In the Guananico section, eight unimodal flute casts indicated paleoflow to the southeast. These paleocurrents were compiled in a regional study of early to mid-Tertiary basinal paleoflow in Hispaniola by Dolan et al. (1991).

Petrography. Framework modal data indicate that the siliciclastic rocks in the central Cordillera Septentrional range in composition from volcanicarenites to quartz-rich, lithic arkoses. Sandstones of the upper Eocene to upper Oligocene age Altamira Formation are characterized by: 1) abundant volcanic lithic fragments; 2) feldspars; 3) biogenic fragments; and 4) the absence of quartz.

REFERENCES

Bourgois, J., Blondeau, A., Feinberg, H., Glaçon, G., and Vila, J., 1983, The northern Caribbean plate boundary in Hispaniola: tectonics and stratigraphy of the Dominican Cordillera Septentrional, (Greater Antilles): Société Géologique de France Bulletin, v. 25, No. 1, p. 83-89

Bourgois, J., Vila, J. -M., and Tavares, I., 1982, Datos geológicos nuevos acerca de la región de Puerto Plata (Republica Dominicana): Caribbean Geological Conference, 9th, Santo Domingo, Dominican Republic, v. 2, p. 633-635

de Zoeten, R., and Mann, P., 1991, Structural geology and Cenozoic tectonic history of the central Cordillera Septentrional, Dominican Republic: in Mann, P., Draper, G., and Lewis, J., eds., Geologic and Tectonic Development of the North America-Caribbean Plate Boundary Zone in Hispanola: Geological Society of America Special Paper 262, p. 265-279.

de Zoeten, R., and Mann, P., Cenozoic El Mamey Group of northern Hispaniola: A sedimentary record of subduction, collisional and strike-slip events within the North America-Caribbean plate boundary zone, in Mann, P., ed., Caribbean Basins: Sedimentary Basins of the World (Series Editor: K. J. Hsu), Elsevier Science, Amsterdam, in press.

Dolan, J. F., Mann, P., de Zoeten, R., Heubeck, C., Shiroma, J. and Monechi, S., 1991, Sedimentologic, stratigraphic, and tectonic synthesis of Eocene-Miocene sedimentary basins, Hispaniola and Puerto Rico: in Mann, P., Draper, G., and Lewis, J., eds., Geologic and Tectonic Development of the North America-Caribbean Plate Boundary Zone in Hispanola: Geological Society of America Special Paper 262, p. 217-263.

Dolan, J., Mullins, H., and Wald, D., 1998, Active tectonics of the north-central Caribbean region: Oblique collision, strain partitioning and opposing slabs, in Dolan, J., and Mann, P., eds., Active strike-slip and collisional tectonics of the northern Caribbean plate boundary zone, Geological Society of America Special Paper 326, p. 1-61.

Mutti, E., and F. Ricci Lucchi, 1978, Turbidites of the northern Appennines: introduction to facies analysis (translation by T. H. Nilsen): International Geological Reviews, v. 20, p. 125-166.

Pickering, K., Stow, D., Watson, M., and Hiscott, R., 1986, Deep-water facies, processes and models: a review and classification scheme for modern and ancient sediments: Earth-Science Reviews, v. 23, p. 75-174.

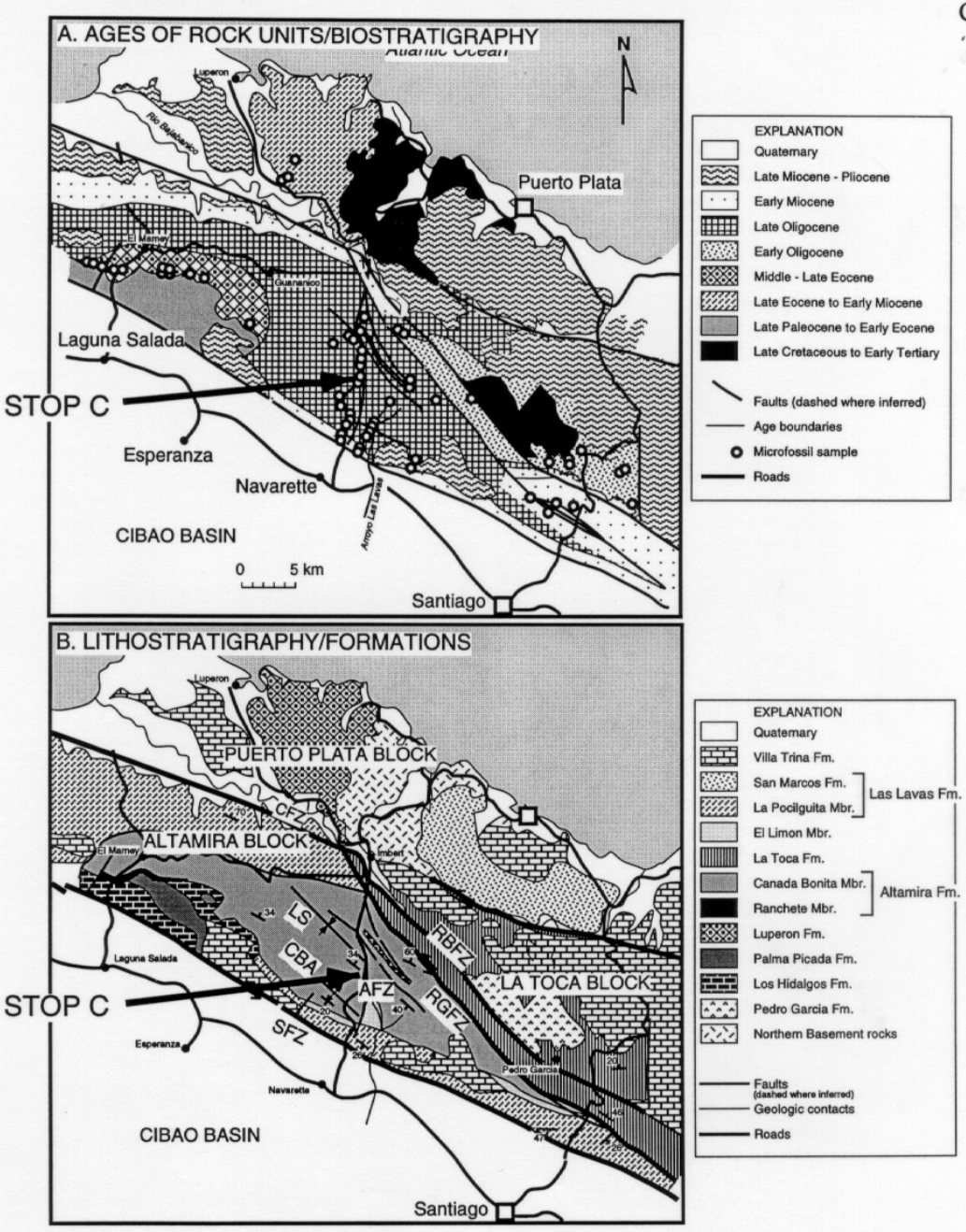

Figure 1. A. Map of the central Cordillera Septentrional showing the age of exposed rock units based on microfossils from 140 sample localities shown by open circles (from de Zoeten and Mann, in press). Contour lines approximate age boundaries and are constrained by both biostratigraphy and stratigraphic relationships. Microfossils used in this map include calcareous nannofossils, planktonic foraminifera, and benthonic foraminifera. This study used systematic biostratigraphy and detailed measured sections to better establish the character and age of lithologic units and correlate them across the central part of the mountain range. **B.** Map showing lithostratigraphy and formations of the central Cordillera Septentrional. The study area is limited to the area between the Septentrional Fault Zone (SFZ) and the Camu Fault Zone (CFZ), and is separated into the Altamira Block and the La Toca Block by the Rio Grande Fault Zone (RGFZ). Key to abbreviations: AFZ=Altamira Fault Zone; RBFZ= Rio Bajabonico Fault Zone; CBA= Canada Bonita Anticline; LS=Llanos Syncline.

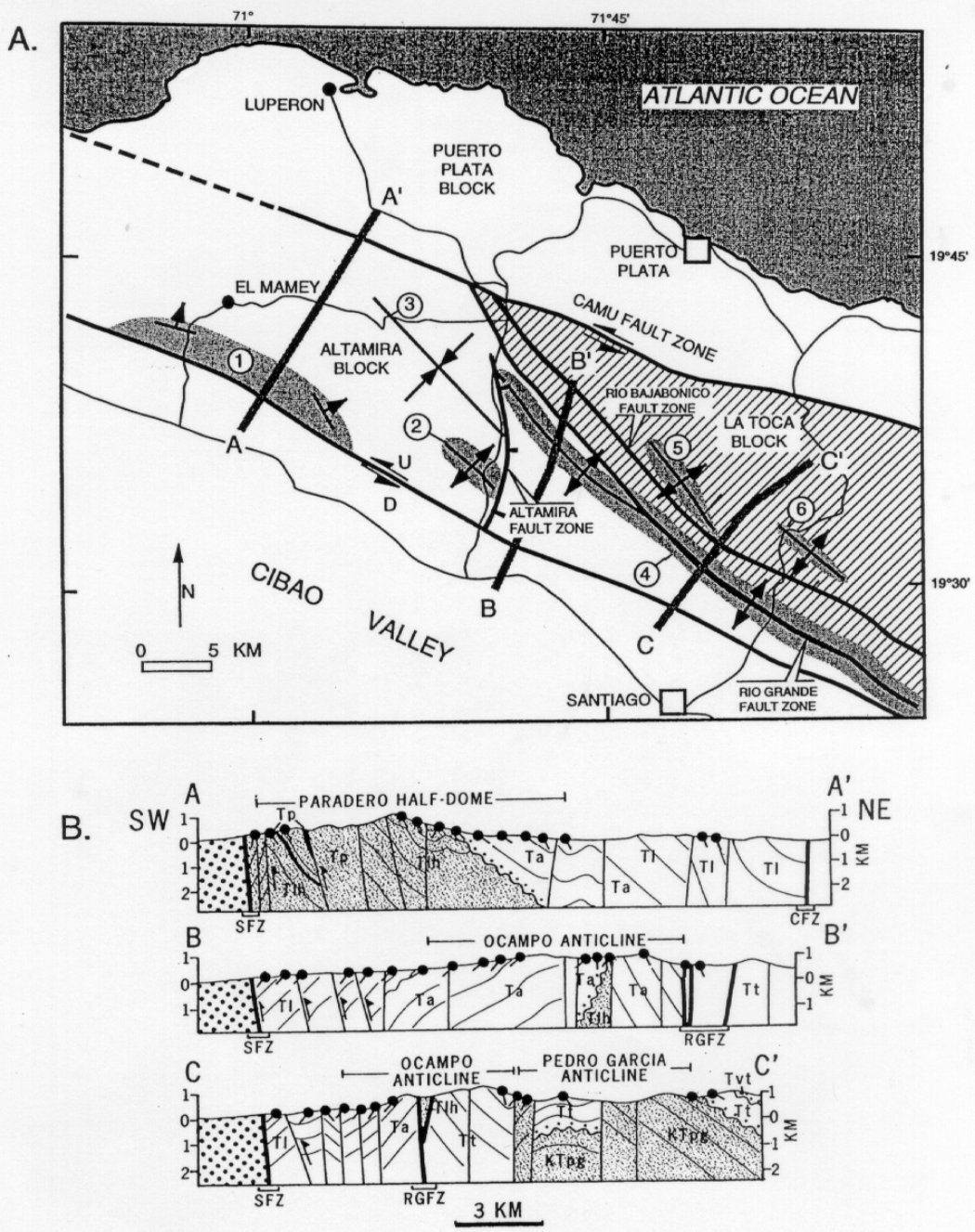

Figure 2. A. Major structural features of the central Cordillera Septentrional from de Zoeten and Mann (in press). Note the *en echelon* arrangement of major folds, which are shaded in gray. Key to numbered folds: 1, Paradero half-dome; 2, Canada Bonita syncline; 3, Llanos syncline; 4, Ocampo anticline; 5, Pedro García anticline; 6, Sonador anticline. Lines A-A', B-B', and C-C' indicate cross sections shown in B. B. One-to-one cross sections of the central Cordillera Septentrional. Key to rock units: KTpg = Pedro Garcia Formation (shaded); Tlh = Los Hidalgos Formation (shaded); Tp = Palma Picada intrusive rocks (shaded); Ta = Altamira Formation; Tt = La Toca Formation; Tl = Las Lavas Formation; Tvt = Villa Trina Formation. Dot pattern indicates Mio-Pliocene sedimentary rocks of the Cibao basin; wavy lines are unconformities. SFZ = Septentrional fault zone; RGFZ = Rio Grande fault zone; CFZ = Camu fault zone. Dip symbols represent the dip of beds measured in outcrop.

Figure 3. Block diagrams summarizing three main tectonic phases in the evolution of the North American-Caribbean plate boundary zone in northern Hispaniola from de Zoeten and Mann (in press).

Phase 1 is marked by Paleogene to early Eocene deposition of hemipelagic, fine grained turbidites (Los Hidalgos Formation=number 5) which are interbedded with arc-related dikes and sills of intermediate composition. Similar deep marine sediments are found to the north (Imbert Formation=number 4) and to the south (Magua Formation=number 6) of the study area and suggest a regionally extensive basin at least 40 km wide. The substrate of the Imbert Formation is a heterogeneous basement consisting of serpentinite, gabbros, volcanic rocks and blueschists (Puerto Plata Basement and and Rio San Juan Complexes=number 3), whereas the substrate of the Magua Formation is greenschist metamorphic rocks intruded by granodiorite plutons (Duarte Complex=number 7). Tuffaceous horizons are common in the Imbert, Los Hidalgos, and Magua Formations and suggest an active arc environment probably to the south along the Hispaniola segment of the volcanic arc. We interpret these geologic relationships in terms of a forearc basin developed above a south-dipping slab of subducted Atlantic ocean floor (number 2). Large-scale, middle Eocene folding and uplift will terminate this tectonic phase of deposition. This compressive event is related to attempted subduction of the Bahamas Platform (number 1) beneath the forearc area.

Phase 2 is marked by upper Eocene to lower Miocene deposition of several kilometers of siliciclastic turbidites (El Mamey Group=number 8; Tabera Group=number 9) in north-northwesterly striking elongate basins. Arrows indicate paleoflow directions based on paleocurrent studies in turbiditic rocks. Source areas for the Tabera Group include Lower Cretaceous metasedimentary rocks (Amina Schists=number 10) and volcanic arc rocks exposed to the east. Source area for the El Mamey Group include folded, hemipelagic rocks of the Los Hidalgos Formation to the south (number 5), the Puerto Plata Basement and Rio San Juan Complexes and Pedro Garcia Formation to the north (number 3). Regional uplift in middle Eocene time is attributed to the initial attempted subduction of the Bahamas Platform (number 1) beneath the Hispaniola arc and Oligocene to Miocene left lateral, strike-slip faulting along the Rio Grande Fault Zone (RGFZ) and the Septentrional Fault Zone (SFZ).

Phase 3 is marked by upper Miocene to lower Pliocene deposition of shallow water carbonate rocks (Villa Trina Formation=number 11). This limestone appears to have covered most of northern Hispaniola as shown by the wide distribution of its remnants. Late Pliocene to present uplift of the Cordillera Septentrional along the transpressional Septentrional Fault Zone has folded the Villa Trina Formation and uplifted it to an elevation of 1250 m. Uplift of the Cordillera Septentrional has accompanied subsidence of coeval rocks in the Cibao basin to depths greater than 3500 m below sea level (Yaque Group=number 12). Coeval sedimentary rocks along the northern edge of the Cordillera Septentrional appear unaffected by uplift concentrated along the Septentrional fault zone.

A. Phase 1: Paleocene to middle Eocene

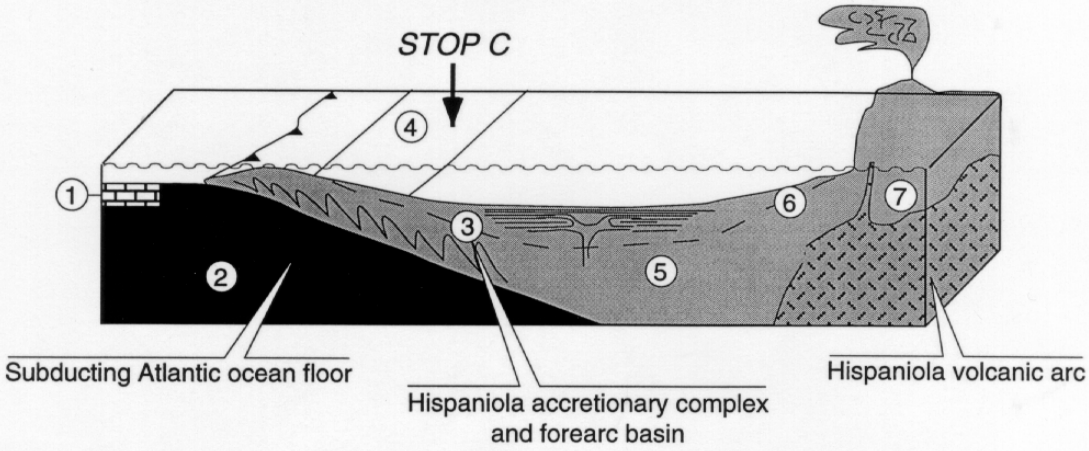

B. Phase 2: late Eocene to early Miocene

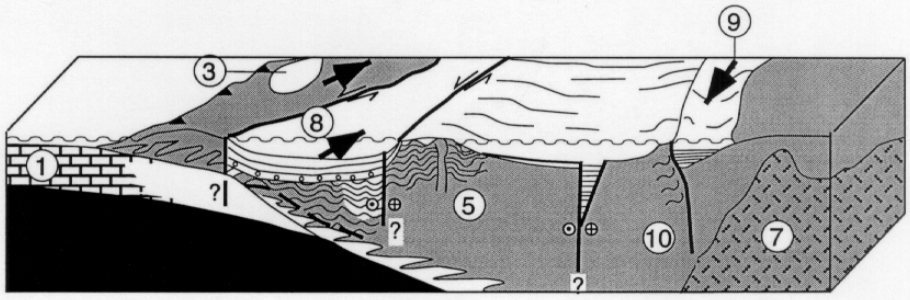

C. Phase 3: late Miocene to Recent

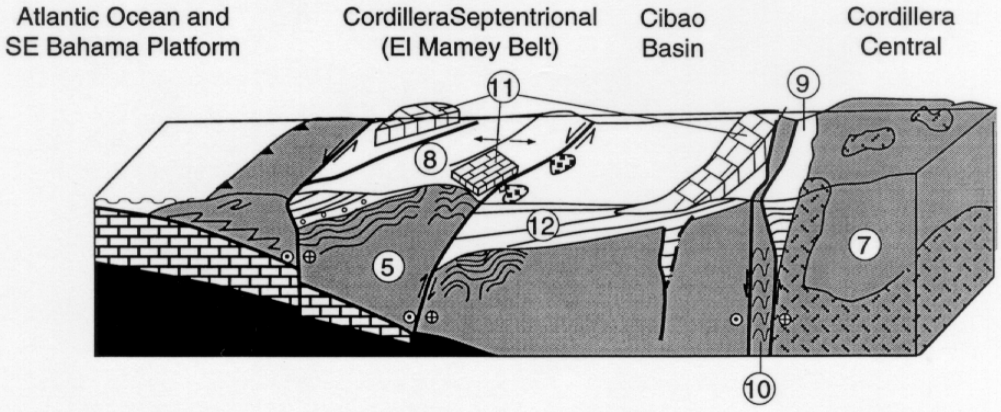

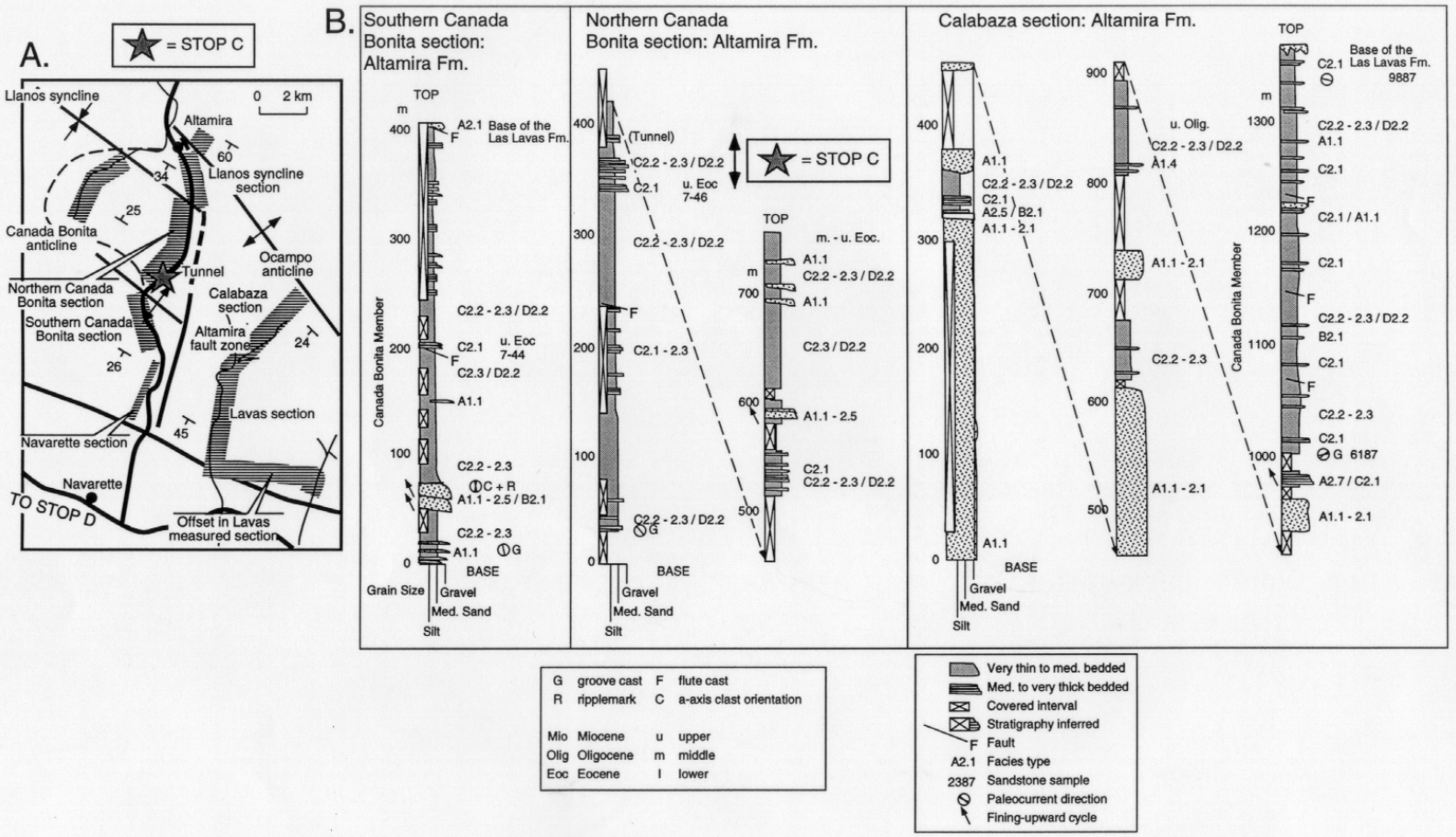

Figure 4. A. Inset map showing measured sections (heavy lines) and major structures in the area of Stop C from de Zoeten and Mann (in press). **B.** Measured sections of deep-marine siliciclastic facies from the southern Canada Bonita, northern Canada Bonita, and Calabaza sections. All sections illustrate lithologies from the upper Oligocene Canada Bonita Member of the Altamira Formation. The location of measured sections are shown in the inset map in A. Note that the Northern Canada Bonita section includes the outcrop at Stop C. The sections summarize facies types, paleocurrent indicators, biostratigraphic sample localities with age determinations, and sandstone sample localities used for point-count analyses. Letter codes of facies types have been been modified slightly from the global classification scheme of Pickering et al. (1986) to account for the common facies types of this study area.

DAY ONE, STOP D: FAULTED ALLUVIAL FAN AT THE JAIBON GRAVEL QUARRY, WEST-CENTRAL CIBAO VALLEY

LEADER: LUIS R. PENA

LOCATION:

This stop is located on the north flank of the Cibao Valley about half way between Navarrete and Castanuela (final Stop E for Day One). The highway in this area runs parallel to the distal edges of alluvial fans and pediment surfaces derived from the erosion of the Cordillera Septentrional located north of the highway. The Cibao Valley lies south of the highway and is dominated by late Quaternary fluvial sedimentation of the Rio Yaque del Norte which is draining the Cordillera Central, the range you can see on the skyline to the south. Immediately south of this stop is an abandonded channel of the Rio Yaque del Norte. The modern channel has shifted southward although the timing of this shift is not known. Its possible that the divergence of the two fault systems in this area has formed a large pull-apart basin in the central part of the valley. On the Landsat images in the introduction, we have attempted to outline some scarps that bound this pull-apart basin in the fluvial part of the valley.

Scarps are well preserved in exposures of Neogene sedimentary rocks along the northern flank of the valley. Scarps are less well exposed in the valley because of the large cultural overprint associated with canal building and intensive agroindustry and because of natural erosion associated with the meandering channels of the Rio Yaque del Sur.

At this stop, quarrying for gravel has exposed recent faults of the Villa Vasquez fault zone. Note on the Landsat image in the overview section that the lineament of the Villa Vasquez fault zone projects through this quarry.

WORDS OF CAUTION! Cactus is mixed in with the underbrush surrounding this site. Some types have long spines that can penetrate your pants and even the soles of shoes and light boots. It you are stuck, gently pull the spine straight out without breaking off tip. Check boots and pants for spines before sitting down!

SIGNIFICANCE:

In this area and to the east of this area, there is a major bifurcation in the western Septentrional fault system. The western Septentrional fault zone extends in a roughly east-west direction across the floor of the Cibao Valley and appears to exit the valley along the northwestern coast of Haiti where it has been mapped on the seafloor. The Villa Vasquez, maintains a more northwesterly strike and is the straight extension of the Septentrional fault zone of the central Cibao Valley. The Moutain Front fault also appears to continue as a straight feature to the northwest coast of the Domincan Republic. To the west of Stop D, the Villa Vasquez and Monte Criste faults appear to interact to form the large Villa Vasquez push-up block (see overview of Cibao Valley). The seaward extensions of the Villa Vasquez, Monte Criste and Moutain Front faults do not appear to be active on the seafloor.

This bifurcation area between the two faults forms a triangular shaped topographic low that I will point out to you as we travel westward from Navarette to this stop. The Septentrional fault is poorly expressed as a faint lineament in the fluvial sediments of the Cibao Valley about 2 km south of this stop (Fig. 1).

DESCRIPTION:

In the quarry walls, you can observe small offset faults with consistent northwest strikes averaging 121° that parallel the trend of the lineament seen on the Landsat image.

The width of the faulted zone is about 80 m. Measured dips on the faults range from 50° to 88° and offsets are apparently normal.

I suggest that you spread out through the quarry and visit the faults I have mapped and attempt to discover more faults on your own. You might also look for any evidence for horizontal offset on these fault surfaces since the Villa Vasquez fault is thought to be a left-lateral strike-slip fault based on the occurrence of a major push-up structure near Villa Vasquez (see Landsat images).

PROBLEMS:

We did not observe evidence for recent activity on the northern faults of the bifurcation (Mountain Front, Villa Vasquez, Monte Criste) in the area 30-50 km west of this stop (Mann et al., 1998). For example at Arroyo Salado on the Monte Cristi fault, a large late Quaternary fan is undisturbed above the fault zone.

The faults at this stop suggest that at least this eastern part of the Villa Vasquez fault may have been recently active. A problem is determining the age of the faulted fan sediments. If anyone sees material that could be dated, please leave in place and let me know. This age would place better constraints on the age of faulting and whether the northwestward continutation of the western Septentrional fault system remains active.

REFERENCE CITED:

Mann, P., Prentice, C. S., Burr, G., Peña, L. R., and Taylor, F. W., 1998, Tectonic geomorphology and paleoseismology of the Septentrional fault system, Dominican Republic: Geol. Soc. Am. Special Paper 326, p. 63-123.

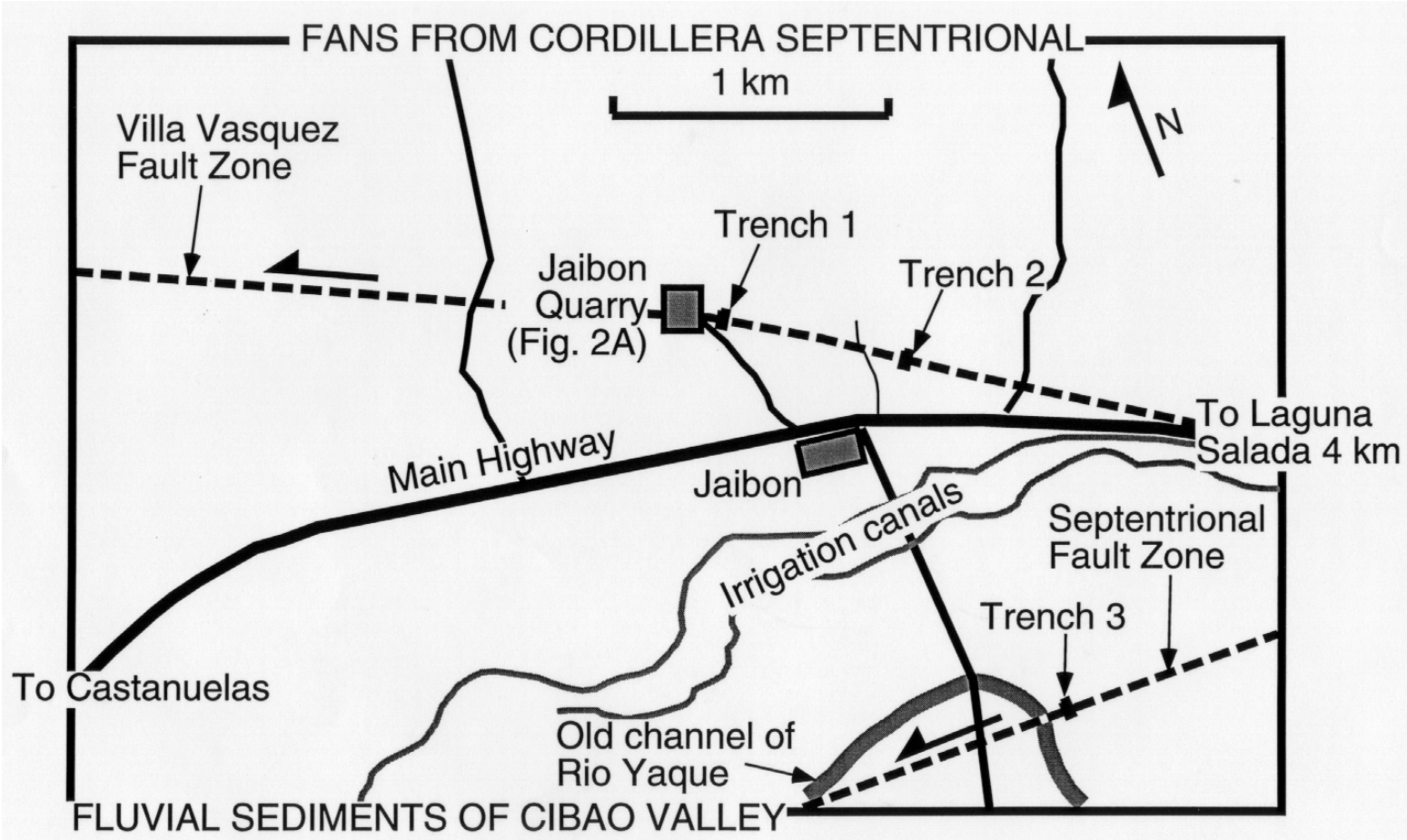

Figure 1. Map of divergent area between the Septentrional fault zone and the Villa Vasquez fault zone. The trace of the latter fault is visible on the Landsat image in the overview of the Cibao Valley. Stop D is in the Jaibon Quarry where recent faults can be seen cutting Quaternary alluvium. Results at trenches 1-3 will be reported on in the poster by Pena at this meeting.

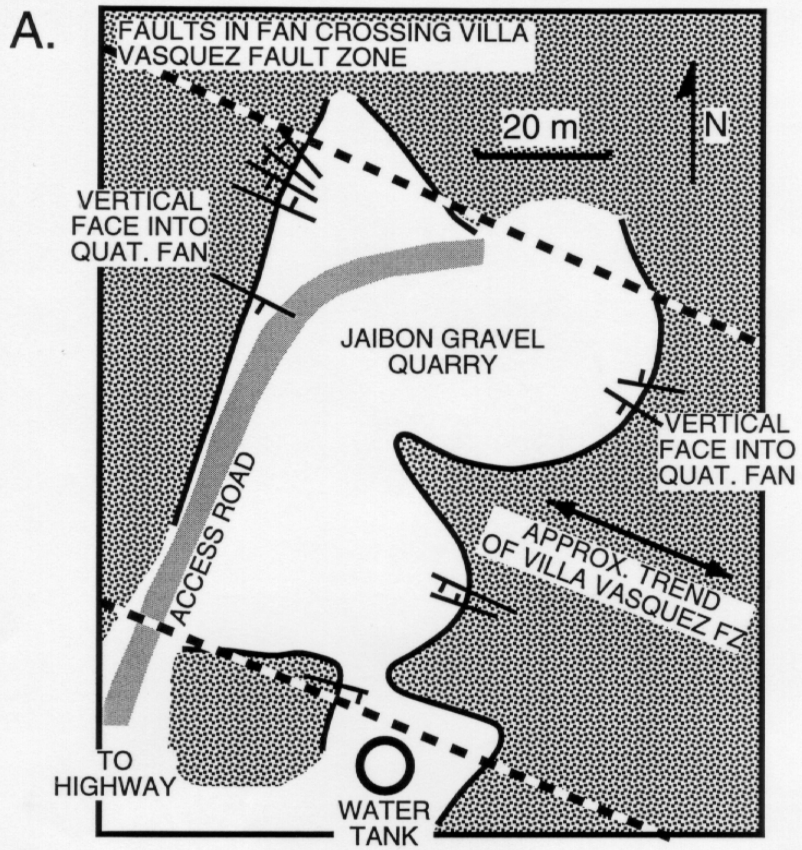

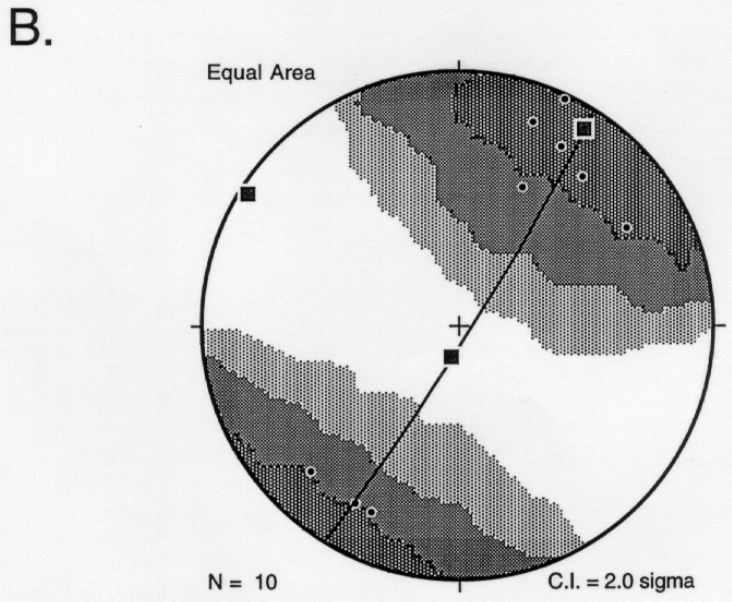

Figure 2. A. Map of small faults in Jaibon quarry with dips indicated. **B.** Equal area plot of poles to faults in quarry showing average strike of small faults in quarry (122°) which agrees well with the strike of the Villa Vasquez fault in this area.

DAY ONE, STOP E: EARTHQUAKE-INDUCED LIQUEFACTION FEATURES ALONG THE RIO YAQUE DEL NORTE, WESTERN CIBAO VALLEY

LEADERS: TISH TUTTLE, LUIS PENA, AND CAROL PRENTICE

LOCATION:

This stop is at liquefaction site,W7, exposed in a cutbank of the Rio Yaque del Norte east of the town of Castanuelas (see landsat image of western Cibao valley in field trip overview and Fig. E1). The site occurs 5 km north of the presumed westward extension of the active trace of the Septentrional fault zone along the southern edge of the Cibao valley and 8-10 km south of the Monte Cristi and Villa Vasquez faults along the northern edge of the valley (Mann et al., 1998; Pena, Penrose abstract). In the western Cibao valley, the Septentrional fault zone is thought to be buried by Holocene alluvial deposits.

Hopefully, the Rio Yaque will be low enough to allow access to the site and to expose sand blows, sand dikes, and the underlying sand deposit that liquefied. After we (in small groups) examine liquefaction features near the stairs, fan out along the cutbank and look for other occurrences. A few troughs and shovels will be available for those who wish to clean off and more closely observe features. Please look for pieces of wood, charcoal, and other datable material in the cutbank. If you find such material, do not remove it. Call one of the field trip leaders who will record its location prior to sampling.

WORDS OF CAUTION! River cutbanks can be unstable. For your safety and that of others, please do not walk close to the edge of the top of the cutbank. Also, do not dig beneath overhangs in the cutbank. We suggest that you avoid contact with river water and apply repellent if mosquitos are present. Several years ago, bee hives were kept in the field above the cutbank. Although the hives may have been removed, we suggest you stay away from this area.

SIGNIFICANCE:

The site at Castanuelas, W7, is one of seven liquefaction sites that we found during reconnaissance along the Rio Yaque between the villages of Guayubin and Castanuelas (landsat image of western Cibao valley in field trip overview and Fig. E1). Building on paleoseismic studies in the central Cibao valley (Prentice et al., 1993 and 1994), we conducted reconnaissance for liquefaction features along the Rio Yaque to extend our knowledge of the behavior of the Septentrional fault towards the west. For the same reason, we conducted reconnaissance along the Rio Yuna in the eastern Cibao valley (landsat image of eastern Cibao valley in field trip overview; see Penrose abstract and poster). Accounts of historic earthquakes gave us reason to think that liquefiable sediments occur along the Rio Yaque and the Rio Yuna. Scherer (1912) reported that springs and ground cracks formed along the Rio Yaque in the vicinity of Santiago (central Cibao valley) during the 1842 earthquake (Fig. E2). He also reported that cracks formed and the ground subsided near Guayubin (western Cibao valley) during the 1897 earthquake. Following the 1946 earthquakes, Lynch and Bodle (1948) reported that high silt banks along the Rio Yuna near Arenoso (eastern Cibao valley) settled in terraces paralleling the river and that sand and water spouts occurred up to 100 m from the river bank. These types of ground failure are often indicative of subsurface liquefaction. Because liquefaction often recurs where susceptible deposits are present, sites of historic liquefaction are prime targets for paleoliquefaction studies (Sims and Garvin, 1995; Tuttle and Seeber, 1991).

Most sand dikes that we found along the Rio Yaque are small to intermediate in size, ranging from 2 to 18 cm in width. Several of the sand dikes are coarse grained, including coarse sand and pebbles, at their bases and grade upwards to medium and fine sand (Fig. E3). Entrainment of pebbles by escaping water is suggestive of high flow velocities resulting from elevated pore-water

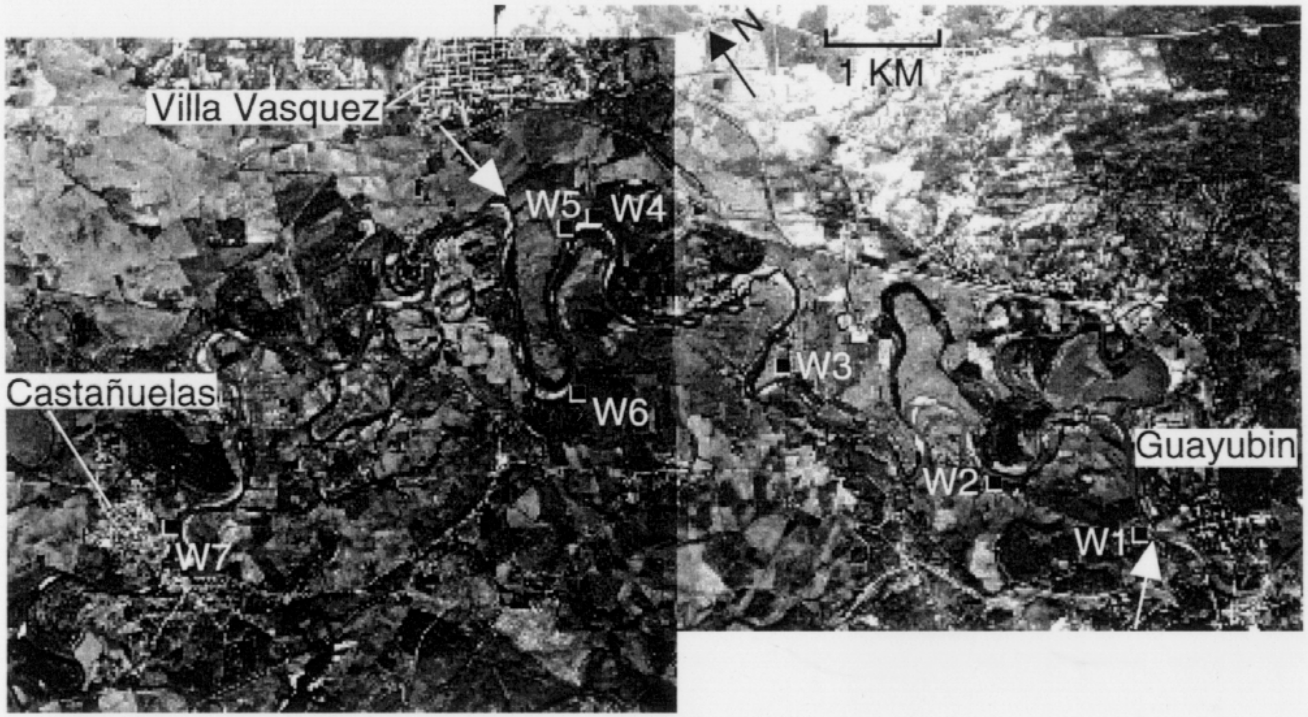

Figure E1. Aerial photographs showing locations of liquefaction sites along Rio Yaque del Norte (see landsat image of western Cibao valley in field trip overview for location). Large white arrows indicate limits of river reconnaissance (site W7 reached independently by car). Aerial photographs Roll 14 Strip 12, 11 January 84, no. 1823 and 1821, original scale 1:40,000.

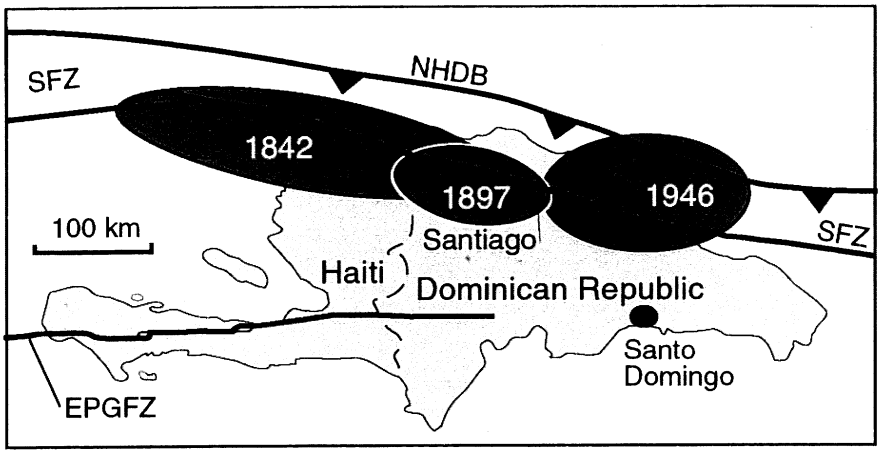

Figure E2. Map of Hispaniola showing regions of strong shaking associated with historic earthquakes that may have induced liquefaction (modified from Kelleher et al., 1973). SFZ = Septentrional fault zone; NHDB = North Hispaniola deformed belt; EPGFZ = Enriquillo-Plantain Garden fault zone; T = trench site in central Cibao valley that exposed liquefaction features associated with 1170-1230 A.D. earthquake (Prentice et al., 1994).

pressures. Sand dikes containing more than 20% pebbles are thought to form as the result of very large ($M \geq 7$) earthquakes (Valera et al., 1994). Sand blows may occur at several of the liquefaction sites but additional excavation is needed to verify this. At one liquefaction site (W1), we collected charcoal near the base of the cutbank from the silt deposit crosscut by sand dikes. The sample yielded a calibrated date of 4580-4000 B.C. and provides a maximum age of liquefaction features observed along the Rio Yaque.

At the Castanuelas site, W7, stratigraphic and structural relations of liquefaction features, including sand blows and sand dikes, indicate that two, possibly three, earthquakes have induced strong ground shaking and liquefaction at this site. Radiocarbon dating at another liquefaction site along the Rio Yaque suggests that these events occurred within the past 6,580 years. Although much work remains to estimate the timing, source areas, and magnitudes of earthquakes that induced liquefaction at this and other sites along the Rio Yaque and Rio Yuna (Tuttle et al., 1998), liquefaction features provide the opportunity to study prehistoric earthquakes in the eastern and western Cibao valley where the Septentrional fault is not available for direct evaluation. In addition, our findings of liquefaction features indicate that there is a potential for liquefaction and lateral spreading during future large earthquakes.

DESCRIPTION:

At the Castanuelas site,W7, liquefaction features, including two, possibly three, generations of sand blows and related feeder dikes, occur within a ~4 m section of silt deposits with multiple paleosols (Fig. E4). The first generation sand blow occurs low in the section (~3 m below the surface), is composed of medium to fine sand up to 6 cm thick, and is fed by at least three sand dikes that are up to 18 cm wide. This sand blow is crosscut by at least one sand dike. This dike, up to 42 cm wide, is a compound feature that appears to have been utilized during two or more episodes of liquefaction. The compound dike is composed of medium to fine sand containing large clasts of the host deposit and exhibits nearly vertical flow structure. The second generation sand blow occurs in the middle of the section (~2.4 m below the surface) and is up to 3 cm thick. A possible third generation sand blow occurs high in the section (~1.5 m below the surface), is composed of very fine sand containing a few small clasts, and is up to 6 cm thick. The sand blow appears to have been fed by a dike that occurs above the large compound dike. A crack, partially filled with sand, extends upward from the compound dike to the feeder dike at the base of the sand blow. The crack probably represents an eroded portion of the feeder dike. The upper sand blow is overlain by silt in which a soil has developed. The soil is in turn overlain by recent alluvium.

Given their cross cutting relations and stratigraphic positions, sand blows and related dikes formed during two, possible three, earthquakes separated in time. Despite sieving of samples of paleosols collected at this site, we found no material for radiocarbon dating, and thus, have not been able to constrain the minimum and maximum ages of these liquefaction features. The upper sand blow may have formed as a result of the1897 earthquake which was responsible for ground cracks and subsidence near Guayubin. Given their depths in the section, the lower sand blows probably formed during prehistoric earthquakes. Radiocarbon dating at another site (W1) along the Rio Yaque suggests that liquefaction features at W7 formed within the past 6,580 years.

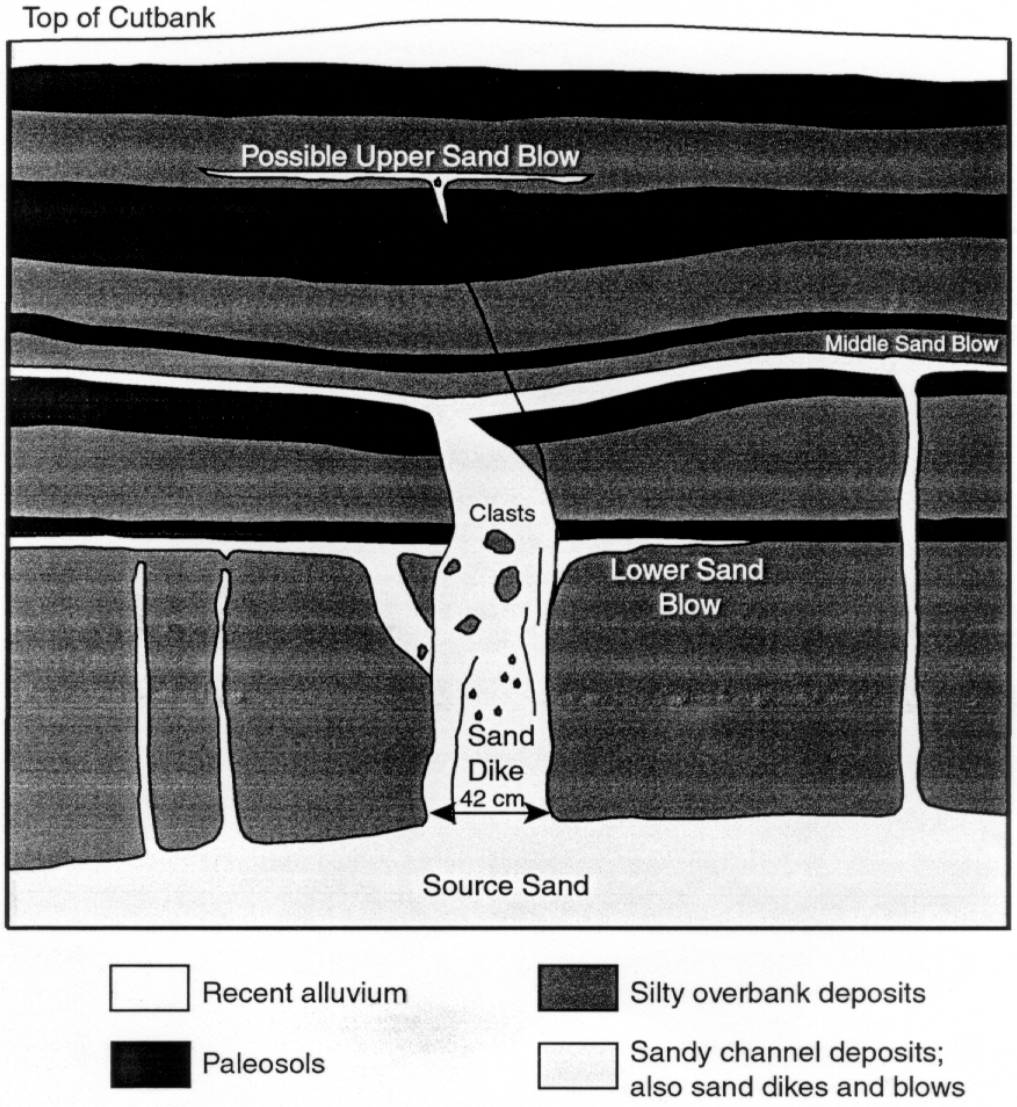

Figure E4. Sketch (not to scale) of liquefaction features exposed in river cutbank at W7. Stratigraphic positions and cross cutting relations of liquefaction features suggest two, possibly three, earthquakes large enough to induce liquefaction during Holocene.

REFERENCES CITED:

Lynch, J. J., and Bodle, R. R., 1948, The Dominican earthquake of August, 1946: Bull. Seismol. Soc. Am., v. 38, 1-17.

Kelleher, J., Sykes, L., and Oliver, J., 1973, Possible criteria for predicting locations and their applications to major tectonic boundaries of the Pacific and Caribbean: Journ. Geophys. Res., v. 78, p. 2547-2585.

Mann, P., Prentice, C. S., Burr, G., Pena, L. R., and Taylor, F. W., 1998, Tectonic geomorphology and paleoseismology of the Septentrional fault system, Dominican Republic: Geol. Soc. Am., Special Paper 326, p. 63-123.

Prentice, C. S., Mann, P., Taylor, F. W., Burr, G., and Valastro, S., Jr., 1993, Paleoseismicity of the North American-Caribbean plate boundary (Septentrional fault), Dominican Republic: Geology, v. 21, 49-52.

Prentice, C. S., Mann, P., Burr, G., and Pena, L. R., 1994, Timing and size of the most recent earthquake along the central Septentrional fault, Dominican Republic [abs.]: *in*, Prentice, et al., 1994, Proceedings of the Workshop on Paleoseismology: USGS Open-File Report 94-568, p. 158.

Scherer, J., 1912, Great earthquakes in the island of Haiti: Bull. Seismol. Soc. Am., v. 2, 161-180.

Sims, J. D., and Garvin, C. D., 1995, Recurrent liquefaction at Soda Lake, California, induced by the 1989 Loma Prieta earthquake, and 1990 and 1991 aftershocks: Implications for paleoseismicity studies: Bull. Seismol. Soc. Am., v. 85, p. 51-65.

Tuttle, M. P., and Seeber, L., 1991, Historic and prehistoric earthquake-induced liquefaction in Newbury, Massachusetts: Geology, v. 19, p. 594-597.

Tuttle, M. P., Schweig, E. S., III, and Sims, J. D., 1998, The use of liquefaction features in paleoseismology: *in* Active faulting and Paleoseismology, Abstracts, European Centre for Geodynamics and Seismology, p. 159-161.

Valera, J. E., Traubenik, M. L., Egan, J. A., and Kaneshiro, J. Y., 1994, A practical perspective on liquefaction of gravels: *in* Prakash, S., and Dakoulas, eds., Ground failures under seismic conditions: American Society of Civil Engineering, Geotechnical Special Publication 44, p. 241-257.

DAY 2, STOP F: RIO LICEY PALEOSEISMIC SITE, SEPTENTRIONAL FAULT, CENTRAL CIBAO VALLEY

LEADERS: CAROL PRENTICE, PAUL MANN, LUIS PEÑA, AND G. BURR

LOCATION

The Rio Licey paleoseismic site is located about 10 km ENE of Santiago, and includes the flood plain and river terraces traversed by the Septentrional fault immediately east of Rio Licey. Coordinates of the site are: 19°28'00" N, 70°35'40" W, and it is located on the Santiago 1:50,000 topographic map, kilometer-grid 53-54 N, 32-33E. Access can be gained on foot either from the road through La Ermita, or from the road between Tamboril and Canca La Piedra. This property is under private ownership.

SIGNIFICANCE

This site is one of four paleoseismic sites that we have studied along the Septentrional fault zone (SFZ) in the central Cibao Valley (Figure F-1). The SFZ is the major strike-slip fault associated with the North American-Caribbean plate boundary at the longitude of the Dominican Republic, and recent GPS data suggest that the rate of motion across the entire plate boundary is about 21 mm/yr (Dixon et al., 1998) (Figure F-2). Dixon et al. (1998) use their geodetic data to model slip rates across the faults in Hispaniola, and suggest a rate of 8±3 mm/yr across the SFZ. The Rio Licey site is one of two localities where we have estimated Holocene slip rates across the SFZ. Both are consistent with the GPS model. Combined with paleoseismic data suggesting that the most recent large earthquake along the SFZ occurred about 800 years ago, the high slip rates suggested by both the geologic and geodetic data imply significant accumulated strain across the SFZ that is currently available for release during a large earthquake.

Paleoseismic excavations and detailed surveying of the Rio Licey site have yielded a maximum estimate of the fault slip rate and dates of prehistoric earthquakes along the Septentrional fault. A fluvial terrace riser is offset a maximum of about 60 meters (Figure F-3); radiocarbon analysis of a charcoal sample collected from fluvial sediments underlying the terrace suggest that the terrace was abandoned 4860-5360 years BP, allowing calculation of a maximum slip rate of 11-12 mm/yr.

We collected data constraining the ages of two pre-historic earthquakes, the penultimate and the most recent events, from two excavations at this site. Relations exposed in trench RL2 suggest that the penultimate event occurred after 30 AD (Figure F-4). Results from the study of trench RL3 suggest the most recent event occurred between 780-1640 AD (Figure F-5). This is consistent with data from other sites suggesting the most recent earthquake occurred between 1150 and 1230 AD (Figure F-6) (Prentice et al., 1993; 1994).

DESCRIPTION

Aerial photographs show terraces associated with Rio Licey traversed by the SFZ (Figure F-7). The higher terraces, labeled Terrace 2 and Terrace 3 on Figure F-3, are separated by a north-facing fault scarp, approximately 8 m in height, and may be offset remnants of the same fluvial terrace. Between T2 and T1 is a south-facing fault scarp, 3-4 m high (Figure F-3). This apparent change in the sense of vertical displacement is due to strike-slip offset. The younger, lower Terrace 1 has been left-laterally juxtaposed against the higher, older Terrace 2, causing a south-facing scarp, though the vertical component of offset is up on the south side along this part of the SFZ (Mann et al., 1997).

The riser between Terrace 3 and Terrace 1 is very prominent south of the SFZ (Figure F-3), and trends nearly perpendicular to the fault. We correlate this riser with the riser between Terraces 1 and 2, north of the fault, and suggest that it has been offset no more than about 60 m. This is a maximum estimate for the amount of offset because some part of the 60-m separation could be the result of a bend in the initial course of the riser. Our projection of the riser to the fault is shown in Figure F-3, and gives a maximum amount the terrace riser has been offset since the time Terrace 1 was abandoned. Radiocarbon analysis of charcoal collected from fluvial sediments underlying Terrace 1 exposed in trench RL2 (Figure F-4) provides an estimate for the time the terrace was abandoned. The 2-sigma calibrated age range is 4860-5260 years BP, giving a maximum slip-rate estimate of 11-12 mm/yr. An earlier study of this site, reported in Mann et al. (1997) used less well constrained age and offset data to estimate a maximum slip rate of 23±7 mm/yr. While the two studies are not contradictory (both provide maximum slip rates) our new data presented here provide better constraints on the maximum slip rate. In particular, the new radiocarbon date is more reliable.

Trench RL2 (Figure F-8a) shows evidence for the penultimate earthquake along the Septentrional fault. We interpret unit 100 (Figure F-4) to represent a colluvial wedge that formed as a result of an earthquake. This unit has in turn been faulted, indicating the occurrence of a later earthquake. We interpret unit 110, a paleosol, as having been the ground surface at the time of the penultimate earthquake. A radiocarbon sample collected from this unit gives a date of AD 30-240, suggesting the penultimate event occurred after AD 30, or within the last approximately 2000 years.

Trench RL3 (Figure 8b) shows evidence for the most recent earthquake. Units 55 and younger are undeformed; sediments older than unit 55 have been folded into an anticline. Radiocarbon dating suggests the most recent earthquake occurred after deposition of a charcoal sample with a date of 780-1220 AD, and before deposition of a charcoal sample with a date of 1430-1640 AD. The earthquake, therefore, occurred between 780 AD and 1640 AD. This is consistent with results from the Ojo de Agua site that show the most recent earthquake occurred between 1150 and 1230 AD (Figure F-6) (Prentice et al., 1993; 1994).

Of the paleoseismic data collected for the Septentrional fault at our four sites, the best-constrained result is that the most recent earthquake occurred prior to 1230 AD. This result is constrained by clear stratigraphic relations at several sites, and by multiple radiocarbon analyses. The maximum age for this event, 1150 AD, is less well constrained. It is based on a single radiocarbon analysis, from one of the trenches at Ojo de Agua, and the stratigraphic relations indicating the sample is older than the earthquake are somewhat ambiguous. The age of the penultimate earthquake is also poorly constrained. Although it has been identified in several excavations (at the Rio Juan Lopez site and at the Tenares site) it is constrained to post 30 AD by only a single radiocarbon date, and the stratigraphic relations suggesting this sample is older than the earthquake are also somewhat ambiguous. More paleoseismic work is needed to better understand the Holocene behavior of the SFZ and the hazard this fault poses to the Dominican Republic and Puerto Rico. However, the work done so far strongly indicates that this fault has accumulated substantial strain in the more than 800 years since it last ruptured, and must be taken seriously as a likely candidate to produce a significant earthquake in the Cibao Valley.

REFERENCES

Dixon, T. H., Farina, F., DeMets, C, Jansma, P., Mann, P., and Calais, E., 1998, Relative motion between the Caribbean and North American plates and related boundary zone deformation from a decade of GPS observations: Journal of Geophysical Research, v. 103, p. 15,157-15,182.

Mann, P., Prentice, C. S., Burr, G., Peña, L. R., and Taylor, F. W., 1998, Tectonic geomorphology and paleoseismology of the Septentrional fault system, Dominican Republic, in: Dolan, J. F., and Mann, P., eds., Active strike-slip and collisional tectonics of the northern Caribbean plate boundary zone: Boulder, Colorado, Geological Society of America Special Paper 326, 174 p.

Prentice, C. S., Mann, P., Taylor, F. W., Burr, G., and Valastro, S., Jr., 1993, Paleoseismicity of the North America-Caribbean plate boundary (Septentrional fault), Dominican Republic: Geology, v. 21, p. 49-52.

Prentice, C. S., Mann, P., Burr, G., and Peña, L. R., 1994, Timing and size of the most recent earthquake along the central Septentrional Fault, Dominican Republic [abs.]: in: Prentice, et al., 1994, ed., Proceedings of the workshop on paleoseismology: USGS Open-File Report 94-568, p. 158.

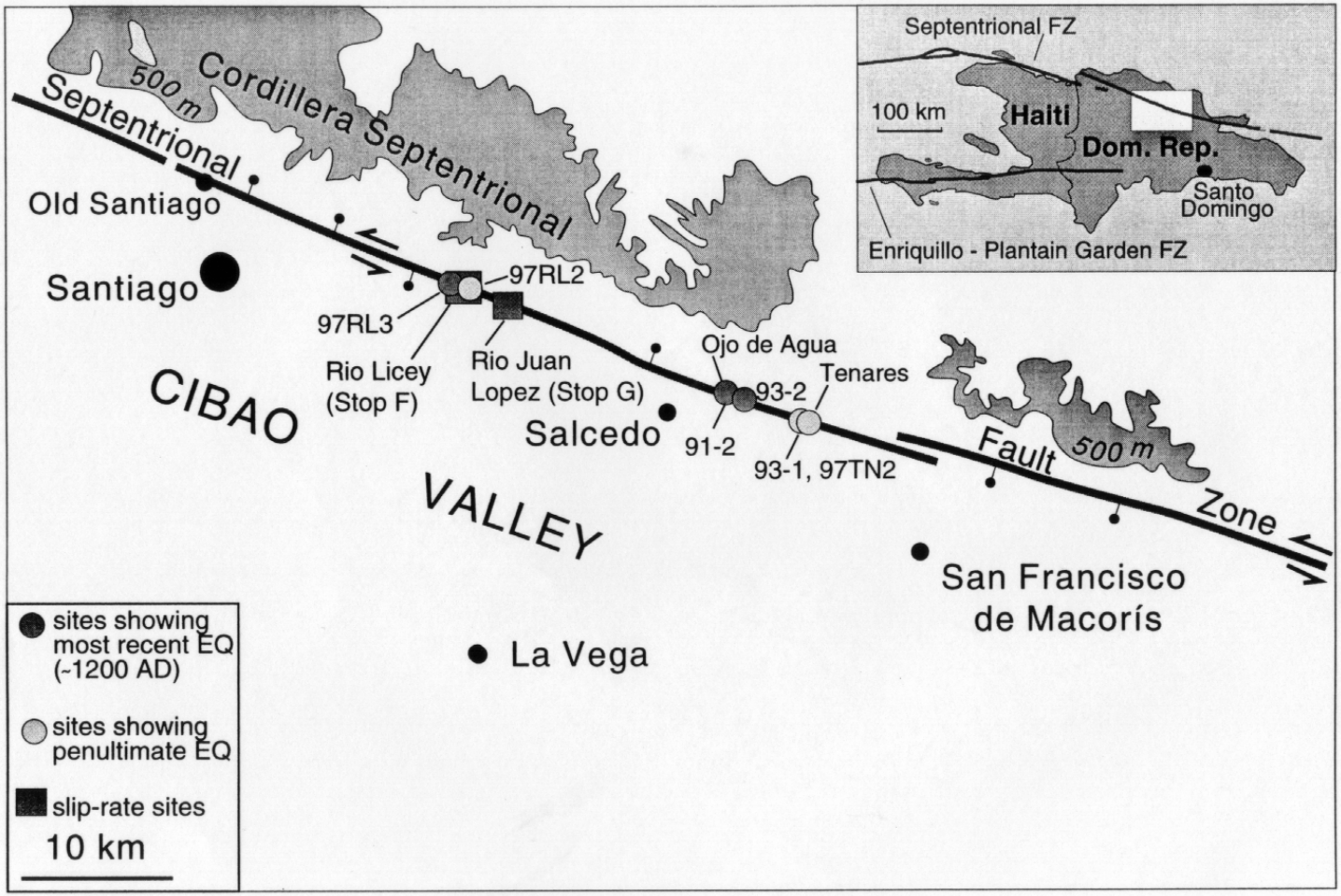

Figure F-1: Map showing locations of paleoseismic sites in the central Cibao Valley.

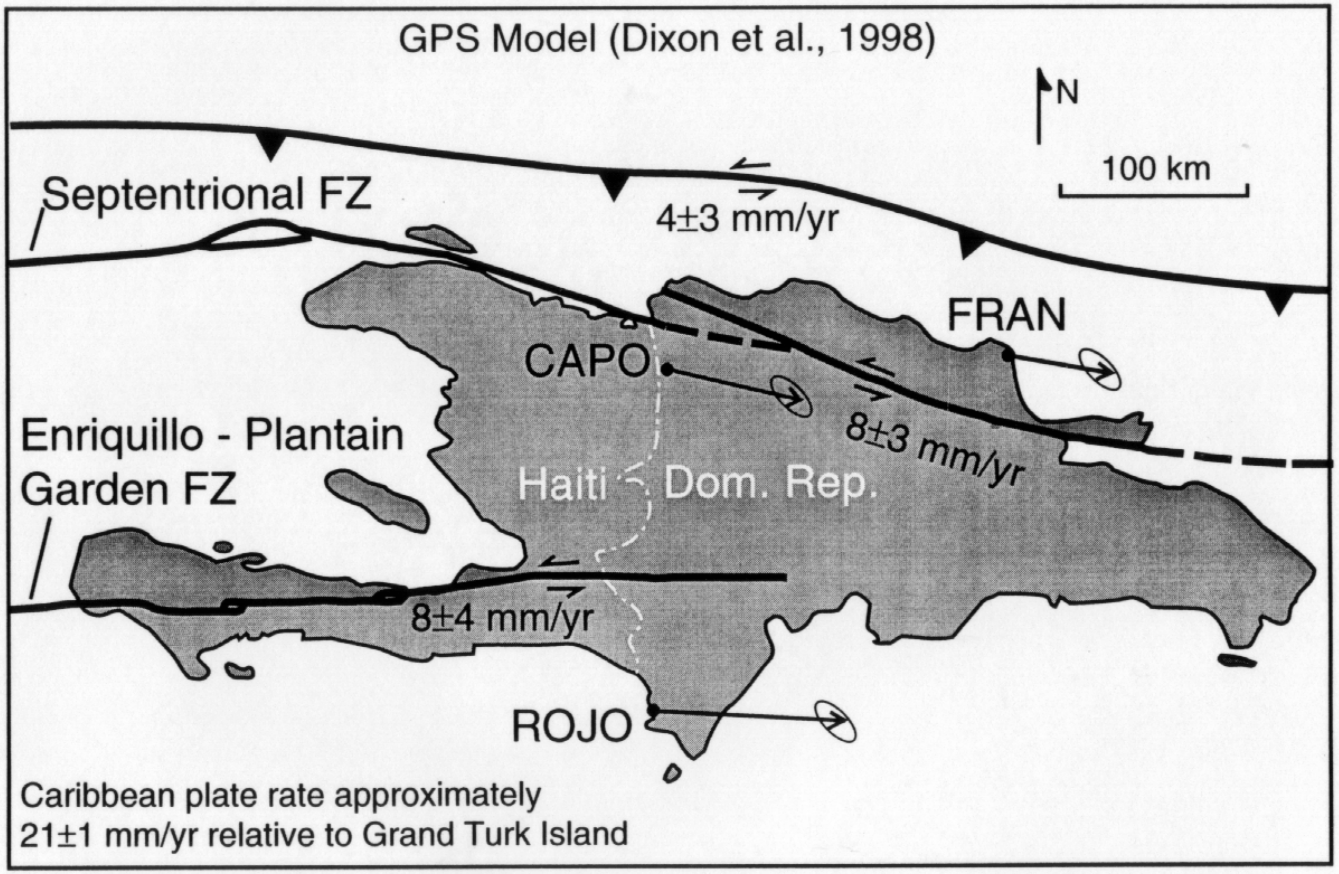

Figure F-2: Modelled slip rates for major faults using GPS data (Dixon et al., 1998)

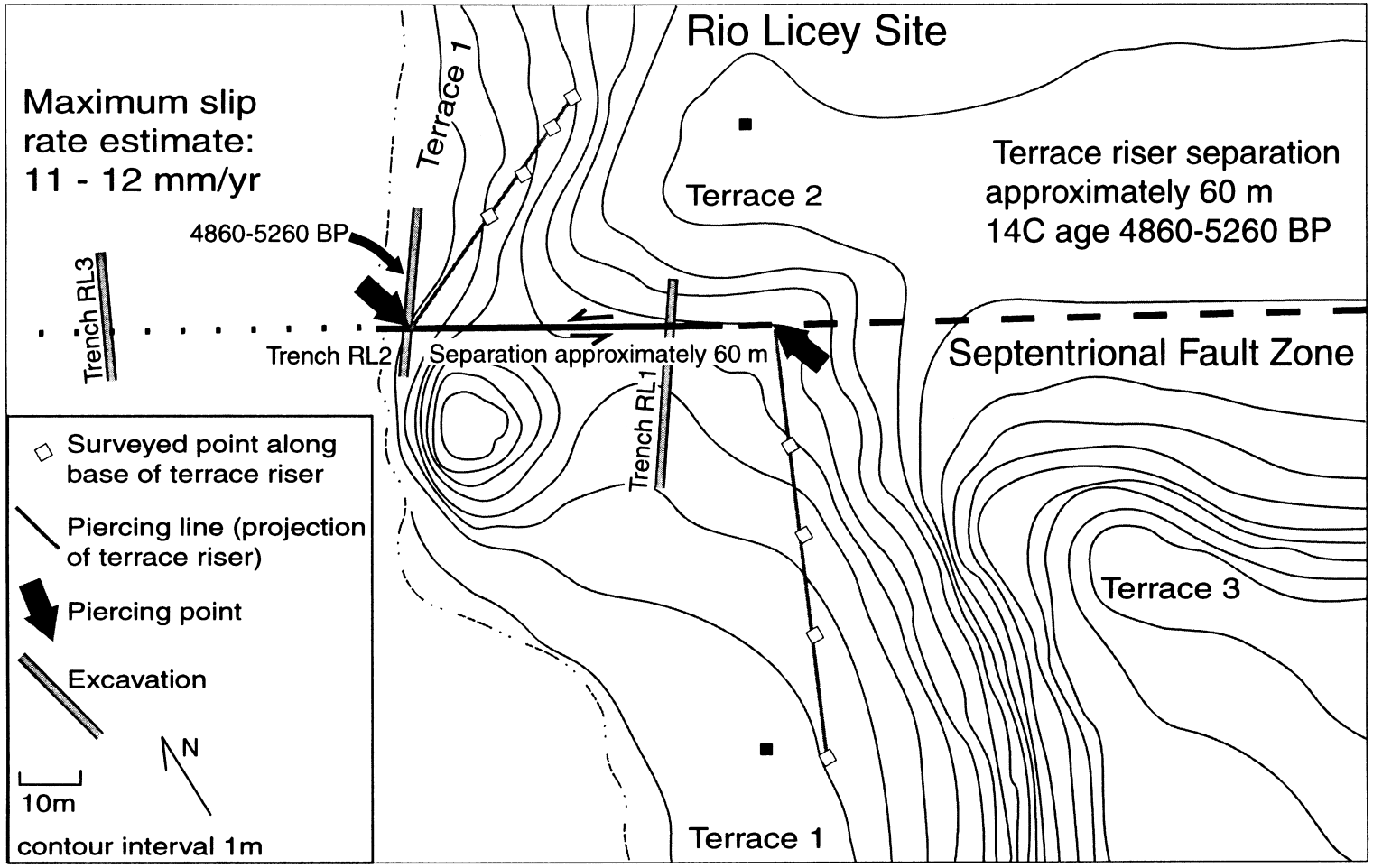

Figure F-3: Surveyed topographic map of Rio Licey site showing locations of trenches and terrace riser used as piercing line to estimate slip rate. Distance between large arrows indicates maximum amount of left lateral slip since terrace was abandoned. Radiocarbon age is from charcoal in uppermost fluvial units exposed in trench 2, and represents time that terrace was abandoned.

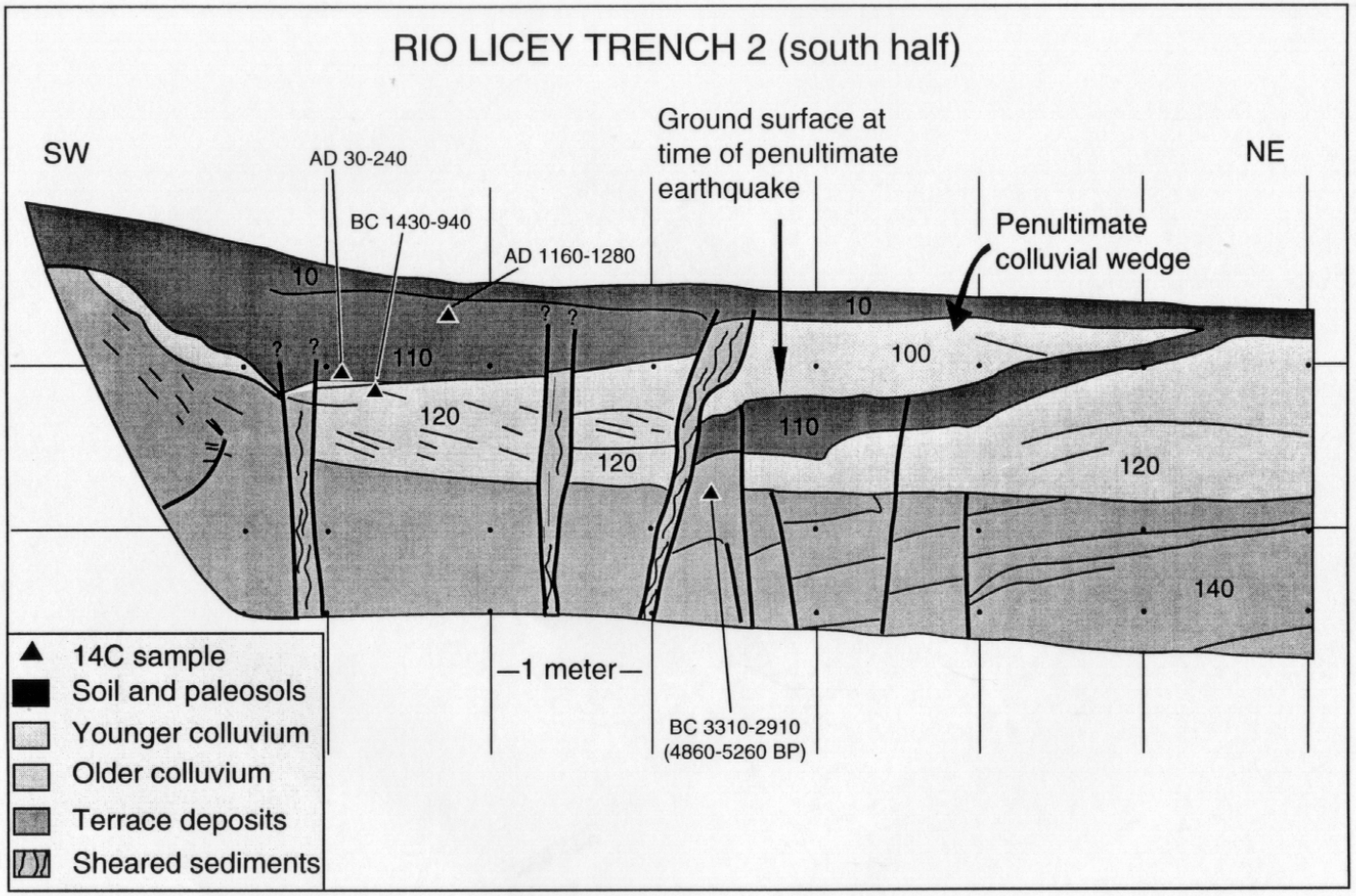

Figure F-4: Part of log of trench RL2. Penultimate earthquake, represented by faulted colluvial wedge (unit 100), occurred when unit 110 formed the ground surface. Charcoal collected from this unit has a radiocarbon date of AD 30-240, indicating penultimate earthquake occurred after this date. Charcoal collected from uppermost fluvial deposits (unit 140) has a radiocarbon date of BC 3310-2910, used to calculate maximum slip-rate estimate (Figure F-6).

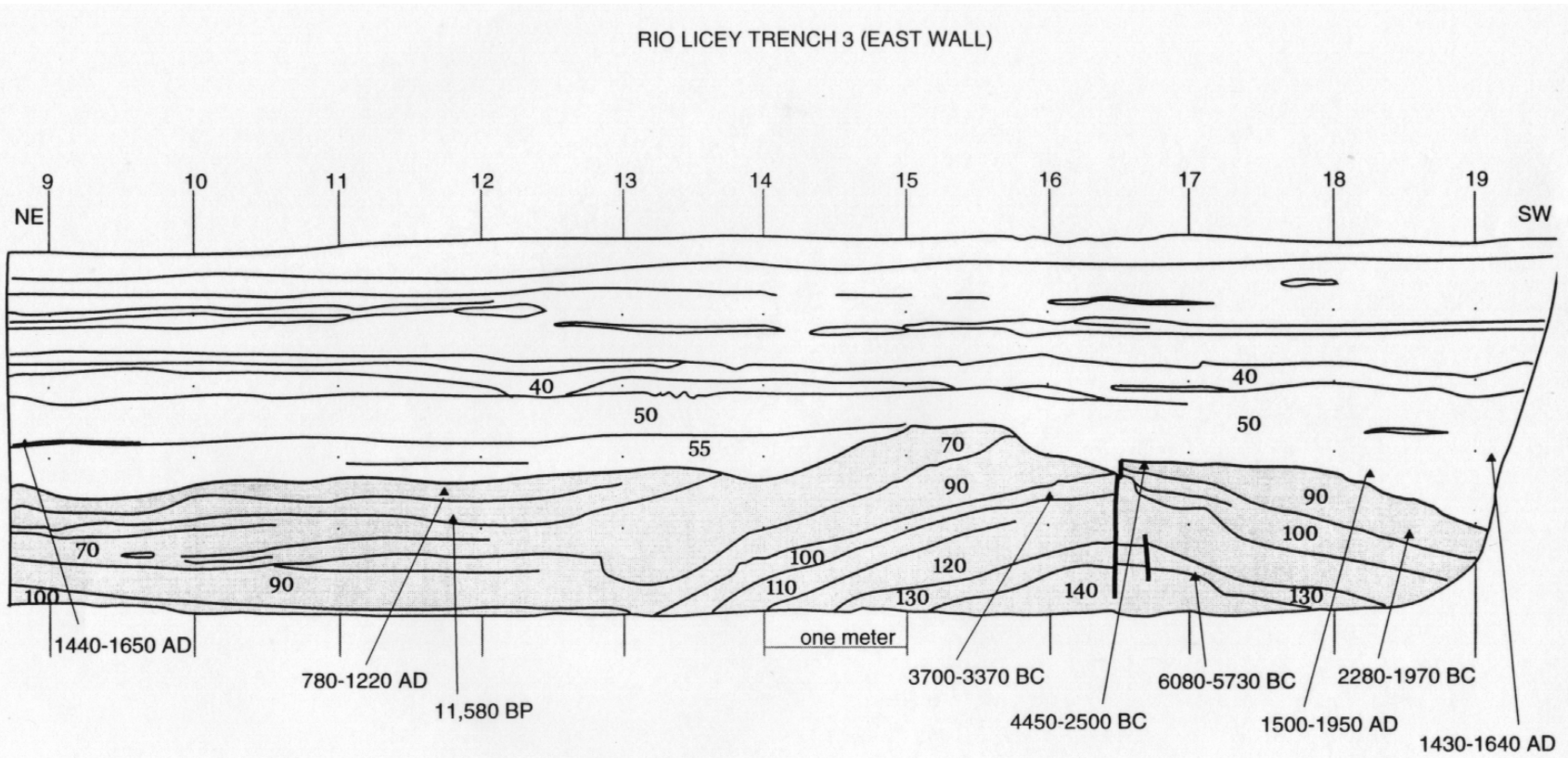

Figure F-5: Partial, simplified log of RL3. Exposed sediments consist of interbedded sand and silt representing fluvial deposits of modern Rio Licey. Units shaded blue were deposited prior to event that caused formation of small anticline, units shaded yellow are undeformed. Radiocarbon analyses are consistent with results from the Ojo de Agua trench site that indicate the most recent earthquake occurred around 1200 AD.

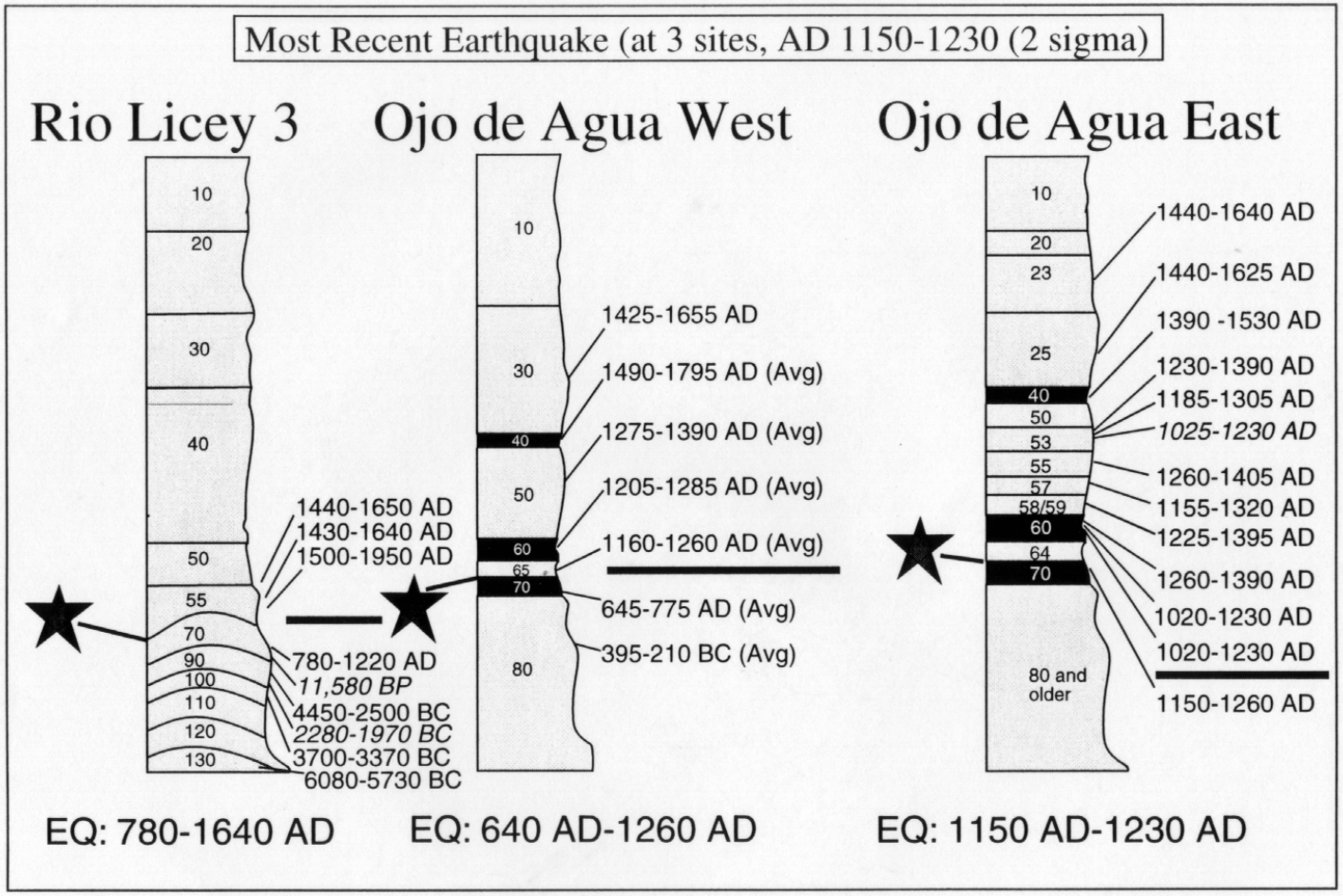

Figure F-6: Summary of results from the three sites that yielded age data for the most recent eathquake on the Septentrional fault in the central Cibao Valley. The minimum date for the earthquake, about 1230 AD, is well constrained stratigraphically and by multiple dates. The maximum date of 1150 AD is less well constrained stratigraphically, and by only a single radiocarbon analysis. Large stars indicate stratigraphic position of event horizon, bars separate pre-event dates from post-event dates. Dates in italics are not in stratigraphic order.

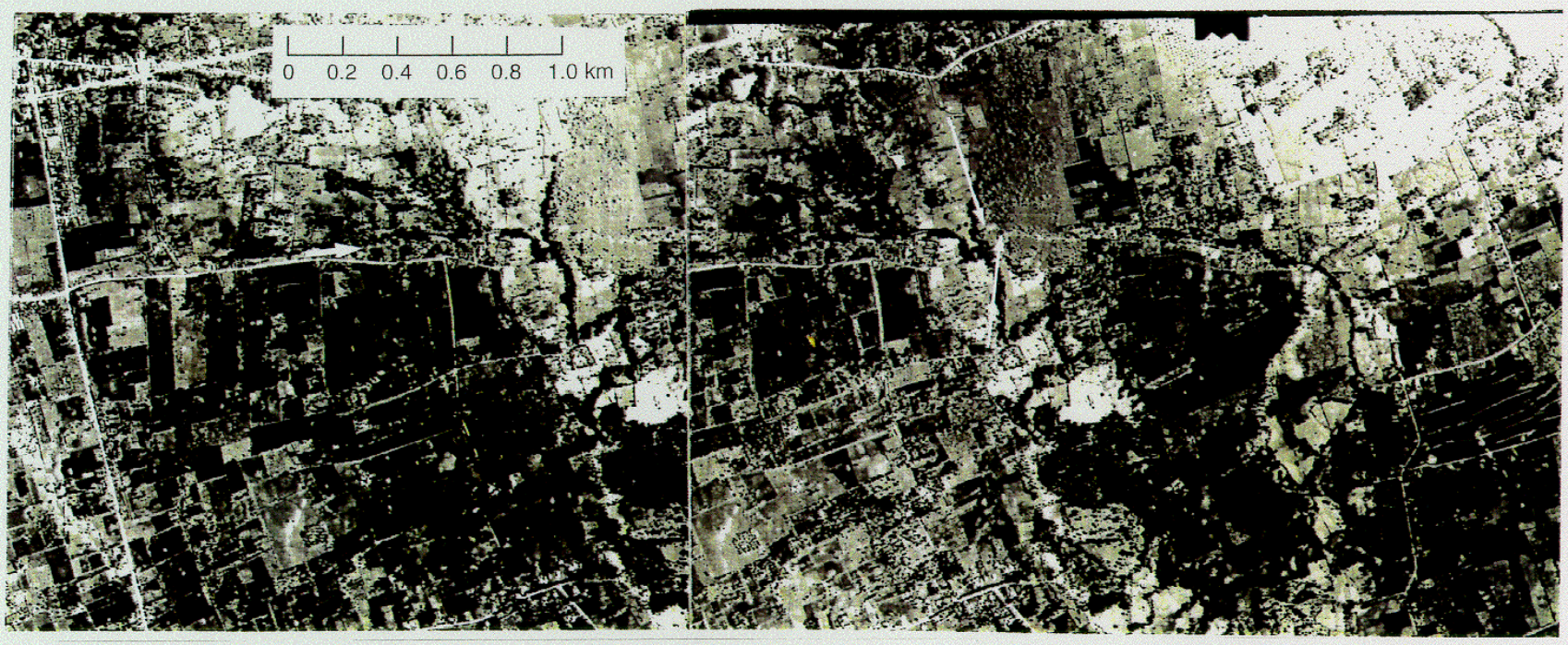

Figure F-7: Stereopair showing Rio Licey area showing fault scarp (shown by large arrows). Two thin arrows indicate left-laterally offset fluvial terrace riser. Offset is no greater than 60 m.

Figure F-8a: Photograph of Trench RL2, showing colluvial wedge (light-colored unit near surface in foreground), faulted by most recent earthquake on SFZ. Dark unit below wedge is a paleosol interpreted to represent the ground surface at the time of the penultimate earthquake.

Figure F-8B: Photograph of Trench RL3, showing undeformed units overlying folded units.

DAY 2, STOP G: RIO JUAN LOPEZ SLIP RATE SITE, SEPTENTRIONAL FAULT, CENTRAL CIBAO VALLEY

LEADERS: CAROL PRENTICE, PAUL MANN, LUIS PEÑA, AND G. BURR

LOCATION

The Rio Juan Lopez site is located about 17 km E of Santiago, and about 4 km NNE of Mocha. The study area includes the river terraces traversed by the Septentrional fault immediately west of Rio Juan Lopez. Coordinates of the site are: 19°25'00"N, 70°30'15" W, and it is located on the Santiago 1:50,000 topographic map, kilometer grid 49-50 N, 41-42E. Access can be gained on foot from the road to Juan Lopez Ariba. The property is privately owned.

SIGNIFICANCE

This site is the second of the two slip-rate sites that we have studied along the Septentrional fault zone (SFZ) in the central Cibao Valley (Figure F-1). The first slip-rate site, Rio Licey (Stop F) yielded data that allow calculation of a maximum slip rate estimate. The slip rate calculated at the Rio Juan Lopez site is also based on the offset of a fluvial terrace riser, however, at Rio Juan Lopez, the data allow a better constrained estimate of the amount of offset, and thus, a better constrained slip rate. Our surveying suggests the riser is left-laterally offset about 35-42 meters (Figure G-1); radiocarbon analysis of a charcoal sample collected from sediments underlying the terrace suggest that the terrace was abandoned 4870-5650 years BP (Figure G-2), allowing calculation of a slip rate estimate of 6-9 mm/yr. This result is consistent with the maximum rate (11-12 mm/yr) determined at Rio Licey, and with the model of geodetic data (Dixon et al., 1998).

DESCRIPTION

Aerial photographs show terraces associated with Rio Juan Lopez traversed by the SFZ (Figure G-3). The higher terrace, labeled T2 in Figure G-1, is vertically offset approximately 4 m across a south-facing fault scarp. On the south side of the fault, T2 is juxtaposed against a lower, younger terrace (T1) across a north-facing fault scarp, approximately 3-4m in height (Figure G-1). This apparent change in the sense of vertical displacement, similar to that seen at the Rio Licey site (Stop F) is due to strike-slip offset. The younger, lower, Terrace 1 has been left-laterally juxtaposed against the higher, older, Terrace 2, resulting in a north-facing scarp, though the vertical component of offset is up on the north side along this part of the SFZ (Mann et al., 1997).

The riser between Terraces 1 and 2 is very prominent north of the SFZ (Figure G-1), and trends nearly perpendicular to the fault. We correlate this riser with the riser between Terraces 1 and 2, south of the fault, and suggest that it has been offset 35-42 meters. Our projections of four different piercing lines associated with the riser are shown on Figure G-1, and give an estimate of the distance this riser has been offset since the time Terrace 1 was abandoned.

We excavated trench RJL across T1 (Figure G-2) to search for radiocarbon samples to determine the time when the riser and terrace were abandoned, and offset of the riser began to accumulate. The sediments exposed in the trench include fluvial sediments associated with T2 south of the fault zone (unit 100), and fluvial sediments associated with T1 north of the fault zone (units 60 and 50). Overlying unit 50 is an organic-rich black clay horizon (unit 40) that we interpret as representing a pond that developed on T1 in response to the onset of growth of the north-facing fault scarp after the terrace was abandoned. Unit

50 is a highly bioturbated horizon that consists of both tan fluvial sands and organic-rich black clay that we interpret as representing the floor of the pond.

Radiocarbon analysis of charcoal collected from lower unit 40 provides an estimate for the time the terrace was abandoned. The 2-sigma calibrated age range is 4870-5650 years BP, giving a slip-rate estimate of 6-9 mm/yr. An earlier study of this site, reported in Mann et al., 1997, used less well constrained age and offset data to estimate a maximum slip rate of 13±4 mm/yr. While the two studies are not contradictory, our new data presented here provide better constraints on the slip rate. In particular, the new radiocarbon date is more reliable, and the amount of offset is better constrained.

Trench RJL also shows evidence confirming that there is a component of south-side-up slip across the fault zone (Figure G-2). This excavation also provides radiocarbon ages for samples collected from T2 sediments that suggest T2 was abandoned less than 20 ka.

The slip rate estimates from the two sites, Rio Licey (Stop F) and Rio Juan Lopez are consistent with the slip rate (8±3 mm/yr) modeled by Dixon et al. (1998), based on geodetic data (Figure F-2). The data of Dixon et al. yielded plate rates much higher than the rate of 11±3 mm/yr determined by the NUVEL-1A model (DeMets et al., 1994). Thus, the geologic slip rate estimates support Dixon et al.'s conclusion that the discrepancy between the NUVEL model and the GPS model is not due to anomalous recent seismic activity. These slip rates, in concert with other paleoseismic data that indicate the last earthquake on this fault occurred more than about 800 years ago, (Prentice et al., 1993; 1994) suggest that the Septentrional fault has accumulated at least about 5 m of slip, and therefore is likely to produce a significant future earthquake.

REFERENCES

DeMets, C., Gordon, R. G., Argus, D. F., and Stein, S., 1994, Effect of recent revisions to the geomagnetic time scale on estimates of current plate motion: Geophysical Research Letters, v. 21, p. 2191-2194.

Dixon, T. H., Farina, F., DeMets, C, Jansma, P., Mann, P., and Calais, E., 1998, Relative motion between the Caribbean and North American plates and related boundary zone deformation from a decade of GPS observations: Journal of Geophysical Research, v. 103, p. 15,157-15,182.

Mann, P., Prentice, C. S., Burr, G., Peña, L. R., and Taylor, F. W., 1998, Tectonic geomorphology and paleoseismology of the Septentrional fault system, Dominican Republic, in Dolan, J. F., and Mann, P., eds., Active strike-slip and collisional tectonics of the northern Caribbean plate boundary zone: Boulder, Colorado, Geological Society of America Special Paper 326, 174 p.

Prentice, C. S., Mann, P., Taylor, F. W., Burr, G., and Valastro, S., Jr., 1993, Paleoseismicity of the North America-Caribbean plate boundary (Septentrional fault), Dominican Republic: Geology, v. 21, p. 49-52.

Prentice, C. S., Mann, P., Burr, G., and Peña, L. R., 1994, Timing and size of the most recent earthquake along the central Septentrional Fault, Dominican Republic [abs.]: in: Prentice, et al., 1994, ed., Proceedings of the workshop on paleoseismology: USGS Open-File Report 94-568, p. 158.

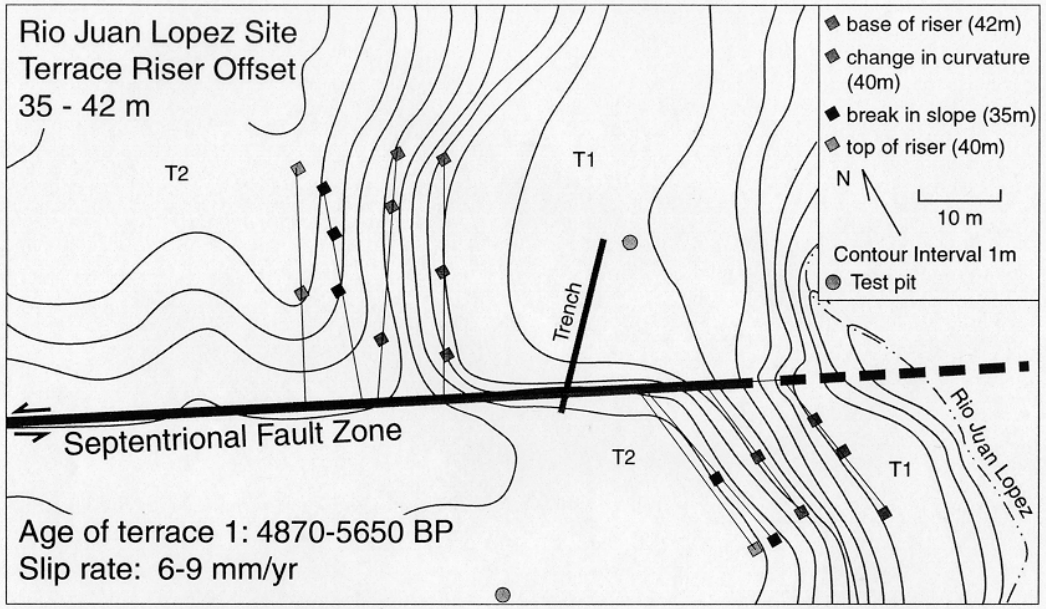

Figure G-1: Surveyed map showing offset terraces of Rio Juan Lopez and location of trench. Diamonds represent surveyed points along topographic features used to estimate amount of left-lateral slip that has accumulated since terrace 1 (T1) was abandoned. Features are offset between 35 and 42 meters. A charcoal sample collected from sediments exposed in the trench yielded a calibrated, 2-sigma radiocarbon age range of 4870-5650 years BP, allowing calculation of a slip-rate of 6-9 mm/yr.

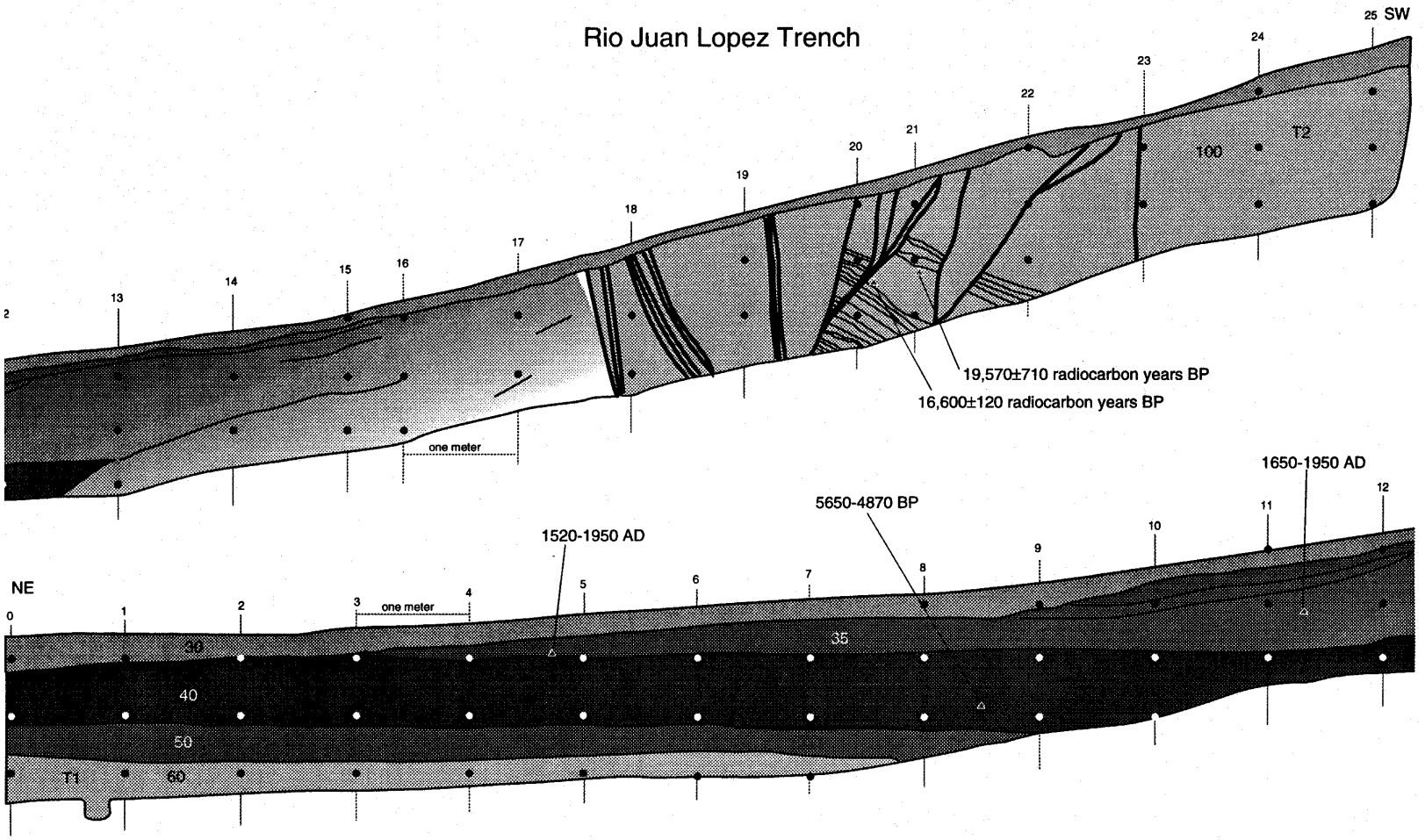

Figure G-2: Log of Rio Juan Lopez trench. Horizon shaded black is an organic-rich clay overlying fluvial deposits associated with Terrace 1. Match line is vertical #12.

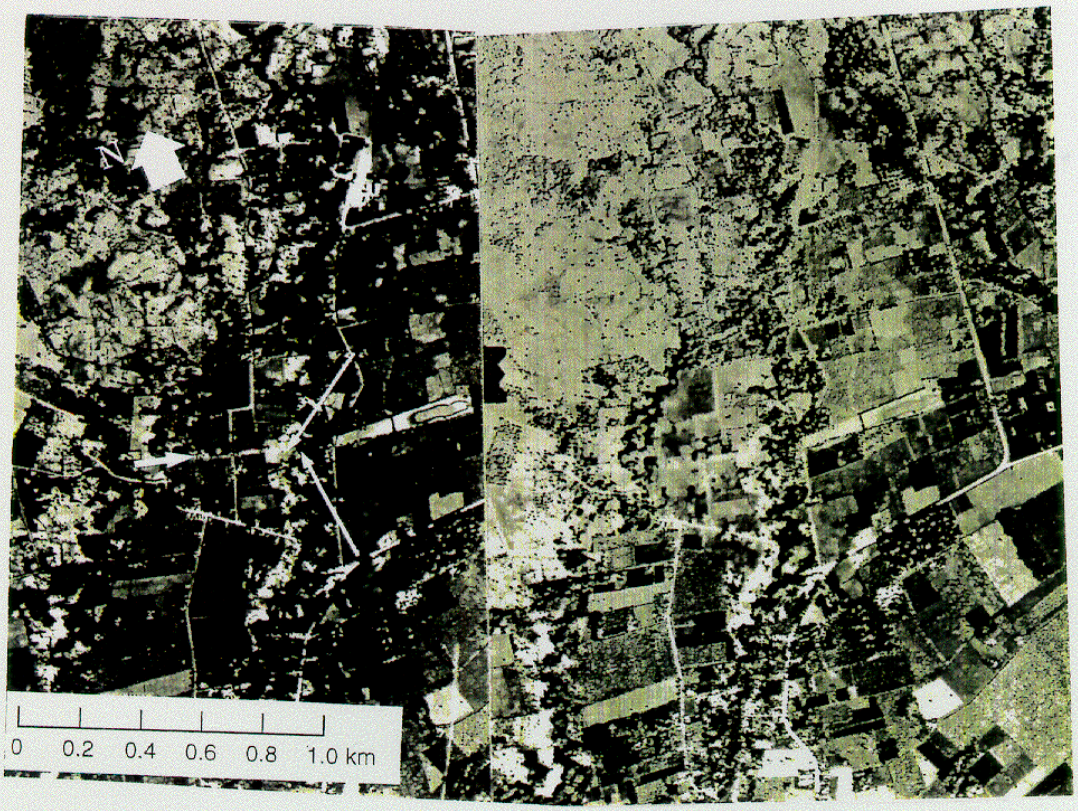

Figure G-3: Steropair showing Rio Juan Lopez area. Short arrow indicates fault scarp. Thin arrows show left-laterally offset terrace riser. Note sag pond east of river.

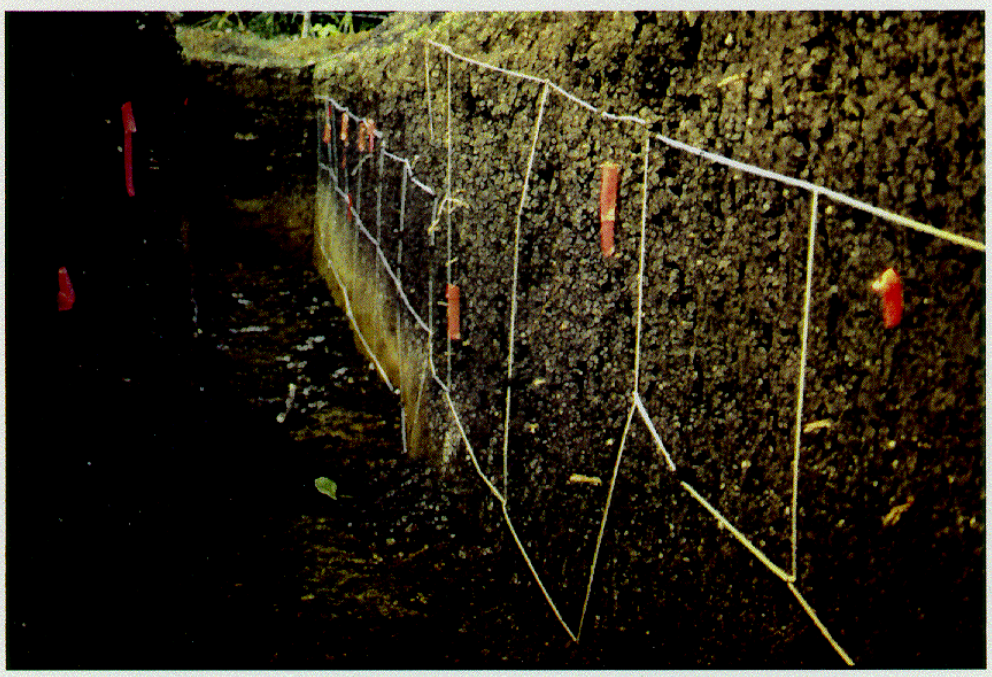

Figure G-4: Photograph of Trench RJL showing T1 fluvial deposits (bottom of trench in distance) and overlying pond deposits (unit 40).

DAY 2, STOP H, MATANCITA, TSUNAMOGENIC POTENTIAL OF THE PUERTO RICO-DOMINICAN MARGIN

LEADER: NANCY GRINDLAY

LOCATION

Matancita, a small town located on the north coast of Hispaniola, is approximately 15 km north of the Septentrional Fault Zone and 45 km south of the surficial trace of the major North America-Caribbean plate boundary thrust fault (Figure H-1 and H-2). Matancita, and many other towns ringing Bahia Escosesa, were inundated by large tsunamis associated with the 1946 earthquake and its subsequent aftershocks.

SIGNIFICANCE

Earthquakes on the active offshore faults associated with the complex northeastern North America-Caribbean plate boundary have historically caused destructive tsunamis and are of concern for the low lying areas of Hispaniola and Puerto Rico. Tsunamis are be generated by the rapid displacement of large sections of the seafloor Displacement can be the result of rupture due to faulting or submarine slides (Moore and Moore, 1984; von Huene et al., 1989; Jiang and Le Blond, 1992; Hampton and Lee, 1996). Although rarely documented directly, ground shaking associated with earthquakes is often inferred to be the triggering mechanism of submarine slides (Hampton and Lee, 1996).

At least four such earthquake-related tsunamis have been documented in the northeastern Caribbean in the recent past. A tsunami associated with the 1842 northern Hispaniola earthquake (Scherer, 1912) was possibly caused by movement along the western, offshore extensions of the Septentrional fault zone. Tsunamis were also associated with the 1887 (Scherer, 1912) and 1946 earthquakes (Dolan and Wald, 1998) along the north coast of Hispaniola. Offshore earthquakes in 1867 and 1918 in the Anegada and Mona Passages, respectively, triggered tsunamis that inundated the southeastern and western coasts of Puerto Rico (McCann, 1985; Reid and Taber, 1919) (Figure H-1).

DESCRIPTION

Knowledge of the distribution, location of active offshore faults and detailed bathymetric maps is crucial in determining the tsunamogenic potential of any region. During a recent marine geophysical expedition to survey the Puerto Rico trench and northern insular margin of the Virgin Islands and Puerto Rico Grindlay et al., (1997) identified several active fault zones within the trench, including one on the south slope of the trench, South Puerto Slope Fault Zone, which lies within 60-100 km of the north coast of Puerto Rico. In addition, Grindlay et al., (1997) corroborated the existence of a major submarine slide first reported by Scanlon et al., (1988) and Schwab et al., (1991) on the south slope of the Puerto Rico trench, located about 37 km north of the city of Arecibo on the island of Puerto Rico (Figure H-1). The presence of active fault zones in the Puerto Rico trench implies that there is a potential threat of repeat submarine slides and accompanying tsunamis.

Marine geophysical data collected during the June-July 1996 cruise on board the *R/V Maurice Ewing* and existing onshore well and outcrop data have be used to provide estimates of the volume and density of material involved in the debris avalanche that formed the large amphitheater-shaped scarp. These data include sidescan sonar imagery which provides information about the reflectivity and nature of seafloor material and structures. High-resolution multibeam sonar bathymetric data provide vertical depth resolutions on the order of 10-15m and swath widths up to 2.5 the water depth. Accurate bathymetric maps

are used to estimate the surface area of the material involved in the slide. Single-channel seismic (SCS) profiles provide information about the subsurface structures, including location of headwall scarps and extent and thickness of units that pre- and post-date the slide. Onshore well data from CPR-4 (Briggs, 1961) and Toa Baja wells (Anderson, 1991) are used to make lithologic and age correlations of seismic reflection data and determine physical properties of these units.

Classification and morphologic description of submarine landslide on south slope of Puerto Rico Trench

On the basis of the geophysical data the landslide that generated the amphitheater-shaped scarp on the south slope of Puerto Rico trench was most likely a debris avalanche. Varnes (1978) define a debris avalanche as a landslide that involves the failure of hundreds to thousands of cubic kilometers of rock and sediment that have disintegrated into relatively smaller pieces (compared to the large slump blocks but can include blocks of many cubic kilometers) and have clearly moved rapidly. Each debris avalanche is thought to represent a single episode of catastrophic slope failure. The bathymetric and sidescan imagery clearly show a giant amphitheater-shaped scarp that is approximately 57 km across (Figures H-3 A& B, and 4A&B). The crown of the headwall scarp lies at depths of 2500 m to 3500 m. The debris deposit shown as dark, highly reflective material in the sidescan imagery extends more than 25 km down the slope to depths of approximately 7000 m (Figures H-3A &B). The seismic profile 20 shows a thin layer characterized by chaotic returns and a hummocky surface that is the uppermost unit on the amphitheater-shaped scarp (Figure H-4).

Description of the stratigraphic units on the south slope of the PR trench

Seismic profiles that extend across the northern insular margin of Puerto Rico show that the offshore stratigraphy of the platform can be divided into three megasequences (Meyerhoff et al., 1983; van Gestel et al., in revision)(Figure H-4, SCS profile 20). On the basis of well data from CPR-4 and Toa Baja wells these sequences can be correlated with lithologic units of defined ages (Meyerhoff et al., 1983; van Gestel et al., in review). The lowest unit, PR1 consists of island arc basement rocks which based on subaerial exposures and samples dredged offshore (Fox and Heezen, 1975; Perfit et al. 1980) are of Cretaceous to Eocene age. The middle unit, PR2, does not correlate to any major formation or group of formations on Puerto Rico (Meyerhoff et al., 1983) but is speculated to be of Eocene age and formed as a basinal fill in a deep marine setting. Meyerhoff et al., (1983) and van Gestel et al., (in revision) note that this unit is offset by large normal faults that extend upward into the overlying unit. It is possible that reactivation of these faults due to recent tectonic activity has resulted in their growth into the overlying unit PR3. The uppermost unit, PR3, consists of Oligocene-Pliocence shallow marine limestones deposited during a tectonically quiescence period (Moussa et al, 1987; Meyerhoff et al., 1983, Reflectors within PR3 can be subdivided in five individual sequences that are conformable with reflectors in the underlying PR2 (van Gestal et al., in revision). Overall, unit PR3 is characterized by continuous parallel reflectors, constant thickness and constant dip that persists through the offshore units. During the past 2.5 m.y. the submarine part of PR3 has subsided more than 4000 m generating a 4.5° regional slope (Birch, 1986).

At the base of south slope SCS profile 20 shows thick onlapping deposits of stratified material characteristic of turbidites. Core and dredge samples show the top portion of this unit to consist of turbidites (Conolly and Ewing, 1967; Fox and Hezzen 1975, Perfit et al. 1980). The source of these deposits is unknown, although it is likely that some portion consists of sediments transported across the shelf and down the scarp face through the submarine canyons. These deposits have been offset vertically and most likely laterally by the South Puerto Rico slope fault. In addition a small, lower headwall scarp is observed cutting these deposits at 7500m.

Estimates of volume and density of material involved in the landslide

SCS Profile 20 suggests that only unit PR3 was involved in the submarine landslide, as it is the only unit to be truncated abruptly at the upper headwall scarp (Figure H-4). Unit PR2 appears to vary little in thickness, although the seismic data do not provide enough penetration to clearly delineate the interface between units PR2 and PR1. On the basis of systematically collected SCS profiles over the platform, van Gestel et al., 1998, estimate that the thickness of unit PR3 ranges from 1500 km to 1300 km (assuming a velocity of 2.75 km/s) at the upper headwall scarp. Given the surface area of failure calculated to be ~ 700 km^2 , a volume of ~ 910-1050 km^3 material is estimated to be involved in the landslide. Geophysical logs from the Toa Baja well (Anderson, 1991) indicate that unit PR3 has a density of 2.2 g/cm^3.

With volume and density estimates of the material involved in the submarine landslide, investigators can use numerical models to estimate potential tsunami propagation and runup for geohazard assessments. Numerical models have been used successfully to simulate historical tsunamis such as the 1960 Chilean tsunami and the resulting flooding in Hilo Bay, Hawaii (Liu et al., 1993) as well as the 1918 tsunami and resulting inundation on the west coast of Puerto Rico (Mercado, 1998).

REFERENCES CITED

Anderson, R., Geophysical logs from the Toa Baja Scientific Drill hole, Puerto Rico, *Geophys. Res. Lett.*, 18, 497-500, 1991.

Birch, F, Isostatic, thermal and flexural models of the subsidence of the north coast of Puerto Rico, *Geology*, 14, 427-429, 1986.

Briggs, R.P., Geology of Kewanne Interamerican Oil Company test well number CPR-4 northern Puerto Rico *in Oil and Gas Possibilities of Northern Puerto Rico*, pp 1-23, 1961.

Conolly, F. and M. Ewing, Sedimentation in the Puerto Rico Trench, *Jour. Sed. Petrology*, 37, 44-59, 1967.

Dolan, J. and D. Wald, The 1943-1953 north-central Caribbean earthquakes: Active tectonic setting, seismic hazards, and implications for Caribbean-North America plate motions, in Dolan, J.F., and Mann, P., eds., Active Strike-slip and Collisional Tectonics of the Northern Caribbean Plate Boundary Zone, Boulder, Co. GSA Special Paper 326, 143-169, 1998.

Fox, J. and B. Heezen, Geology of the Caribbean crust, in *The Ocean Basins and Margins*, eds. A Nairn and F. Stehli, pp. 421-466, New York, NY, 1975.

Grindlay, N., P. Mann, and J. Dolan, Researchers investigate submarine faults north of Puerto Rico, *Eos, Trans. AGU*, 78, 404, 1997.

Grindlay, N., P. Mann, J. Dolan, and J-P van Gestal, Oblique collision of the Bahamas Platform in the Hispaniola-Puerto Rico area, northeastern Caribbean 2: Puerto Rico trench and northern Puerto Rico Island Slope, *J. Geophys. Res.*, in prep.

Hampton, M., H. Lee and J. Locat, Submarine landslides, *Rev. of Geophys*, 34, 33-59, 1996.

Haq, B., J. Hardenbol and P.R. Vail, Chronology of fluctuating sea levels since the Triassic, *Science*, 235, 1156-1167, 1987.

Jiang, L., and P.H. LeBlond, The coupling of a submarine slide and the surface waves which it generates, *J. Geophys. Res.*, 97, 12,731-12,744, 1992.

Lui, P., Yoon, S.B., Seo, S.N., and Cho, Y. Numerical simulation of tsunami inundation at Hilo, Hawaii, Poc. *IUGG/IOC International Tsunami Symposium*, TSUNAMI '93, 257-270, 1993.

McCann, W.R., On the earthquake hazards of Puerto Rico and the Virgin Islands, *Bull. Seism. Soc. Am.*, 75, 251-262, 1985.

Mercado, A., Numerical simulation of the 1918 Puerto Rico tsunami, *Jour. of Natural Hazards*, in press.

Meyerhoff, A., E.A. Krieg, J.D. Cloos, and I. Taner, Petroleum potential of Puerto Rico, *Oil and Gas Jour.*, 81, 113-120, 1983.

Monroe, W., Stratigraphy and petroleum possibilities of middle Tertiary rocks in Puerto Rico, *AAPG Bull.*, 57, 1086-1099, 1973.

Moore, G. and J.G. Moore, Deposit from a giant wave on the island of Lanai, *Science*, 226, 1312-1315, 1984.

Moussa, M.T., G.A. Seiglie, A.A. Meyerhoff and I. Taner, The Quebradillas Limestone (Miocen-Pliocene), northern Puerto Rico and tectonics of the northeastern Caribbean margin, *GSA Bull*, 99, 427-439, 1987.

Perfit, M.R., B.C. Heezen, M. Rawson and T. Donnelly, Chemistry, origin and tectonic significance of metamorphic rocks from the Puerto Rico trench, *Marine Geology*, 34, 125-156, 1980.

Reid, H. and S. Taber, The Puerto Rico earthquakes of October-November 1918, *Bull. Seism. Soc. Am*, 9, 95-127, 1919.

Scanlon, K., D. Masson and R. Rodriguez, GLORIA sidescan-sonar survey of the EEZ of Puerto Rico and US Virgin Islands, *Trans. Caribb. Conf., 11th*, Barbados, 32:1-32:9, 1988.

Scherer, J., Great earthquakes in the island of Haiti: Seismological Society of America Bulletin, v.2, p. 161-180, 1912.

Submarine Landslides: Selected Studies in the U.S. Exclusive Economic Zone, ed. W. Schwab, H. Lee, D. Twichell, US Geological Survey Bull., 2002, 1993.

Schwab, W.C., W.W. Danforth, K. Scanlon, and D. Masson, A giant submarine slope failure on the northern insular slope of Puerto Rico, *Marine Geology*, 96, 237-246, 1991.

van Gestel, J-P, P. Mann, J. Dolan and N. Grindlay, Structure and tectonics of the upper Cenozoic Puerto Rico-Virgin Islands carbonate platform as determined from seismic reflection studies, *J. Geophys. Res.*, 1998.

van Gestel, J-P., P. Mann, N. Grindlay, and J. Dolan, Three-phase tectonic evolution of the northern margin of Puerto Rico as inferred from an integration of seismic reflection, well and outcrop data, *Marine Geology*, in revision.

Varnes, D.J. , Slope movement types and processes, *in Landslides--Analysis and Control*, eds. R.L. Schuster and R.J. Krizek, Spec. Rep. 176, pp. 12-33, Transp. Res. Board, Natl. Res. Counc., Washington, DC, 1978.

von Huene, R. , J. Bourgois, J. Miller, and G. Pautot, A large tsunamogenic landslide and debris flow along the Peru Trench, *J. Geophys. Res.*, 94, 1703-1714, 1989.

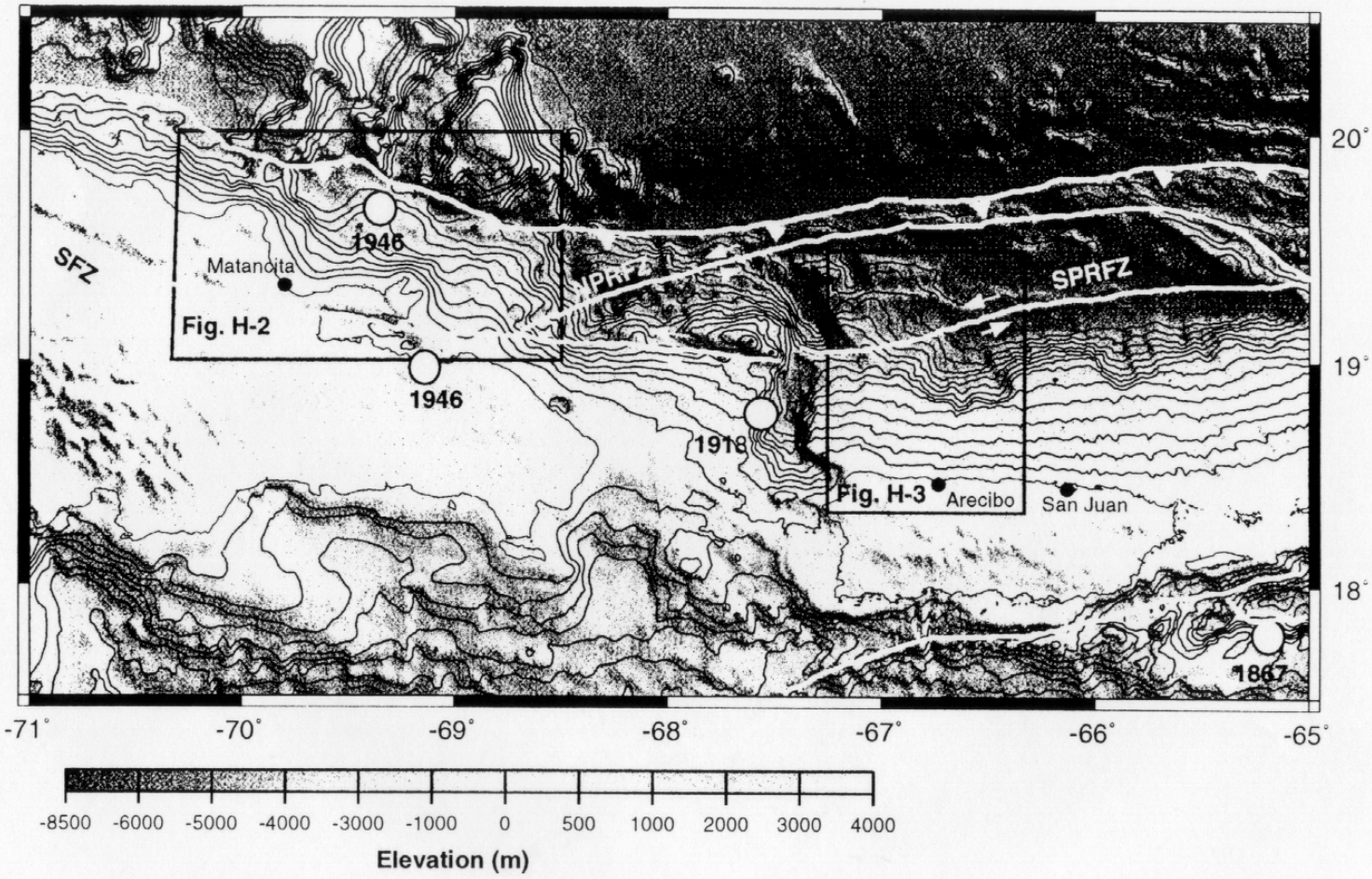

Figure H-1. Shaded relief map of topography and offshore bathymetry of the northeastern Caribbean-North America plate boundary zone. Boxes indicate location of figures H-2 and H-3. Epicenters of tsunami-generating earthquakes are shown as yellow circles. NPRFZ = North Puerto Rico Fault Zone, SPRFZ=South Puerto Rico Fault Zone, SFZ= Septentrional Fault Zone.

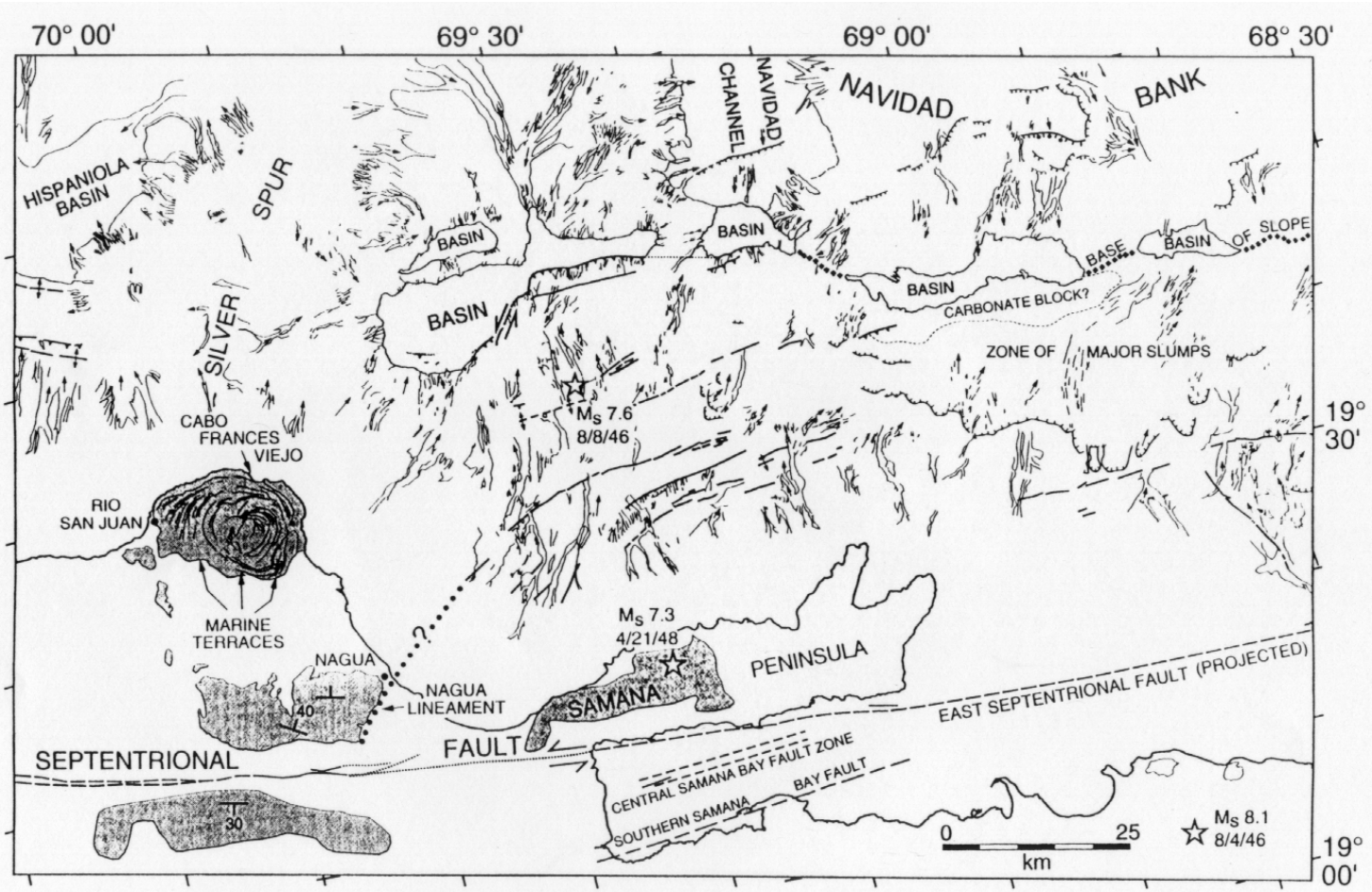

Figure H-2. Interpretation of major structures in the central part of survey area. Dark gray shading shows outcrop of Miocene-Pliocene Villa Trina Formation limestones (known as the La Canita Formation on the Samana Peninsula). The carbonate outcrop east of Rio San Juan encompasses younger (Pleistocene?) limestones that are lithologically similar to those of the Villa Trina Formation (see text for discussion). Onshore data from de Zoeten and Mann (1991) and de Zoeten et al. (1991), except for outcrop of the La Canita Formation, which is from Joyce (1991), and the pattern of Rio San Juan Peninsula terraces, which are from this study. Pale gray shading denotes flat-floored, turbidite-filled basins. Epicenters (stars) of 1946 Northeastern Hispaniola earthquake, its August 8, 1946, aftershock, and the April 21, 1948, Samana earthquake are from Kelleher et al. (1973). FROM DOLAN ET AL., 1998

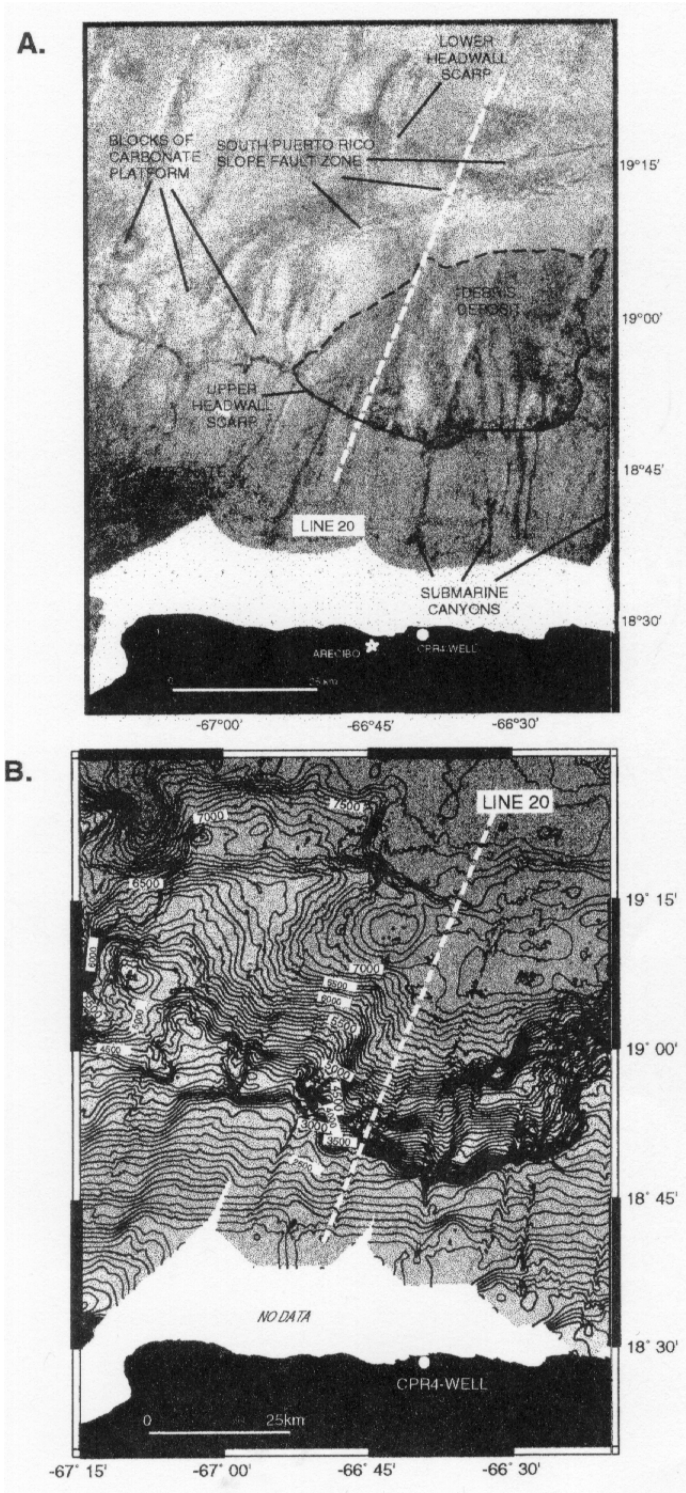

Figure H-3 **A**. Sidescan sonar imagery (HMR1) of amphitheater-shaped scarp cut into the northern Puerto Rico insular margin and debris deposit downslope. Also identified are a possible lower headwall scarp at the base of the slope, the SPRFZ, and submarine canyons cut into the Oligocene-Miocene carbonate platform. The north coast of Puerto Rico is shown in black, areas of no data are in white. The location of the seismic profile, Line 20, shown in figure H-4 is marked by a dashed white line. **B**. Bathymetric map (250m-grid interval) of the study area at the same scale as the sidescan imagery. Contour interval is 100m. The crown of the amphitheater-shaped scarp ranges from 2500-3500m. The base of the upper scarp lies at ~7000m water depth.

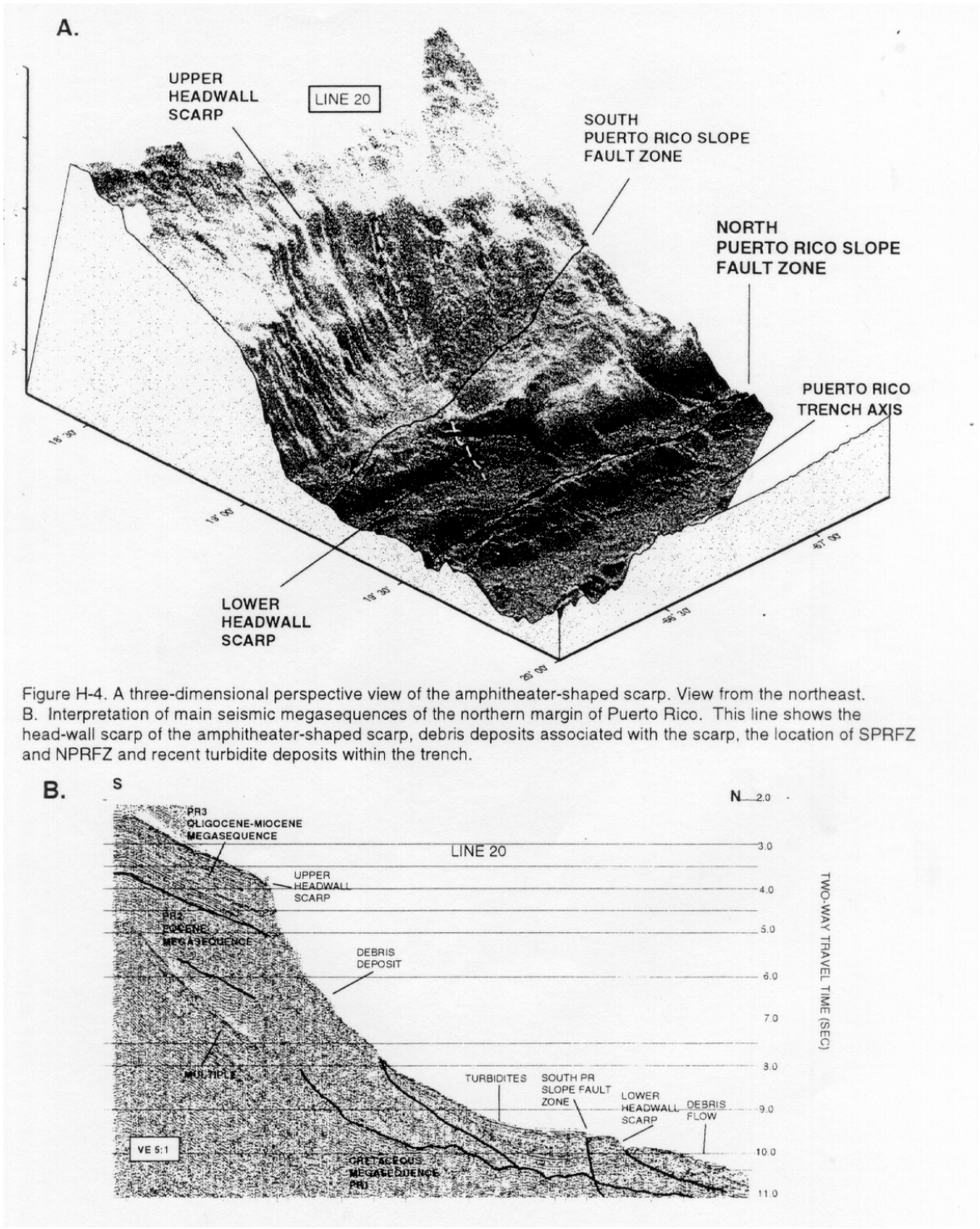

Figure H-4. A three-dimensional perspective view of the amphitheater-shaped scarp. View from the northeast. B. Interpretation of main seismic megasequences of the northern margin of Puerto Rico. This line shows the head-wall scarp of the amphitheater-shaped scarp, debris deposits associated with the scarp, the location of SPRFZ and NPRFZ and recent turbidite deposits within the trench.

DAY 2, STOP I-a, CABO FRANCES VIEJO, LOCUS OF MAXIMUM UPLIFT IN THE ACTIVE HISPANIOLA-BAHAMAS COLLISION ZONE
LEADER: JAMES DOLAN

NOTE: DANGER!!! THIS SITE IS LOCATED NEXT TO A VERTICAL 20-M-TALL CLIFF THAT IS MASKED BY VEGETATION. PLEASE DO NOT VENTURE NEAR THE EDGE AS A FALL COULD PROVE TO BE FATAL.

LOCATION

Cabo (Cape) Frances Viejo lies at the northeastern tip of a small peninsula along the northeastern edge of the much larger Rio San Juan Peninsula (Figure ONC 4; Note: Figures labelled "ONC-x" refer to figures in the section of your field guide entitled "Overview of the Field trip for the Northern Coast"). The Rio San Juan Peninsula is visible on regional maps as a prominent 'bump' that projects ~20 northward from the overall west-northwest-trending coastline of the northern Dominican Republic.

Driving north from our lunch stop just south of Nagua (Matancita), you will see a conical hill ahead of us and to our left. Look carefully at the outlines of the hill. You will see that the hill is composed of a number of 'stairsteps'. These are uplifted marine terraces that represent the most prominent onshore deformation associated with the active Hispaniola-Bahamas collision.

SIGNIFICANCE

We are stopping at Cabo Frances Viejo for two reasons: (1) there is a GPS station (first surveyed in 1986) at the site that will be discussed in detail in a few minutes by Eric Calais; and (2) the peninsula is capped by the youngest of a series of spectacularly developed marine terraces. From this vantage point we will view these uplifted marine terraces and discuss their significance for the active tectonics of the region. We will use the presence of the terraces as a lead-in to a description of the offshore geology of the Hispaniola-Bahamas collision zone.

DESCRIPTION

The Rio San Juan Peninsula--The Rio San Juan Peninsula (RSJP) is a 17 km by 13 km promentory that projects northward from the west-northwest trending coastline of north-central Hispaniola (Figure ONC-4). The peninsula is dominated by a 420 m-high, dome-shaped hill that exhibits a spectacular flight of more than 15 well-developed marine terraces (Figures I-1 and ONC-4). With the exception of the lowest terrace, which comprises an uplifted coral-reef (visible beneath our feet at the lighthouse or in the seacliff just below us), the terraces consist of marine abrasion platforms cut into shallow-marine limestones composed mainly of medium- to coarse-grained calcarenites (grainstones) that contain only local, displaced coral heads. The limestones exhibit varying degrees of karst weathering, with the degree of weathering generally increasing with elevation.

In the absence of detailed biostratigraphic age determinations from the RSJP limestones, they are tentively correlated with the Villa Trina Formation, a widespread unit of Pliocene-Pleistocene shallow-marine limestones that cap ridge crests throughout the Cordillera Septentrional and coastal mountains of the northern Dominican Republic (Figures ONC-3 and ONC-4; de Zoeten and Mann, 1991; De Zoeten et al., 1991; Dolan and others, 1991). However, at this locality the RSJP terrace limestones may be

considerably younger than the majority of the Villa Trina Formation; the youngest terraces of the RSJP are certainly younger than the youngest biostraigraphic age (early Pleistocene?) determined for the Villa Trina Formation exposed elsewhere in the northern Dominican Republic (de Zoeten and Mann, 1991; De Zoeten et al., 1991; Dolan et al., 1991). The RSJP terrace limestones lie with angular unconformity above metamorphic rocks of the Cretaceous Rio San Juan Complex, which is thought to represent the remains of an ancient accretionary prism (Draper and Nagle, 1991).

Uplifted Marine Terraces of the Rio San Juan Peninsula--The spectacularly well-developed flight of marine terraces of the RSJP is unique along the coast of north-central Hispaniola; similar flights of terraces do not occur nearby either to the east or west of the peninsula. The nearest well-developed flights of multiple terraces are located in northwestern Haiti, 500 km to the west (Mann et al., 1995), and along the Samana Peninsula, 200 km to the east of the RSJP (Joyce, 1991). The area immediately to the east of the RSJP is characterized by extremely low-lying, swampy conditions, whereas the area to the west exhibits only one well-developed marine terrace (resumably the oxygen isotope stage 5e terrace) at an elevation of 8-10 m above sea level.

Around the northern and eastern perimeter of the peninsula the lowest well-developed terrace, which presumably extends inland as far as the base of the second terrace, is approximately 500 to 1800 m wide (we are standing on it at the Cabo Frances Viejo stop). Exposed coral-reef deposits can be traced inland for >100 m from the modern seacliff, where they are buried by debris from the second terrace.

Approximately 15 well-developed terraces can be traced laterally for distances of up to 20 km (Figure I-1). However, reconnaissance mapping indicates that many smaller, highly discontinuous terraces also occur on the peninsula. Terrace height for the well-developed terraces ranges from a few meters to >50 m, whereas some the smaller, discontinuous terraces appear to be as little as 1 to 2 m in height. Individual terraces are generally roughly concentric in plan view, although some terraces 'pinch out' laterally (Figure I-1). Except for the very wide lowest terrace, most of the RSJP terraces range in width from ~50 m to a few hundred meters. The oldest terraces in the central 'core' of the hill have been topographically inverted by karst weathering.

The well-developed coral-reef terrace atop the modern seacliff and the second lowest terrace are the most laterally continuous terraces on the peninsula (Figure I-1). Both of these terraces reach maximum elevations along the northern part of the peninsula, in the area from Cabo Frances Viejo and just to the west. The paleo-seacliff along the seaward edge of the second lowest terrace is locally more than 50 m high along the northern part of the peninsula. Locally, paleo-sea stacks similar to those along the modern shoreline occur at the base of some terrace risers. The terraces systematically diminish in height systematically and become generally less pronounced from near Cabo Frances Viejo westward towards the city of Rio San Juan. Aside from the lowest terrace above the modern seacliff, uplifted terraces cannot be reliably traced west of about Rio San Juan.

At Cabo Frances Viejo, along the northern RSJP, the lowest coral terrace occurs at an elevation of ~18-19 m above sea level. The terrace slopes upward inland and may reach heights of 25 m or more; the inland limit of the terrace is poorly defined. However, at this locality the next well-developed terrace riser is located more than 1800 m inland from the seaward edge of the lowest terrace. The lowest terrace contains abundant colonies of *Acropora palmata* and *Montastrea annularis* reef-crest corals, most of which appear to be slightly too weathered for isotopic dating (F. Taylor, written communication, 1993). Despite the lack of an exact age for the terrace, the terrace most likely formed during the last interglacial highstand of sea level (oxygen isotope stage 5e; ~120,000-130,000 yr B. P.), which is believed to have reached about +6 m. The next well-developed terrace scarp inland is clearly much older, as indicated by the extreme weathering and recrystallization of the corals. Assuming a 120,000 year age for the lowest terrace, its 18-19 m minimum height indicates that the north-central part of the RSJP has been uplifted ~12-13 m in the

last 120,000 years. These values yield a rather low long-term uplift rate of approximately 0.11 mm/yr along the highest part of the uplifted terrace. Although the terrace inner edge is somewhat higher in elevation, the uplift rate is still no more than a few tens of a millimeter/year.

It is extremely unlikely that the lowest terrace corellates with oxygen isotope stages 5a or 5c because if the wide, lowest terrace is associated with stages 5a or 5c, then there should be a prominent stage 5e terrace at approximately 40 m above sea level that contains relatively well-preserved corals. Instead, there are only poorly preserved corals in heavily weathered emerged sea cliffs at this elevation. Furthermore, none of the uplifted RSJP terraces are as aerially extensive as the lowest terrace. Thus, although the lowest terrace has not been isotopically dated, it probably corellates with late Pleistocene oxygen isotope stage 5e.

The ~120 ka stage 5e terrace decreases systematically in height both to the east and west of the northern Rio San Juan Peninsula to values of only 8-10 m. This indicates minimal uplift of only 2-4 m of uplift in 120,000 years in other parts of the peninsula, yielding an uplift rate of only 0.02-0.03 mm/yr. Similarly, 8-10 m 120 ka terrace elevations from outside the peninsula (e. g., at Sosua, 70 km west of Cabo Frances Viejo) indicate extremely low late Quaternary uplift rates along the northern coast of Hispaniola (F. Taylor, personal communication, 1991; Dolan, unpubl. data).

Implications for Collisional Underthrusting of Silver Spur--Comparison of the location of the Rio San Juan Peninsula terraces with offshore side-scan sonar and bathymetric data indicates that the peninsula and the terraces have been formed during underthrusting of a prominent, ~2-km-tall submarine carbonate ridge (Silver Spur) near the western edge of a 200-km-long zone of active oblique collision between Hispaniola and the high-standing carbonate banks of the southeastern Bahamas (Figure ONC-4).

On August 4, 1946 this part of the northern Domincan Republic was rocked by a M~8 earthquake, which was caused by rupture of a 200-km-long segment of the shallowly south-dipping thrust interface between Hispaniola and the underthrust Bahamas carbonate banks (Figures ONC-1 and 4) (Dolan and Wald, 1998). The aftershock zone of this event exactly matches the limits of the active part of the collision zone defined by the side-scan sonar data (Dolan et al., 1998). The focal mechanism for this earthquake reveals oblique left-lateral/thrust motion (Dolan and Wald, 1998).

What does the morphology of the Rio San Juan Peninsula terraces tell us about the kinematics of the Silver Spur collision? Using topographic maps, a tilt axis for the second terrace can be defined by connecting a line between the intersections of the 80 m elevation contour with the second terrace crest along the northwestern and eastern parts of the peninsula (Figure 11). Terrace elevations are higher to the north of the N70W tilt axis, indicating that the peninsula has been tilted down to the southwest during the Silver Spur collision. Although they are not as laterally continuous as the lowest terraces, the oldest, highest terraces on the San Juan Peninsula also exhibit a general south-westward tilt. The shape of the terraces, however, suggests that earlier tilt axes were oriented more northerly; a probable tilt axis for the highest well-developed terrace strikes approximately N55W. The temporal variation in tilt rates probably reflects east-to-west lateral propagation of the collision.

The morphology of the peninsula, coupled with modern drainage patterns also provide details of the progression of the collisional underthrusting of Silver Spur. The 50 km-long, north-trending eastern coastline of the Rio San Juan Peninsula is highly anomolous with respect to the rest of the WNW-trending coastline of northern Hispaniola to the west of the RSJP (Figure ONC-4). In addition, all active drainages on the eastern part of the peninsula are assymetric to the east, implying that the eastern part of the peninsula has been tilted down to east (Draper and Nagle, 1991). These features probably developed in response to oblique southwestward passage of the main topographic crest of the underthrust portion of Silver Spur during the ongoing collision. As the oblique collision progressed topographic

support for the eastern part of the peninsula was progressively removed as the main crest of Silver Spur moved southwestward. Dolan et al. (1998) suggest that this may have resulted in collapse of the eastern, trailing edge of the collision, forming the north-trending coastline, and down-tilting of the eastern part of the peninsula. This model implies that the main, active part of the collision lies along the western edge of the RSJP, an inference that is supported by the occurrence of the 1953 Ms 7.0 Sosua earthquake just west of western edge of the peninsula. Dolan and Wald (1998) show that this earthquake extended the main 1946 rupture plane to the far western, leading edge of the Silver bank collision. The 1953 event terminated the westward-propagating 1946-1953 sequence of earthquakes, suggesting that the earthquakes were limited to a zone of enhanced mechanical coupling associated with underthrusting of relatively buoyant Bahamas crust; "normal" oceanic crust to the west in more readily subductible and the degree of interplate coupling there may be less than within the collision zone (Dolan and Wald, 1998).

REFERENCES

de Zoeten, R., and Mann, P., 1991, Structural geology and Cenozoic tectonic history of the central Cordillera Septentrional, Dominican Republic, *in* Mann, P., Draper, G., and Lewis, J. F., eds., Geologic and tectonic development of the North America-Caribbean plate boundary: Geol. Soc. Amer. Special Paper 262, p. 265-279.

de Zoeten, R., Draper, G., and Mann, P., 1991, Geologic map of the northern Dominican Republic, scale 1:100,000, *in* Geologic and Tectonic development of the North America-Caribbean plate boundary in Hispaniola, P. Mann, P., Draper, G., and Lewis, J., eds., Geol. Soc. Am.Special Paper 262, Plate 1.

Dolan, J. F., Mann, P., de Zoeten, R., Heubeck, C., Shiroma, J., and Monechi, S., 1991, Sedimentologic, stratigraphic, and tectonic synthesis of Eocene-Miocene sedimentary basins, Hispaniola and Puerto Rico, *in* Mann, P., Draper, G., and Lewis, J. F., eds., Geologic and tectonic development of the North America-Caribbean plate boundary, GSA Special Paper 262, p. 217-263.

Dolan, J. F., Mullins, H. T., and Wald, D., 1998, Active tectonics of the north-central Caribbean: Oblique collision, strain partitioning, and opposing subducted slabs: GSA Special Paper 326 *Active tectonics of the north-central Caribbean*, (eds.) Dolan, J. F., and P. Mann, p. 1-61.

Dolan, J. F., and Wald, D., 1998, The 1943-1953 north-central Caribbean earthquake sequence: Active tectonic setting, seismic hazards, and implications for Caribbean-North America plate motions: GSA Special Paper 326 *Active tectonics of the north-central Caribbean*, (eds.) Dolan, J. F., and P. Mann, p. 143-169.

Draper, G., and Nagle, F., 1991, Geology, structure, and tectonic development of the Rio San Juan Complex, northern Dominican Republic, *in* Mann, P., Draper, G., and Lewis, J. F., eds., Geologic and tectonic development of the North America-Caribbean plate boundary in Hispaniola: GSA Special Paper 262, p. 77-95.

Joyce, J., 1991, Blueschist metamorphism and deformation on the Samana Peninsula; a record of subduction and collisison in the Greater Antilles, *in* Mann, P., Draper, G., and Lewis, J. F., eds., Geologic and tectonic development of the North america-Caribbean plate boundary in Hispaniola: GSA Special Paper 262, p. 47-76.

REFERENCES (cont.)

Mann, P., Taylor, F., Edwards, R. L., and Ku, T., 1995, Actively evolving microplate formation by oblique collision and sideways motion along strike-slip faults: An example from the northeastern margin of the Caribbean plate: Tectonophysics, v. 246, p. 1-69.

FIGURE CAPTIONS

Figure I-1. Reconnaissance map of inner edges of marine etrraces on the Rio San Juan Peninsula, northern Dominican Republic (J. F.. Dolan, unpubl. data based on air photo interpretation). Tilt axis derived by connecting 80-m contour lines at two points on several terraces.

NOTE: Figure ONC-xxx refer to figures in the section of your field guide entitled "Overview of the Field Trip on North Coast Geology"

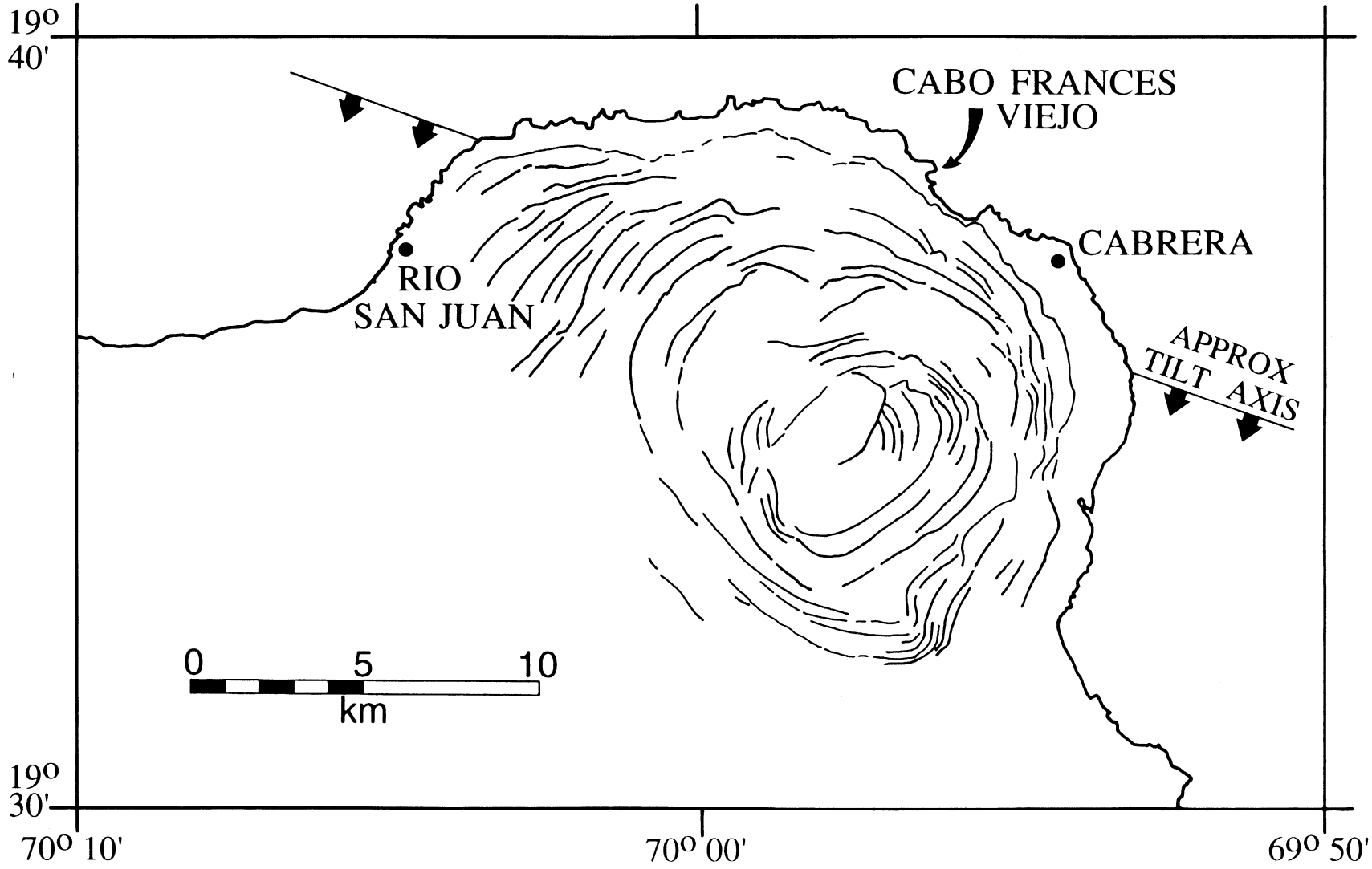
19° 40'
CABO FRANCES VIEJO
CABRERA
RIO SAN JUAN
APPROX TILT AXIS
0 5 10
km
19° 30'
70° 10'
70° 00'
69° 50'

DAY TWO, STOP Ib: GPS SITE, CABO FRANCES VIEJO
LEADER: ERIC CALAIS

NOTE: DANGER!!! THIS SITE IS LOCATED NEXT TO A VERTICAL 20-M-TALL CLIFF THAT IS MASKED BY VEGETATION. PLEASE DO NOT VENTURE NEAR THE EDGE AS A FALL COULD PROVE TO BE FATAL.

BACKGROUND

Relative motion of the Caribbean plate with respect to the North American plate is accomodated across a 200-km-wide deformation zone, which includes the island of Hispaniola. The relative motion of the two plates is poorly defined in global plate motion models because of a lack of constraining data such as transform azimuths and ocean ridge spreading rates. In addition, earthquake slip vectors are likely to be biased by deformation partitioning in a kinematic setting where strike-slip and convergence coexist (DeMets, 1993). The distribution of strain within the plate boundary zone remains also poorly constrained in spite of clear evidences for active deformation. The major active faults in Hispaniola have been identified from field observations, aerial photos, and satellite images. Late Quaternary tectonic activity is clearly recognized for both the Enriquillo and Septentrional fault zones (e.g. Mann et al., 1984, 1995). Trenching across the Septentrional fault indicates that it last ruptured 730 years ago, slipping about 5 m horizontally and 2 m vertically (Prentice et al., 1993). Holocene terraces offset by the Septentrional fault indicate 13-23 mm/yr of slip over the past 3000 years (Mann et al., 1998). Historical and recorded seismicity show several earthquakes of magnitude greater than 6.5 associated with the Septentrional and Enriquillo fault zones (Robson, 1964; Sykes et al., 1982; Calais et al., 1992). Significant seismicity and active deformation have also been identified offshore along the North Hispaniola Trench (Dillon et al., 1992; Russo and Villasenor, 1995; Dolan and Wald, 1998; Dolan et al., 1998) and the Muertos Trench to the south (Ladd et al., 1977). However, the strain distribution among these active features is not yet quantified and the slip rate of the major active faults is not known.

SCIENTIFIC OBJECTIVES

The main objectives of GPS measurements in the northeastern Caribbean are:

--To determine the present-day motion of the Caribbean plate.
--To determine the slip rate and level of elastic strain accumulation along the major active faults.
--To determine how the Caribbean/North America motion is partitioned by the faults that separate the two plates in the vicinity of Hispaniola and Puerto Rico.
--To determine the amount of localized versus diffuse deformation across the plate boundary zone.
--To extract information about the dynamics of the plate boundary by modeling elastic strain and extracting block rotation from the GPS-derived velocity field.

GPS MEASUREMENTS

In 1986, a sparse network of geodetic sites was occupied by GPS in the northeastern Caribbean, as part of a NASA program to test and validate this new technology in a humid tropical environment (Dixon et al., 1991 and Figure 1). Three of the sites were installed in

the Dominican Republic (Cabo Frances Viejo, Capotillo, and Cabo Rojo). In 1994, this network was reoccupied and a number of new sites were added, in particular in the Dominican Republic. Some of these sites have been reoccupied in 1995, 1996, and 1998. In addition, 27 new sites have been established in September 1998, that will be occupied during a two-week campaign in January-February 1999. Figures 3 and 4 show a typical field setup during a GPS campaign. The measurements will be made with dual-frequency Trimble receivers and choke-ring antennas. Each site will be occupied during three consecutive 24-hour sessions by four field teams. The conventional tripods will be replaced by specially designed spike mounts in order to eliminate antenna height measurement problems and to minimize systematic errors associated with classical tribrachs.

PRELIMINARY RESULTS

The analysis of GPS data collected in 86, 94, and 95 (Dixon et al., 1998; Figure 2) shows an eastward motion of the Caribbean plate at a rate of 17 mm/yr relative to North America, measured at Cabo Rojo, southern Dominican Republic. This velocity is significantly higher than the NUVEL-1A prediction of 11±3 mm/yr. Additional measurements at ROJO performed in September 98 confirm this result, with slightly faster velocities (18 to 21 mm/yr). Preliminary elastic strain models (Dixon et al., 1998), based on 3 velocities only in the Dominican Republic (ROJO, CAPO, FRAN), had suggested:
4±3 mm/yr of slip on the North Hispaniola fault offshore the north coast of Hispaniola;
8±3 mm/yr of slip on the Septentrional fault in northern Dominican Republic;
8±4 mm/yr of slip on the Enriquillo fault in southern Haiti and Dominican Republic.
The September 98 measurements allowed us to compute velocities at three additional sites (CONS, SDOM, and MOCA, Figure 1). These new results, together with 3 dimensional elastic strain models, will be presented at the conference.

REFERENCES

Calais, E., BÈthoux, N., and B. Mercier de LÈpinay, 1992, From transcurrent faulting to frontal subduction: A seismotectonic study of the northern Caribbean plate boundary from Cuba to Puerto Rico, Tectonics, v. 11, p. 114-123.

DeMets, C., 1993, Earthquake slip directions and estimates of present-day plate motion, J. Geophys. Res., v. 98, p. 6703-6714.

Dillon, W.P., Austin, J.A., Scanlon, K., M., Edgar, N.T., and Parson, L.M., 1992, Accretionary margin of north-western Hispaniola: Morphology, structure, and development of the northern Caribbean plate boundary, Marine and Petroleum Geology, v. 9, p. 70-92.

Dixon, T., Farina, F., DeMets, C., Jansma, P. ,Mann, P., and Calais, E., 1998, Relative motion between the Caribbean and North American plates and related boundary zone deformation based on a decade of GPS observations, J. Geophys. Res., v. 103, p. 15157-15182.

Dixon, T.H., G. Gonzalez, S.M. Lichten and E. Katzigris, 1991, First epoch geodetic measurements with the Global Positionning System across the Northern Caribbean plate boundary zone, Jour. Geophys. Res., v. 96, p. 2397-2415.

Dolan, J.F., and Wald, D.J., 1998, Strain accumulation and seismic energy release localized along collisional asperities: the 1946 and 1948 north-central Caribbean

earthquakes: GSA Special Paper 326 Active Tectonics of the North-Central Caribbean, (eds.) Dolan, J. F., and P. Mann, p. 143-169.

Dolan, J. F., Mullins, H. T., and Wald, D., 1998, Active tectonics of the north-central Caribbean: Oblique collision, strain partitioning, and opposing subducted slabs: GSA Special Paper 326 Active Tectonics of the North-Central Caribbean, (eds.) Dolan, J. F., and P. Mann, p. 1-61.

Ladd, J.W., J.L. Worzel, and J.S. Watkins, 1977, Multifold seismic reflection records from the northern Venezuela basin and north slope of Muertos trench, in Island Arcs, Deep Sea Trenches and Back-Arc Basins, Maurice Ewing Ser., vol.1, edited by M. Talwani and W.C. Pitman III, p. 41-56, AGU, Washington D.C.

Mann P., Burke K. and Matumoto T., 1984, Neotectonics of Hispaniola plate motion, sedimentation and seismicity at a restraining bend: Earth and Planetary Science Letters, v. 70, p. 311-324.

Mann, P., F.W. Taylor, R. Edwards, and T.L. Ku, 1995, Actively evolving microplate formation by oblique collision and sideways motion along strike-slip faults†: An example from the Northeastern Caribbean plate margin, Tectonophysics, v. 246, p. 1-69.

Mann, P., E. Calais, C. DeMets, T. Dixon, J. Dolan, N. Grindlay, P. Jansma, and C. Prentice, Integrated geologic and geophysical data suggest high seismic risk for the Dominican Republic, Haiti, and Puerto Rico, EOS, submitted, 1998.

Prentice, C., P. Mann, F.W. Taylor, G. Burr, and S. Valastro, 1993, Paleoseismicity of the North American plate boundary (Septentrional fault), Dominican Republic, Geology, v. 21, p. 49-52.

Robson, G.R., An earthquake catalog for the eastern Caribbean, 1630-1960, Bull. Seism. Soc. Amer., v. 54, p. 785-832.

Russo, R.M., and Villasenor, A., 1995, The 1946 Hispaniola earthquakes and the tectonics of the North America-Caribbean plate boundary zone, northeastern Hispaniola, J. Geophys. Res., v. 100, p. 6265-6280.

Sykes, L.R., McCann, W.R., and Kafka, A.L., 1982, Motion of the Caribbean plate during the last 7 million years and implications for earlier Cenozoic movements, J. Geophys. Res., v. 87, p. 10,656-10,676.

FIGURE CAPTIONS

Figure 1. Map of the GPS sites observed in 1986, 1994, and 1998 (red stars) and planned to be observed in January-February 1999 (white squares).

Figure 2. GPS site velocities with respect to Grand Turk (yellow vectors) and a North America reference frame (red vectors). Error ellipses are two-dimensional, 95% confidence (Dixon et al., 1998).

Figure 3. A GPS antenna installed on a tripod at Cabo Frances Viejo, 1994 CANAPE campaign.

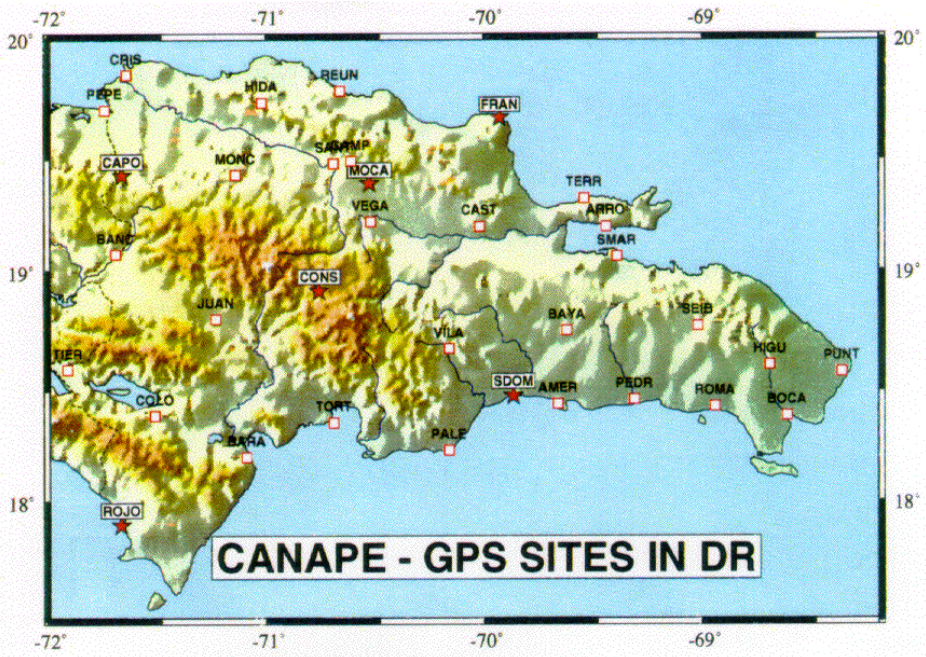

Figure 1 : Map of the GPS sites observed in 1986, 1994, and 1998 (red stars) and planned to be observe in January-February 1999 (white squares).

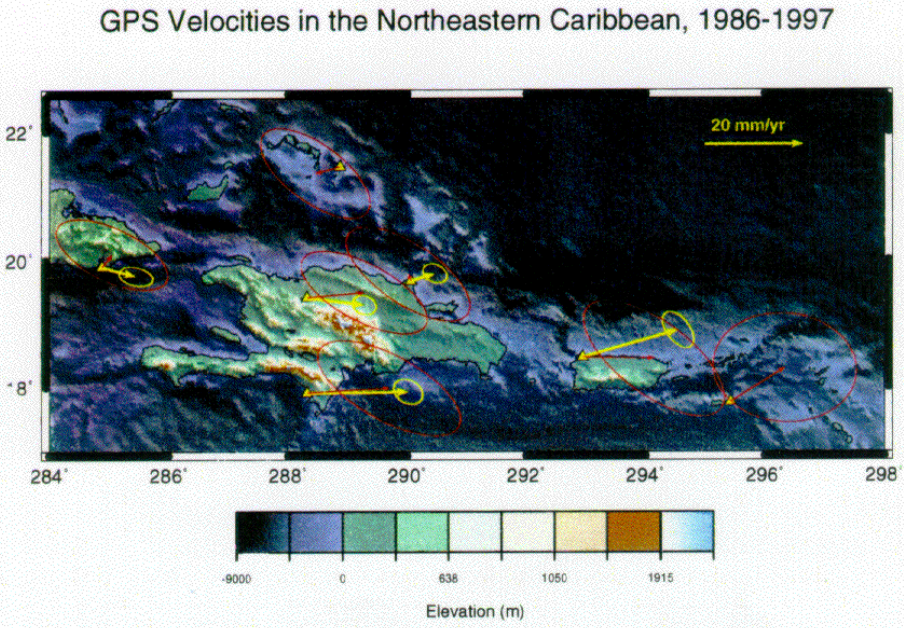

Figure 2 : GPS site velocities with respect to Grand Turk (yellow vectors) and a North America referenc frame (red vectors). Error ellipses are two-dimensional, 95% confidence (Dixon et al., 1998).

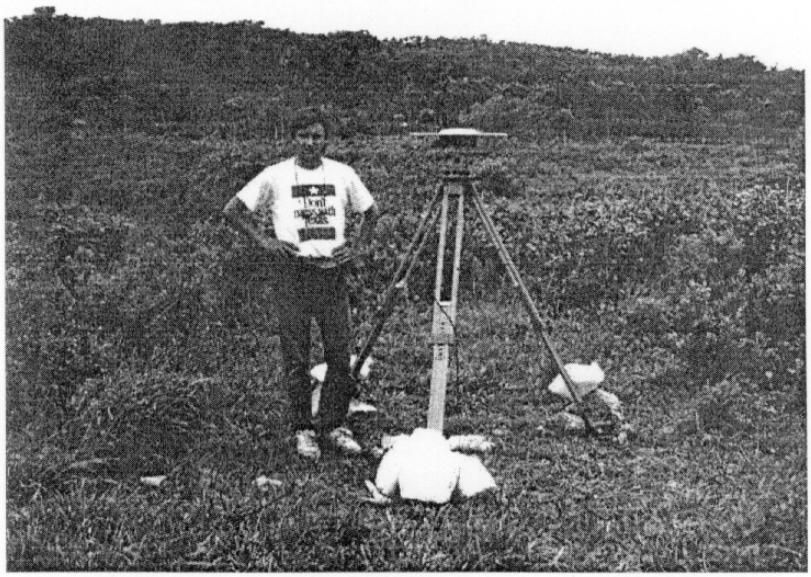

Figure 3 : A GPS antenna installed on a tripod at Cabo Frances Viejo, 1994 CANAPE campaign.

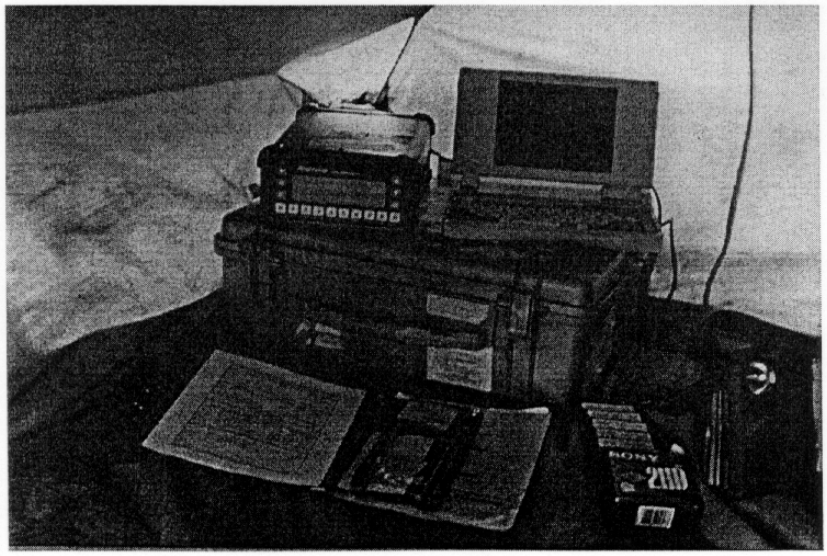

Figure 4 : GPS field equipment : receiver (right), portable computer, floppy disks, and log book.

DAY TWO, STOP J: LATE CRETACEOUS, HIGH-PRESSURE, LOW-TEMPERATURE METAMORPHIC ROCKS - THE RIO SAN JUAN COMPLEX

LEADER: GRENVILLE DRAPER

LOCATION

Outcrops of the Gaspar Hernadez serpentinite can be seen on the south side of the coastal highway between the towns of Rio San Juan and Gaspar Hernandez (Fig. 1). This serpentinite contains diabase blocks, but no HP/LT metamorphic blocks have yet been found in this unit.

To reach Stop J, turn south off the main road at La Cantera and continue to the small outcrop opposite the military post near the entrance to the Guzman farm. Stop J is a small exposure of the Arroyo Sabana melange that is in a lenticular outcrop bound by strands of the Camu fault (Fig. 2) that continues westward to the Puerto Plata area (see Stops A and B). Blocks of fine grained blueschists can be seen in a serpentinite matrix. The blocks contain glaucophane -epidote- phengite- quartz-pyrite assemblages. If you have a geologic hammer and hand lens, please share with a neighbor.

SIGNIFICANCE

The area south of the Gaspar Hernandez - Rio San Juan exposes the largest area of Cretaceous basement rocks exposed along the north coast of Hispaniola and is the principal evidence of Cretaceous subduction in the area (Nagle, 1966; 1974). The rocks are known as the Rio San Juan Complex from the river that runs through the complex (Eberle et al, 1982).

DESCRIPTION

According to Draper and Nagle (1991) the complex is made up of the following units (Figs. 1, 2)

The **Imbert Formation**, a Paleocene to lower Eocene series of interbedded sandstone, conglomerate, white tuff and sedimentary serpentinite, that is also found in the Puerto Plata area (see Stops A and B).

Three coherent HP metamorphic are present: The **Hicotea schists**, pervasively fractured, mafic greenschists with patchily developed glaucophane and lawsonite; the **Puerca Gorda schists**, dominantly mafic, foliated greenschists, also with patchily developed glaucophane and lawsonite; and the **El Guineal schists**, fine grained, dominantly felsic schists. The protoliths of these units are tuffaceous in many cases and have island arc geochemical signatures (Anam, 1994).

Two separate melanges are present, both of which have a highly metasomatically altered and hydrated serpentinite matrices. The first of these is the **Jagua Clara mélange**, which contains retrograded eclogite and garnet blueschist blocks. In contrast, the Arroyo Sabana mélange has fine grained blueschist, marble, altered volcanic and mica-plagioclase blocks. Renne (1991) used $^{40}Ar/^{39}Ar$ to obtain dates from a single hornblende-phengite-chlorite block in the Jagua Clara mélange, and found an 85 ± 2.4 Ma retention age for the hornblende and evidence for a 61 ± 1.8 Ma thermal overprint event.

A third serpentinite unit is the **Gaspar Hernandez serpentinite**, which is less hydrated and contains only blocks of diabase.

The southern area of the complex is structurally simpler and consists of the **Cuaba amphibolites** which are mafic to felsic gneisses. Recent studies by Abbott and Draper

(1998) have shown that symplectic intergrowths of plagioclase and clinopyroxene are present that are the result of the breakdown of omphacite, and that hornblende is a late stage mineral. Thus the Cuaba seems to have origianlly been a high temperature eclogite that has retrograded to an amphibolite. The Cuaba amphibolite is intruded by the **Rio Boba Intrusive Suite**, which is a large composite pluton consisting of layered gabbros, diorites and ultramafic cumulates.

TECTONIC ORIGIN AND UPLIFT HISTORY OF THE RIO SAN JUAN COMPLEX

The Hicotea, Puerca Gorda and El Guineal schists were metamorphosed in a Late Cretaceous subduction zone where they were faulted at depth against the Jagua Clara and Arroyo Sabana mélanges. The southern part of the complex was formed in a higher temperature environment closer to the Hispaniola magmatic arc. The Rio Boba Suite which has an intrusive contact with Cuaba amphibolites may represent an example of forearc magmatism. The southern area was tectonically juxtaposed against the northern area before the Paleocene, but the mechanism by which this was achieved is unclear. Strike-slip faults in the forearc, formed in response to oblique convergence may be one mechanism. Exposure of the assembled complex had occurred by the Eocene, but the complex was probably covered by clastic sediments during Late Eocene to Miocene times. Both the Cretaceous subduction complex and the mid-Tertiary clastic cover were disrupted and deformed by Neogene, E-W trending, sinistral, transcurrent movements. Major fault displacements of tens to hundreds of kilometers separated the Puerto Plata area from the Rio San Juan complex, and both areas from southeastern Cuba. Minor displacements occurred within the Rio San Juan complex on sinistral oblique and strike slip faults Transcurrent faulting continues to the present and has resulted in eastward tilting of the Rio San Juan complex and the establishment of its present drainage systems.

REFERENCES

Abbott, R. N. and Draper, G., 1998, Retrograded eclogite in the Cuaba amphibolites of the Rioa San Juan Complex, northern Hispaniola, Fifteenth Caribbean Geological Conference, Articles, Field Guides & Abstracts, Contributions to Geology, U.W.I. Mona, no.3, p. 71

Anam, K,, 1994, Petrology and geochemistry of some high presssure rocks from the northern part of the Rio San Juan Complex, Dominican Republic, unpublished MS thesis, Florida International University, 126pp.

Draper, G. and Nagle, F., 1991, Geology, structure and tectonic development of the Rio San Juan Complex, northern Dominican Republic: in Mann, P., Draper, and Lewis, J.F. (eds.), Geological and tectonic development of the North American-Caribbean plate boundary in Hispaniola, Geol. Soc America, Special Paper 262, p. 77-95.

Eberle, W., Hirdes, W., Muff, R., and Pelaez, M., 1982, The geology of the Cordillera Septentrional (Dominican Republic), in Transactions, 9th Caribbean Geological Conference, Santo Domingo, Dominican Republic, 1980, p. 619-632.

Nagle, F., 1966, Geology of the Puerto Plata area, Dominican Republic [Ph.D. thesis]: Princeton University, 171 p.

Nagle, F., 1974, Blueschist, eclogite, paired metamorphic belts, and the early tectonic history of Hispaniola: Geological Society of America Bulletin, v. 85, p. 1461-1466.

Renne, P. R., 1991, Appendix, $^{40}Ar/^{39}Ar$ data and thermochronologic implications for a block from the Jagua Clara mélange of the Rio San Juan complex, in Draper, G. and Nagle, F., 1991, Geology, structure and tectonic development of the Rio San

Juan Complex, northern Dominican Republic: in Mann, P., Draper, and Lewis, J.F. (eds.), Geological and tectonic development of the North American-Caribbean plate boundary in Hispaniola, Geol. Soc America, Special Paper 262, p. 91-95.

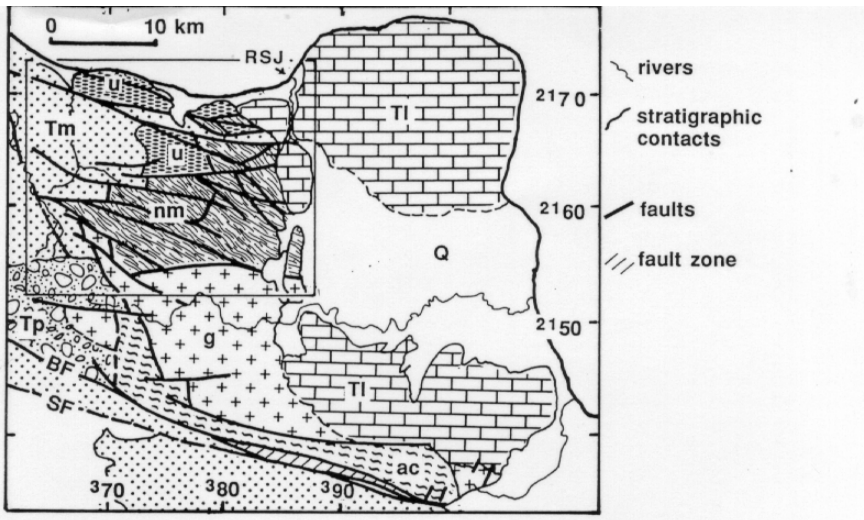

Figure 1. Geologic map of the entire Rio San Juan complex from Draper and Nagle (1991). Grid numbers shown at sides of Figures 1 and 2 refer to the grid shown on 1:50,000 topographic maps of the Dominican Republic. Key to abbreviations: **GH** = Gaspar Hernandez, **RSJ**= Rio San Juan, **ac** = Cuaba Amphibolites, **g** = Rio Boba Intrusive Suite, **u** = Gaspar Hernandez Serpentinites, **nm** = metamorphic rock units of the northern part of the complex (including Imbert Formation). Sedimentary rocks associated with the complex are: **Tm** = Upper Eocene to Oligocene clastic sedimentary rocks of the Mamey Group (principally the La Toca Formation), **Tl** = Neogene limestones (mainly Villa Trina Formation), **Q** = Quaternary alluvium and reef deposits. **SF** and **BF** indicate the traces of the Septentrional and Bajabonico Faults respectively. Box indicates area of northern Rio San Juan complex shown in Figure 2.

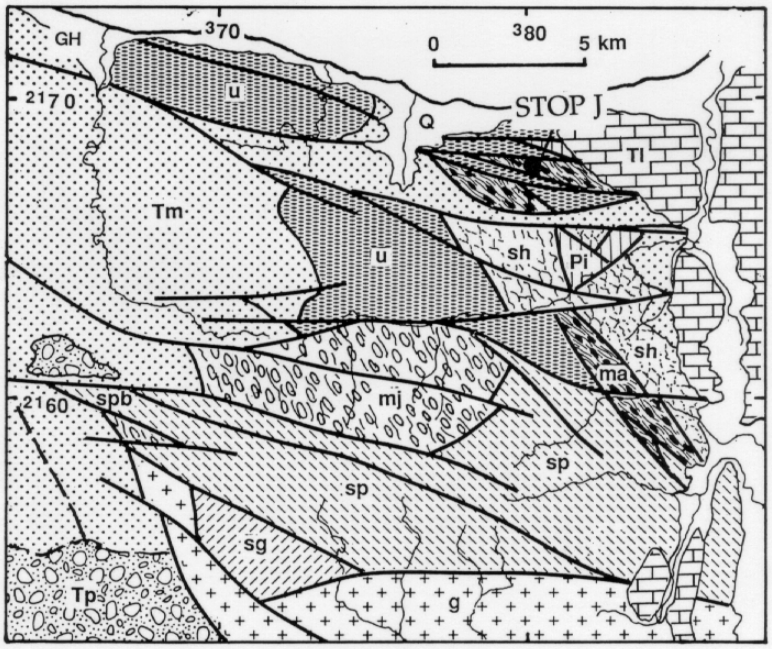

Figure 2. Geologic map of the northern part of the Rio San Juan complex and setting of Stop I from Draper and Nagle (1991). Key to abbreviations: **Pi** = Imbert Formation, **mj** =Jagua Clara mélange, **ma** = Arroyo Sabana mélange, **sh** = Hicotea schists, **sp** = Puerca Gorda schists, **spb** = anomalous brecciated unit in the Puerca Gorda schists, **sg** = El Guineal schists, **Pi** = Imbert Formation. All other symbols are the same as Figure 1.